National Aeronautics and Space Administration

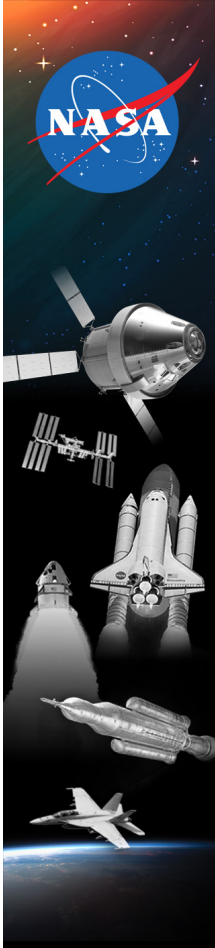
NESC

NASA Engineering & Safety Center

Technical Bulletins 2007-2022

Critical knowledge captured from NESC assessments in the form of new engineering information or best practices in a one-page format.

nesc.nasa.gov



NESC tech bulletin

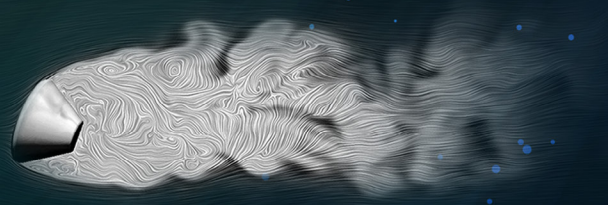
09/19/22 Doc 20210009638

National Aeronautics and Space Administration

NASA ENGINEERING & SAFETY CENTER

Why the NESC Exists

The Columbia Accident Investigation Board (CAIB) specified a need for a technically strong, program-independent resource to provide an alternate perspective on difficult technical issues and provide independent technical investigations (study, analysis, test, etc.) for NASA programs and projects.





The NESC Highlights NASA's Traditional Safety Philosophy

- Strong in-line checks and balances
- Healthy tension between organizational elements
- Value-added independent assessments

The Mission

To perform value-added independent testing, analysis, and assessments of NASA's high-risk projects to ensure safety and mission success.



NESC Technical Bulletins

NESC Technical Bulletins can result from NESC independent testing, analysis, and assessments. The process is shown below. A technical bulletin captures critical knowledge in the form of new engineering information or best practices in a one-page format. NESC Technical Bulletins are available at nesc.nasa.gov.

NESC Assessment Flow

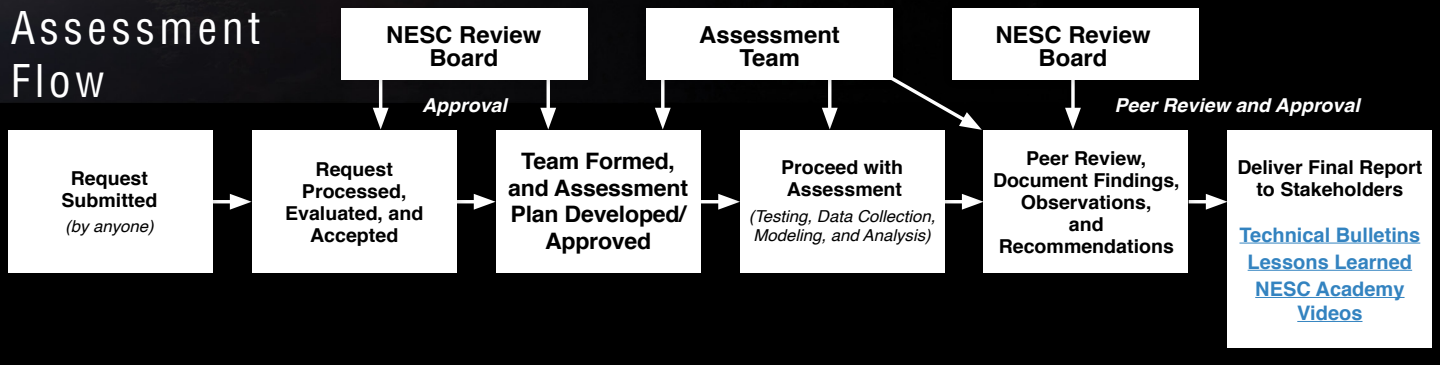
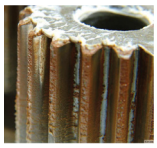
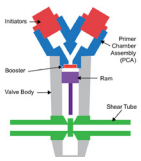


TABLE OF CONTENTS



No. 07-01 - Braycote Grease Storage ..... page 9

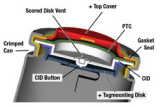
Braycote™ greases that are in mechanisms in controlled storage retain their tribological properties for an extended period of time. Testing on aged and separated Braycote™ grease obtained from several sources showed no detrimental effect on lubricity. Additionally, Thermal Gravimetric Analysis testing demonstrated no significant decrease in performance due to static, controlled storage. Tribological action, heat, or other forces are required to effect the performance of Braycote™ grease.



No. 09-01 - Pyrotechnic Valves Failure ..... page 10

Investigation of recent pyrovalve failures reveals timing of redundant initiator firings is crucial for reliable operation of pyrovalves. Simultaneous firing, i.e., within a very narrow time frame, was found to be the primary cause of the valve failing to operate. Testing of both single and dual initiators revealed important design characteristics affecting pyrovalve device performance. They include Primer Chamber Assembly (PCA) geometry and material properties, as well as operational effects on combustion product flow, and resulting energy transfer to the booster.

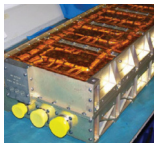
The CONAX PCA design has evolved slowly over time undergoing incremental changes to correct known issues. These piecewise changes were verified by limited test, without a full understanding of the overall system impact or effect on margins. Adequate system performance margins may be adversely affected in existing or future systems incorporating a pyrovalve actuated by simultaneous firing of dual initiators.



No. 09-02 - Battery Protection ..... page 11

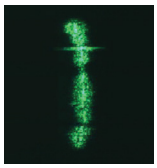
Most commercial cylindrical 18650 Lithium-Ion (Li-Ion) cells have two internal protective devices: the Positive Temperature Coefficient (PTC) and the Current Interrupt Device (CID). The PTC protects the cells under external short conditions and the CID protects the cells under overcharge conditions. While proven to be effective at the single cell and small-size battery levels, these devices do not always offer protection when used in high- voltage and high-capacity battery designs.

No. 09-03 - Battery Database/Guideline ..... page 12



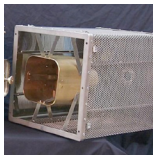
Lithium-Ion (Li-Ion) batteries are fast becoming the battery chemistry of choice for aerospace applications requiring (rechargeable) power supplies. These batteries offer high-energy density and high-specific energy combined with excellent rate capability and cycle potential. The increased energy content and operational characteristics of this system require defined safety and handling procedures to ensure the safe implementation. Standardized approaches to defining, determining, and addressing safety, handling, and qualification for Li-Ion batteries have been developed and published as an NESC-sponsored Li-Ion Battery Guidelines Document. A data base was established cataloging cells and batteries that have been considered for aerospace applications.

No. 09-04 - Penetrant NDE Capability ..... page 13



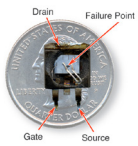
As the desired crack detection size is decreased and approaches the physical limitations of liquid penetrant inspection techniques, the approach of performing a probability of detection (POD) validation test at a single aspect ratio, and then extending the results to other aspect ratios based on equivalent area predictions may not be valid. POD testing for penetrant inspection of metallic pressure vessels and COPV liners should be performed at the bounds of the required range of crack aspect ratios.

No. 09-05 - Self-Contained Oxygen Generator ..... page 14



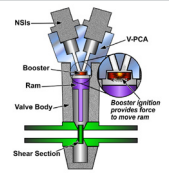
A Self-Contained Oxygen Generator (SCOG) produces breathable oxygen (O^2) by using chemically-reactive briquettes that begin producing O^2 when mechanically ignited. Contamination with organic material of, or manufacturing defects in, the briquettes have been shown to lead to conditions that can cause an explosive failure.

No. 10-01 - Power MOSFET Thermal Instability ..... page 15



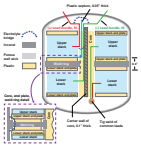
In the quest for faster switching times and lower “on resistance” the Metal-Oxide Semiconductor Field-Effect Transistor (MOSFET), produced since 1998, has achieved most intended goals. Unfortunately, lower “on resistance” and higher switching speeds in the designs now being produced allow the charge carrier dominated region to develop conditions that could lead to thermal runaway. Temperatures above 450° C on any location within the part can cause the metals to begin migrating causing a fatal short circuit.

TABLE OF CONTENTS



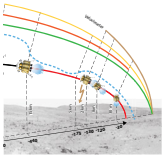
No. 10-02 - Potential Failure of Dual Simultaneously Initiated Pyrotechnic Operated Valve.....page 16

The NASA Engineering and Safety Center (NESC) Technical Bulletin No. 09-01 reported an independent investigation of four pyrovalve failures that occurred while using aluminum (Al) pyrovalve primer chamber assemblies (PCAs) during ground testing. The investigation revealed that simultaneous firing (within a few microseconds) of the NASA Standard Initiators (NSIs) was the primary reason why the booster charge failed to ignite and the pyrovalves subsequently failed to operate. A second investigation of a new stainless steel (SS) PCA design with separate flame channels was completed in 2010. The new SS configuration was found to be improved in most respects; however, no improvement was noted in the temperature delivered to ignite the booster during dual simultaneous NSI firings. Simultaneous firings should be avoided when using either the Al or the SS PCA design.



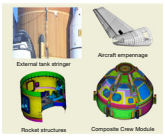
No. 11-01 - Nickel-Hydrogen (NiH2) Common Pressure Vessel (CPV) Cell Capacity Loss and Voltage Collapse.....page 17

During an investigation of anomalous voltages during a NASA scientific mission, a NASA Engineering and Safety Center (NESC) team discovered that the design of NiH 2 CPV batteries may be susceptible to a unique electrolyte bridging between the two internal cells resulting in undesired ionic current flow. This condition can lead to depletion of the capacity within one of the two cells.



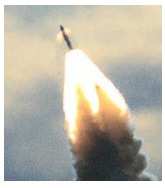
No. 12-01 - Simulation Framework for Rapid Entry, Descent, and Landing Analysis.....page 18

The NASA Engineering and Safety Center has archived a number of key historic Entry, Descent, and Landing (EDL) simulation models and developed several new models to enhance the capability of the Agency to evaluate a wide range of EDL systems for system analysis studies, preliminary design, mission development and execution, and time-critical assessments. The simulation models developed in this activity can be used to help define the required architectures and investment strategies for future robotic and human exploration missions.



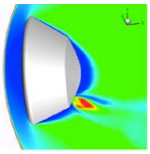
No. 12-02 - Structural Analyses and Margins of Safety.....page 19

There is an increasing reliance on modeling and simulation to verify, quantify, and certify designs of complex structures. The availability of a range of commercial modeling and simulations tools and packages with a variety of capabilities, in conjunction with increased computational resources, is allowing analysts to rapidly perform detailed analyses. However, care should be taken to understand specific tool limitations, assumptions, and boundary conditions as erroneous results can be generated without being recognized by the analysts. In addition, the reported margins of safety should be carefully interrogated to identify any false positive or negative margins and highlight any areas for structural concern.



No. 14-01 - Designing for Flight Through Periods of Instability.....page 20

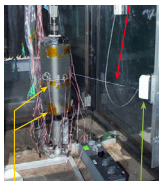
An NESC assessment of the Ares 1 flight control sensitivity to slosh dynamics in the Orion service module raised questions for Neil Dennehy, NASA Technical Fellow for Guidance, Navigation, and Control (GNC), about stability margins, the degree of conservatism flight control system (FCS) engineers put into designs, the linear and nonlinear analysis tools they use, and how it all related to safely flying a vehicle through brief periods of control instability. As stability is a mantra for GNC experts, Dennehy began capturing what the GNC community was learning about stability margins with respect to control instability, resulting in this technical bulletin that suggests FCS designers not limit themselves, and look beyond the frequency domain approach when designing flight control systems.



No. 14-02 - Aerodynamic Reaction Control System (RCS) Orientation and Jet Interaction (JI) Model Validation.....page 21

A historical perspective on jet interaction prediction issues combined with NESC analysis gleaned from a Mars Science Laboratory assessment led to this technical bulletin's guidance on the placement and orientation of reaction control system (RCS) jet thrusters on hypersonic entry vehicles. Dr. David Schuster, NASA Technical Fellow for Aerosciences, concluded that taking the proper precautions in the development of an RCS system, paired with computational fluid dynamics calculations and wind tunnel testing, yields a more accurate view of controllability and the flow characteristics behind those vehicles.

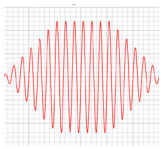
TABLE OF CONTENTS



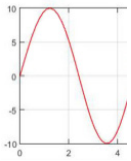
No. 14-03 - COPV Mechanical Model Validation ..... page 22
When issues surrounding the understanding of composite overwrapped pressure vessel (COPV) mechanics surfaced in two previous NESC assessments, Dr. Lorie Grimes-Ledesma of the Composite Pressure Vessel Working Group discovered that even with the availability of vendor-supplied finite element tools, there was a lack of accuracy in understanding COPV liner and composite response. And that lack of accuracy was propagating in subsequent fracture and stress rupture analysis. A look back to fundamentals in understanding autofrettage and a subsequent correlation study between finite element analysis and measured response on COPVs led to this technical bulletin's best practices for COPV model validation.



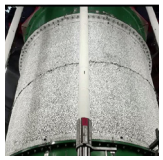
No. 15-01 - Preventing Incorrect Installation of Polarized Capacitors..... page 23
Concerns that the incorrect installation of polarized capacitors has continued, despite lessons learned from past installation issues, Dr. Christopher Iannello, NASA Technical Fellow for Electrical Power, and Andrew Ging, an industry partner on the NESC Electrical Power Technical Discipline Team, initiated this technical bulletin to shed new light on a timeworn problem. Using an NESC assessment of an anomaly on board the International Space Station as an example, Dr. Iannello and Mr. Ging highlight the ways in which reverse installation can occur, and provide a short list of best practices — from procedure review to the correct use of symbols on schematics — to help eliminate any future issues with reverse installation.



No. 15-02 - Best Practices for Use of Sine Burst Testing ..... page 24
For more than two decades, sine burst testing has provided a method of strength testing for aerospace hardware that not only minimizes potential for damage to the test item, but can be performed on a shaker table along with other tests to maximize efficiency. But with all testing comes potential risk. In this Technical Bulletin, Mr. Daniel Kaufman, NESC Discipline Deputy for Loads and Dynamics, identifies top risks such as unintended over-test or erroneous calculations, and provides best practices to help mitigate those risks and take full advantage of what sine burst testing provides.



No. 15-03 - Best Practices for Use of Sine Vibration Testing ..... page 25
Sine vibration testing replicates the low-frequency launch environment. This test method is used mainly on flight articles to determine if they can survive the harsh launch environment. Testing involves accepting calculated risk, but failure to follow best practices for sine vibration testing has resulted in avoidable damage to flight hardware. Dr. Curtis Larsen, NASA Technical Fellow for Loads and Dynamics, Mr. Daniel Kaufman, NESC Discipline Deputy for Loads and Dynamics, and their Technical Discipline Team identified top risks and documented best practices to help mitigate those risks and take full advantage of what sine vibration testing has to offer.



No. 16-01 - Buckling Knockdown Factors for Composite Cylinders ..... page 26
It took decades to figure out the complex buckling behavior of metallic cylindrical launch vehicle structures and the knockdown factors (KDFs) that account for the unknown variability in the geometry, loading, and material imperfections. The KDFs, established by Apollo-Era engineers, are still in use today by NASA and by industry world-wide, as captured in NASA SP-8007 Buckling of Thin-Walled Circular Cylinders from 1968. Developed with conservatisms warranted by the technology of the time, these KDFs are likely adding unnecessary weight to today's modern aerospace structures. That was the catalyst behind Dr. Mark Hilburger's NESC-sponsored proposal to develop and implement updated shell buckling KDFs, now in use by the Space Launch System Program. Designers of composite cylinders, however, still turn to SP-8007, often using KDF=0.65 in their composite designs, a number for which the technical justification is unclear. As a result, Dr. Marc Schultz, working with Dr. Hilburger, is investigating KDFs for modern composite cylinders. Their work has led to the development of this Technical Bulletin, which emphasizes that composite cylinders are outside the scope of SP-8007 and why caution must be taken when using the universal KDF in composite designs.



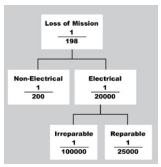
No. 16-02 - Damage Tolerance Life Issues in COPVs with Thin Liners..... page 27
While Composite Overwrapped Pressure Vessels (COPVs) with thin liners offer weight savings, they present fracture control challenges. Current methods for estimating damage tolerance life may be limited for thin-lined vessels. This Technical Bulletin explains the challenges present when COPVs with thin liners are used, why additional qualification tests may be necessary, and what steps the NESC is taking to develop a path forward for their future use.

TABLE OF CONTENTS



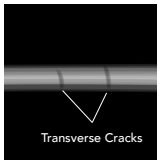
No. 17-01 - Development of NASA Standards for Enabling Certification of Additively Manufactured Parts ..... page 28

As NASA approaches certification of manned spaceflight components made from additively manufactured (AM) parts, Mr. Richard Russell, NASA's Technical Fellow for Materials, initiated this NESC technical bulletin to underscore the need for an Agency standard that outlines the requirements for AM parts design, manufacture, and certification. The AM field is experiencing rapid growth. NASA, as well as its commercial crew partners, are using these parts in several programs such as the Orion Multi-Purpose Crew Vehicle and the Space Launch System (SLS) – programs that will by flying before industry and international standards agencies can complete the AM standards they are currently developing. Marshall Space Flight Center, took the initiative to write a Center-level standard - MSFC-STD-3716 "Standard for Additively Manufactured Spaceflight Hardware by Laser Powder Bed Fusion in Metals," 2017, and an accompanying specification - MSFC-SPEC-3717, "Specification for Control and Qualification of Laser Powder Bed Fusion Metallurgical Processes," 2017, encompassing the laser power bed fusion (L-PBF) process.



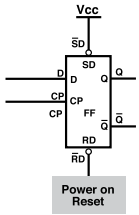
No. 19-01-1 - Avoiding Single Event Upsets in Commercial Parts Used in Space Applications ..... page 29

The current and former NASA Technical Fellows for Avionics have led several NESC assessments to better understand and quantify the risks of using commercial electrical, electronic, and electromechanical parts in space-based architectures. These complex architectures rely on highly integrated electronics that provide state-of-the-art functionality, but commercial components having high levels of functionality are potentially more susceptible to radiation that can result in single event upsets that may or may not be recoverable. Because the impact of single event effects (SEEs) to system reliability are not always accounted for in analyses, this Technical Bulletin relays the best practices learned from NESC assessments to mitigate the effects of SEEs. The goal is to help the NASA avionics community better prioritize radiation testing to areas that will have the greatest impact on reliability.



No. 19-02 - 90/95 POD Radiography Concern for COPVs and Metal Tank Welds ..... page 30

Inspecting all-metal tanks and composite overwrapped pressure vessels using radiography presents significant challenges, particularly when inspecting for cracks in the tank welds. Recent evaluations performed by Nondestructive Evaluation experts at Johnson Space Center found that X-rays, which must penetrate two-wall thicknesses of a welded tank, cannot guarantee detection of a crack with the same level of reliability demonstrated in the typical single-wall test. This lack of visibility into the weld cracks can mean fracture risk is not fully understood. This Technical Bulletin aims to highlight that risk and suggests methods to better understand it until further research can determine more effective techniques for evaluating damage tolerance on these tanks.



No. 20-01 - Latching Safety Critical Signals in Pyrotechnic Circuits ..... page 31

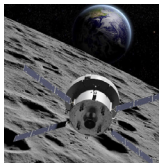
When a shock test of safety-critical pyrotechnic circuits resulted in an inadvertent firing, it revealed a sensitivity to electrical noise in the latching circuits, which store the state-of-control signals in pyro control circuitry. This technical bulletin, developed by Dr. Robert Hodson, NASA Technical Fellow for Avionics, recommends enhancements to recent designs of these circuits that would reduce this sensitivity and the susceptibility of the circuit to unintentional firing. These best practices offer simple improvements such as qualifying data signals and adding filters to the design of these critical circuits that are vital to the safe operation of spacecraft.



No. 20-02 - Effective and Environmentally Compliant Cleaner - Solstice Performance Fluid ..... page 32

Historically, NASA has used Hydrochlorofluorocarbon-225 (HCFC-225 or AK-225) solvent to clean and verify propulsion systems that use liquid and gaseous oxygen, but when the EPA implemented restrictions regarding its use, NASA began efforts to find an acceptable replacement. This Technical Bulletin highlights the cleaning capabilities and compatibility of alternative fluids, Honeywell's Solstice® Performance Fluid (PF), PF-high purity (HP), and PF-HP spray, that may be used in a variety of cleaning applications. The bulletin is provided by Mr. Steven Gentz, NESC Chief Engineer at Marshall Space Flight Center, who through NESC assessments, supported the Agency's initiative to identify and test alternatives to AK-225.

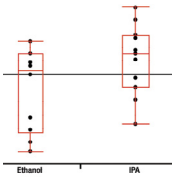
TABLE OF CONTENTS



No. 20-03 - Navigation Filter Design Best Practices..... page 33
This Technical Bulletin introduces a new handbook that aggregates NASA's extensive knowledge base on navigation estimation systems and filters, which are used extensively throughout the Agency on both crewed and uncrewed missions. Targeted to mission designers, the handbook provides a comprehensive reference to NASA's best practices for navigation filter designs, which have safely and reliably supported missions since the Gemini/Apollo era. The handbook's development was, in part, an outgrowth of an NESC assessment of best practices for rendezvous navigation filter design, led by the NASA Technical Fellow for Guidance, Navigation, and Control, Mr. Neil Dennehy.



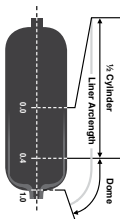
No. 20-04 - Alternative O-Rings for Hypergolic Propellant Systems ..... page 34
The commercial company Parker-Hannifin has stopped production of O-rings using the material E0515. NASA programs such as the Multi-Purpose Crew Vehicle, the Commercial Crew Program, Mars 2020, the Europa Clipper, and the International Space Station have used O-rings made of this material to seal high pressure lines that contain liquid engine propellants and gases. As NASA reserves of the E0515 O-rings will soon be depleted, Dr. Daniel Dorney, NASA Technical Fellow for Propulsion, led an NESC assessment team that tested potential replacement candidates. This Technical Bulletin provides the results of that testing as well as recommendations for replacement O-rings that are compatible with hypergolic propellant applications.



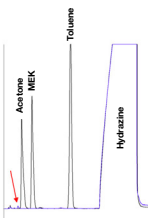
No. 20-05 - Determination of Autogenous Ignition Temperature of Isopropyl Alcohol and Ethanol..... page 35
Following a liquid rocket engine shutdown investigation, NASA was requested to provide any available data on the autoignition temperature (AIT) of isopropyl alcohol (IPA) in a pressurized, gaseous oxygen environment. IPA is commonly used as a solvent or cleaner in launch vehicle and spacecraft propulsion systems. When the data was found to be focused primarily on air and for much lower pressures than needed, the NASA Technical Fellow for Propulsion, Dr. Daniel Dorney, led an NESC assessment to determine the AIT of IPA, as well as ethanol, in the required conditions. The new data was provided to interested programs and projects across NASA and industry. This Technical Bulletin summarizes those findings.



No. 20-06 - Material Compatibility Assessment of Spacecraft Oxidizer Systems..... page 36
After recognition that an ignition vulnerability existed between certain materials and oxidizers used in spacecraft propulsion, the NESC researched ignition mechanisms to better understand the potential risk to NASA and industry. An assessment focused on the flammability/ignition behavior of titanium and oxidizers such as nitrogen tetroxide but revealed that other metals may also be susceptible. While the oxidizer compatibility assessment process is on-going, this technical bulletin discusses the immediate steps NASA is taking to mitigate this risk until these ignition mechanisms are fully understood and thresholds and operating envelopes can be determined.

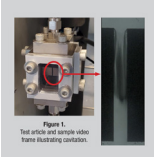


No. 20-07 - Evaluating and Mitigating Liner Strain Spikes in COPVs..... page 37
Based on NESC analysis of cracks and leaks that occurred in flight Composite Overwrapped Pressure Vessels (COPVs), a failure mode due to liner strain spikes was observed through measurement and predicted by analysis. The failure mode may be present in COPVs used on NASA programs and by the aerospace industry. This technical bulletin was developed to alert manufacturers and the user community to this failure mode and contains approaches to evaluate COPVs for susceptibility to this failure mode.



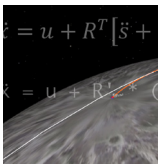
No. 20-08 - Assessment of Ketazine Derived High Purity Hydrazine for Spacecraft Propellant Systems..... page 38
Hydrazine and its derivatives have dominated the class of hypergolic liquid propellants for bipropellant propulsion systems, and is used as a monopropellant in auxiliary power units and thrusters. With continued use of hydrazine in current and future spacecraft and payloads, it is necessary to understand the historical and current states of synthesis for the commodity and possible purity implications that may arise from changes in production processes for the United States stock. This technical bulletin describes these issues in detail.

TABLE OF CONTENTS



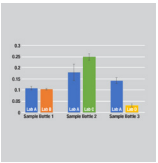
No. 21-01 - Experimental and Computational Study of Cavitation in Hydrogen Peroxide ..... page 39

Cavitation in liquid propulsion systems can lead to performance degradation and hardware failures. The NESC sponsored an investigation to measure and model cavitation in pressurized hydrogen peroxide flow. The experimentally measured and computationally predicted cavitation lengths were compared as a function of cavitation number. The measured and predicted data exhibited close agreement over the range of pressures and temperatures studied, and no calibration of the cavitation model coefficients was needed.



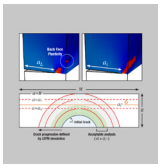
No. 21-02 - Genesis Flight Mechanics Simulation ..... page 40

The NASA Engineering and Safety Center (NESC) consolidated and modernized a suite of legacy flight mechanics simulations, including the Flight Analysis and Simulation Tool (FAST), resulting in Genesis, a generic, multi-vehicle, variable-degree-of-freedom flight mechanics simulation for ascent, aerocapture, entry, descent, and landing (A2EDL) trajectory design.



No. 21-03-1 - Best Practices for the Elemental Profiling of High-Purity Hydrazine ..... page 41

Trace contaminants in high-purity hydrazine (HPH) propellant impact a wide variety of commercial, Department of Defense (DoD), and NASA missions. Depending on thruster design, elemental contaminants must be kept at extremely low levels and are verified as such by routine analysis. A number of these contaminants have recently undergone an assessment to shed light on their quantities present following changes in the HPH supply chain. A round robin analysis utilizing four separate laboratories resulted in unacceptably high variability in the quantification of these contaminants. The principal objective of this technical bulletin is to signal the availability of a new analysis methodology which yields accurate and repeatable quantification by providing best practices for both quantitation methodology and strategies for avoiding sample contamination during analysis.



No. 21-04 - Evaluating Appropriateness of LEFM Tools for COPV and Metal Pressure Vessel Damage Tolerance Life Verification ..... page 42

Human spaceflight composite overwrapped pressure vessels (COPVs) and metal pressure vessels can use linear elastic fracture mechanics (LEFM) analysis to demonstrate damage tolerance life in some cases per ANSI/AIAA-S-081 for COPVs and ANSI/AIAA-S-080 for metal pressure vessels. LEFM analysis assumptions require that the crack tip plastic zone is small relative to the crack size and is completely surrounded by elastically responding material. Test and analysis have shown that LEFM tools (e.g., NASGRO*) can provide unconservative crack growth predictions for cracks in COPV liners that violate LEFM assumptions. COPV and metal pressure vessel designers should evaluate and address the violation of LEFM plasticity assumptions before using LEFM analysis tools for damage tolerance life verification.



No. 21-05 - Industry Recommendations from Arecibo Observatory Zinc Spelter Socket Joint Failure Analysis ..... page 43

A structural analysis and forensic investigation concluded that the Arecibo Observatory M4N socket joint failure in August 2020 was primarily due to cumulative damage caused by initially low structural design margins and a high percentage of sustained load, resulting in zinc creep deformation, progressive internal socket wire damage, and eventual loss of joint capacity. Open spelter sockets of this type are used throughout industry in stay cables. Recommendations are proposed to prevent failures of similar socket joints, including verification of positive stress margins in socket joint wires for all failure modes, periodic visual inspections with pass/fail criteria for zinc extrusion that are tied to structural qualification, and revisiting codes/industry standards to capture lessons learned.



No. 22-01 - Detecting Flow-Induced Vibration in Bellows ..... page 44

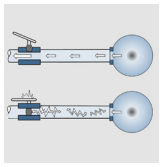
The NESC performed testing to determine if high-speed video techniques can be used to predict the onset of flow-induced vibrations (FIV) in bellows. A comprehensive test matrix was established to determine if Motion Magnification (MM) and Digital Image Correlation (DIC) can be used to determine the onset of FIV in straight and gimbaled bellows. Several of the tests were intended to determine if MM and DIC can establish the resonant frequencies of the bellows with no a priori knowledge. The results of the MM and DIC were compared with data from strain gages and microphones. Although the testing was limited to one single-ply unshielded bellows, this effort provided the proof-of-concept that MM and DIC are feasible methods for determining the onset of FIV in bellows.

TABLE OF CONTENTS



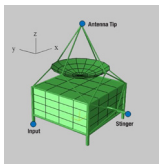
No. 22-02 - Revisiting Filtration Standards and Definitions for Spaceflight Propulsion and Pressurant Systems..... page 45

The NESC performed an assessment of existing filtration standards and guidance documents for propellant and pressurant systems. The assessment included a vendor survey to better understand concerns about filtration systems, defined a common set of filtration and contamination-related terms, and developed guidelines for system filtration design and implementation.



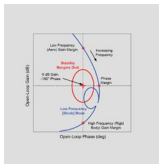
No. 22-03 - Treatment of Transient Pressure Events in Space Flight Pressurized Systems ..... page 46

Analytical and experimental evidence shows that fast-moving dynamic pressure fluctuations caused by valve actuation, fluid-system priming, fluid discharge, vibration, and flow disturbances can elicit adverse structural response and must be considered in the space flight pressure system design and verification process.



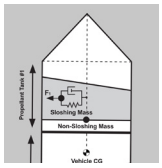
No. 22-04 - Uncertainty Quantification of Reduced Order Structural Dynamic Models..... page 47

Uncertainty quantification (UQ) provides statistical bounds on prediction accuracy based on finite element model (FEM) uncertainty. An alternate method for UQ, called the Hybrid Parametric Variation (HPV) combines a parametric variation of the Hurty/Craig-Bampton (HCB) fixed-interface (FI) modal frequencies with a non-parametric variation (NPV) method. This provides a UQ method that can be traced to test data, which can be updated as additional data and improved correlated models become available.



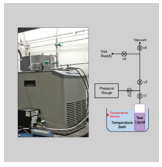
No. 22-05 - Launch Vehicle Flight Control Stability Margin Reduction Considerations..... page 48

Launch vehicle ascent stability analyses typically rely on a combination of frequency and time domain analyses. Frequency domain analysis uses a sequence of high-fidelity linear models with constant parameters spanning the ascent trajectory. Complementary time domain analysis is performed using high-fidelity, nonlinear 6-DOF simulations. Analyses are typically dispersed to verify robustness to parameter variations by showing the vehicle meets frequency domain stability margin requirements and time domain performance metrics. This Technical Bulletin outlines standard stability margin best practices and provides recommendations for treatment of deviations from industry-standard launch vehicle stability margins due to vehicle flexibility, slosh dynamics, aerodynamics, other offending dynamics, or coupling thereof.



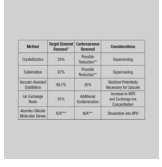
No. 22-06 - Treatment of Slosh Stability Margin Reductions for Human-Rated Launch Vehicles ..... page 49

Slosh dynamics pose a stability concern for human-rated launch vehicles during ascent. Historical perspectives on the treatment of slosh dynamics, newly developed rules of thumb, the utility of flight data, and methods for analyzing and dispositioning slosh instability risks should be considered when linear stability margins are lower than typically accepted for human-rated systems.



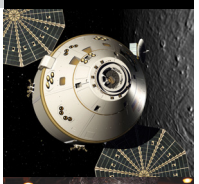
No. 22-07 - Helium Solubility in MMH and NTO ..... page 50

A test program to characterize the solution of helium in nitrogen tetroxide/mixed oxides of nitrogen (NTO)/(MON) and monomethylhydrazine (MMH) at anticipated flight-representative pressures/temperatures was completed. Updated relations for helium solubility in MMH and NTO were generated and documented.



No. 22-08 - Contaminant Reduction in High Purity Hydrazine ..... page 51

Hydrazine and its derivatives are used ubiquitously in liquid propulsion systems. In smaller thruster systems, contaminant build up has historically caused flow decay and consequently performance losses. Many of these contaminants are not controlled by the current revision of MIL-PRF-26536 [1], the High Purity Hydrazine (HPH) procurement specification, yet have been observed to be present in HPH at variable concentration and, often exceed potentially problematic levels for small thrusters. This technical bulletin outlines recent work aimed at identifying appropriate separation processes to remove specific target elemental and carbonaceous contamination in HPH.









Braycote™ Grease retains tribological properties for 17 years in controlled storage

Braycote™ greases that are in mechanisms in controlled storage retain their tribological properties for an extended period of time. Testing on aged and separated Braycote™ grease obtained from several sources showed no detrimental effect on lubricity. Additionally, Thermal Gravimetric Analysis testing demonstrated no significant decrease in performance due to static, controlled storage. Tribological action, heat, or other forces are required to effect the performance of Braycote™ grease.

Applicability

Braycote™ 601 grease on space flight and ground system mechanisms

Background

A scheduled inspection of the Rudder/Speed Brake actuators on Space Shuttle orbiter OV-103 revealed fretting corrosion, micropitting, wear and discoloration of the lubricant Braycote™ 601. A decision was made to replace the actuators with the existing spares, a single ship set which had been in controlled storage for the past 17 years. Data did not exist on the lubricity of Braycote™ 601 grease after extended storage.

Data and Analysis

Testing and analysis were undertaken to investigate two key issues:

Issue 1: Oil separation of grease into its component oil and thickener is known to occur in storage. Its effect on lubricity is not known.

Results: Lubricity testing was performed on aged grease, and grease that exhibited oil separation obtained from several sources, including grease that had been removed from the OV-103 actuators. Three test protocols were used: (1) Falex Block on Ring; (2) Spiral Orbit Tribometer (SOT); and (3) Wedeven Associates Machine (WAM) testing. In all cases, no detrimental effect on lubricity was observed due to storage and/or grease that experienced oil separation.

Issue 2: Chemical reactions involving the grease and the gear/housing material, 9310 steel, could lead to formation of Lewis acids, resulting in corrosion, pitting, and cracking. The degree to which the chemical reactions were occurring in the actuators was unknown.

Results: Investigations into potential chemical reactions of the grease with the actuator steel were addressed in three ways: (1) an extensive literature review; (2) WAM testing to duplicate the conditions observed in the used actuators; and (3) Thermodynamic analysis, using Thermal Gravimetric Analysis (TGA), to bound the amount of degradation/mass loss that might occur during 17 years of controlled storage. The literature review revealed that absent tribological action, i.e., no stress on the lubricant, no significant mass loss should occur below 190ºC. The WAM testing was successful in duplicating the fretting corrosion and micropitting effects observed on OV-103 by high frequency low amplitude wear testing, thus reinforcing the results reported in the literature for similar material/lubricant combinations. The TGA testing and thermodynamic analysis predicted no significant corrosive effects from static, controlled storage for 17 years.



NASA

White Braycote™ grease on top of a used actuator gear. The discoloration present on the gear surfaces is normal for Braycote™ grease in contact with steel.

References

Orbiter Rudder Speed Brake Actuator Braycote™ Grease Independent Technical Assessment/Inspection (ITA/I) Report, NESC RP04-03/03-003-E, May 2004

This work was led by Dr. Paul Munafo, Marshall Space Flight Center

For further information contact the NESC at www.nesc.gov

NESC tech bulletin

Failure of Pyrotechnic Operated Valves with Dual Initiators

Investigation of recent pyrovalve failures reveals timing of redundant initiator firings is crucial for reliable operation of pyrovalves. Simultaneous firing, i.e., within a very narrow time frame, was found to be the primary cause of the valve failing to operate. Testing of both single and dual initiators revealed important design characteristics affecting pyrovalve device performance. They include Primer Chamber Assembly (PCA) geometry and material properties, as well as operational effects on combustion product flow, and resulting energy transfer to the booster.

The CONAX PCA design has evolved slowly over time undergoing incremental changes to correct known issues. These piecewise changes were verified by limited test, without a full understanding of the overall system impact or effect on margins. Adequate system performance margins may be adversely affected in existing or future systems incorporating a pyrovalve actuated by simultaneous firing of dual initiators.

Applicability

Pyrovalves are used frequently in propulsion systems built by NASA and industry.

Background

Four spacecraft propulsion system pyrovalve "no-fire" failures were recently investigated by the NESC (NASA Engineering and Safety Center). In all four cases, a normally-closed pyrovalve failed to actuate during tests in which simultaneous firing of dual initiators failed to ignite the booster charge. In each failure, a common aluminum Y-shaped PCA (Y-PCA) manufactured by CONAX was used to mechanically accommodate the two initiators and to direct the individual output products of each initiator towards the booster charge. Booster charge ignition is intended to generate sufficient pressure to actuate the pyrovalve.

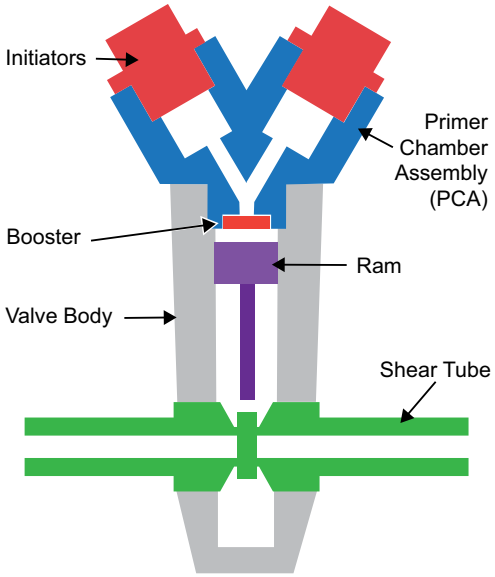
Findings and Conclusions

The primary finding from this investigation is that dual simultaneous firing (< 10 microseconds skew) is not as robust as a single firing and should be avoided. When close sequential firing of the redundant initiator is necessary, the NESC recommends the skew time between initiator firings should ideally be longer than the flow duration for single fire. Thus the NESC recommendation that use of the device should be constrained to single fire operation (or dual with skew greater than 2 milliseconds) to ensure robustness of booster ignition.

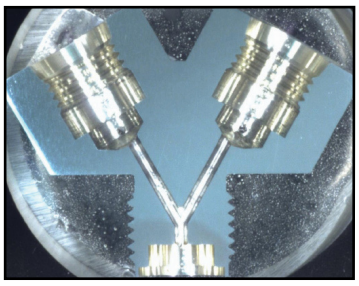
The NESC has forwarded this finding, and others related to critical PCA parameters and device qualification issues, to projects using the current design. In addition, the NESC contributed to a new stainless steel PCA design activity initiated by the Mars Science Laboratory project. Recommendations outlining other follow-on tasks have been communicated to the NASA Pyrotechnic Working Group.

References

CONAX Y-PCA Booster Anomaly Investigation Report, NESC Document Number RP-08-111, NASA Technical Memorandum (TM) Number TM-2008-215548



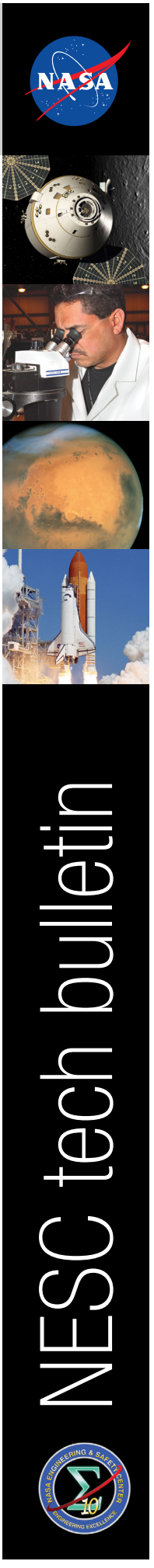
A normally closed pyrovalve



Unfired PCA sectioned at midline

This work was led by Michael Hagopian, Goddard Space Flight Center, and Andreas Dibbern, Kennedy Space Center.

For information contact the NESC at www.nesc.nasa.gov



NESC tech bulletin

Limitations of Internal Protective Devices in High-Voltage/High-Capacity Batteries Using Lithium-Ion Cylindrical Commercial Cells

Most commercial cylindrical 18650 Lithium-Ion (Li-Ion) cells have two internal protective devices: the Positive Temperature Coefficient (PTC) and the Current Interrupt Device (CID). The PTC protects the cells under external short conditions and the CID protects the cells under overcharge conditions. While proven to be effective at the single cell and small-size battery levels, these devices do not always offer protection when used in high-voltage and high-capacity battery designs.

Applicability

This information is applicable to those considering the use of Li-Ion batteries comprised of cells with PTC and CID internal protective devices.

Background

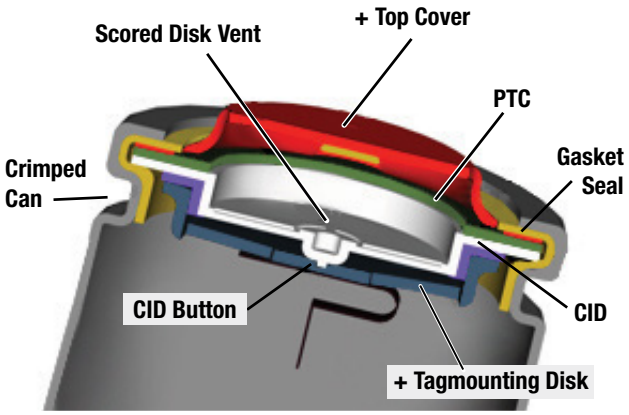
The internal protective devices (PTC and CID) used in the most common commercial-off-the-shelf (COTS) Li-Ion cells (cylindrical 18650's) have been extremely reliable at a single-cell level and have resulted in total prevention of the cell reaching a hazardous condition. However, test programs have indicated that batteries built with cylindrical COTS cells in multi-cell configurations (series and/or parallel) have experienced thermal runaway under various test conditions. Test data analysis indicated that the two major causes for the thermal runaway are overvoltage (overcharge) and external short conditions.

In these cases, the internal protective devices were either not protecting as expected or were a cause for the hazards encountered. PTC ignition above its withstanding (threshold) voltage has been shown to cause thermal runaway under external short conditions in high-voltage battery modules. Thermal runaway has also been observed during overcharge conditions in high-voltage and high-capacity modules, indicating that the CIDs did not protect the cells from catastrophic events, as seen in single cells. The NESC-sponsored study was conducted to understand the causes for the thermal runaway in high-voltage and high-capacity battery modules, and to determine the limitations of the cell internal protective devices.

Data and Analysis

PTC characteristics and limitations vary with cell manufacturer and are rarely provided. This information should be obtained by testing prior to considering a battery design for a specific application. The cell series voltage should not exceed the PTC withstanding voltage. For high-voltage batteries, diodes added to a series string of cells can improve their safety under external short conditions. The diodes must be carefully matched to battery characteristics.

In high-voltage and high-capacity batteries where the CID is used as a level of safety control, overcharge tests need to be performed to confirm its safe operation. The number of cells recommended for use in parallel depends on the charge current. The total charge current used to charge a bank (cells in parallel) should in no way cause an increase in PTC resistance of any single cell. In other words, in the event that all cell CIDs but one have opened, the current seen by the remaining cell should not cause an increase in PTC resistance. The CID voltage tolerance should also be characterized. The charger voltage limit should be set so that the difference between the voltage limit value and the end-of-charge battery voltage does not cause CID arcing. The main causes of failure that prevent the CID from proper safing are the charge current (causing inadvertent PTC activation), high temperatures (causing PTC activation or uncontrollable thermal runaway), and high voltages (causing PTC ignition).



Cross-Section of a Typical 18650 Cylindrical Li-Ion cell showing the PTC (in green) and CID (in white)

References

NASA Aerospace Flight Battery Program Year 1 Report – Part 1, Volumes 1 and 2, Generic Safety, Handling and Qualification Guidelines for Lithium-Ion (Li-Ion) Batteries, Li-Ion Batteries, Maintaining Technical Communications Related to Aerospace Batteries (NASA Aerospace Battery Workshop), NESC Document Number RP-08-75.

This work was led by Judith Jeevarajan, NASA Johnson Space Center, and Michelle Manzo, NASA Glenn Research Center.

For information contact the NESC at www.nesc.nasa.gov



NESC tech bulletin

Data Base and Guidelines Document Developed for Lithium-Ion Battery

Lithium-Ion (Li-Ion) batteries are fast becoming the battery chemistry of choice for aerospace applications requiring (rechargeable) power supplies. These batteries offer high-energy density and high-specific energy combined with excellent rate capability and cycle potential. The increased energy content and operational characteristics of this system require defined safety and handling procedures to ensure the safe implementation. Standardized approaches to defining, determining, and addressing safety, handling, and qualification for Li-Ion batteries have been developed and published as an NESC-sponsored Li-Ion Battery Guidelines Document. A data base was established cataloging cells and batteries that have been considered for aerospace applications.

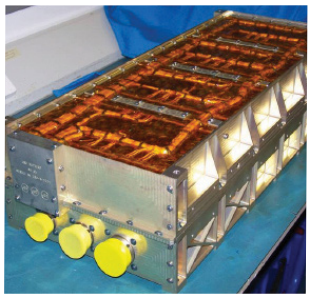
Applicability

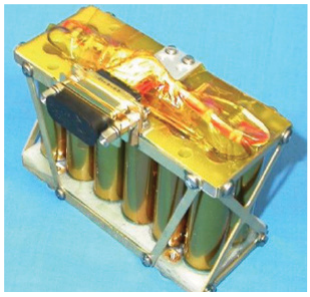
These resources are applicable to missions and applications considering the use of Li-Ion batteries in the energy storage subsystem.

Background

Li-Ion batteries are an attractive alternative to traditional alkaline-based battery systems. They offer reduced weight and volume and additional rate capability over the nickel-cadmium (Ni-Cd), nickel-hydrogen (Ni-H2) and silver-zinc (Ag-Zn) battery systems they will replace.

To be considered for aerospace mission applications, Li-Ion batteries must meet stringent safety and performance requirements. These considerations have been defined in documents from various sources that address safety, use, issues, qualification, and testing of aerospace Li-Ion batteries. To facilitate and ensure the safe implementation of this technology, important guidelines and recommendations were compiled, and then revised and enhanced in the NESC-sponsored Li-Ion Battery Guidelines Document.





Li-Ion batteries flown on NASA Missions: Mars Exploration, Rover, and the Lunar Reconnaissance Orbiter.

To date, cells and batteries from several manufacturers have been qualified for use in specific aerospace mission applications. A survey was also conducted (both within and outside the United States) on existing Li-Ion battery manufacturers' capabilities to meet future NASA mission needs.

Li-Ion Battery Database

A Microsoft® Excel®-based database of Li-Ion batteries and cells appropriate for aerospace applications was established. The database describes the performance of cells and batteries along with the reported testing that they have undergone (either at the manufacturer or by other government agencies). The database includes batteries and cells appropriate for multiple NASA mission needs including: Low Earth Orbit (LEO), Geostationary Orbit (GEO), and the Constellation Program. Additionally, the database contains commercial-off-the-shelf cells and batteries.

Li-Ion Guidelines Document

The Li-Ion Guidelines Document addresses the issues and concerns associated with the use of Li-Ion chemistries resulting from their inherent high-specific energy combined with flammable electrolytes.

The guidelines document provides background on the technology; basic operational information discussing the electrochemical reactions that take place within the cells; a summary of factors that affect battery performance; battery design considerations; cell and battery hazards and controls; battery requirements; cell and battery handling and procedures; typical Li-Ion cell and battery test procedures; and definitions. A listing of references that provide more detail on program-specific requirements is also included.

It is recommended that all users considering this technology for space applications, especially for applications involving humans, consult this document for guidance prior to implementation due to the extreme importance of appropriate design, test, and hazard control of Li-Ion batteries.

References

NASA Aerospace Flight Battery Program Year 1 Report – Part 1, Volumes 1 and 2, Generic Safety, Handling and Qualification Guidelines for Lithium-Ion (Li-Ion) Batteries, Li-Ion Batteries, Maintaining Technical Communications Related to Aerospace Batteries (NASA Aerospace Battery Workshop), NESC Document Number RP-08-75.

This work was led by Michelle Manzo, Barbara McKissock, NASA Glenn Research Center, and Paul Schmitz, PCS/NASA Glenn Research Center.

For information contact the NESC at www.nesc.nasa.gov

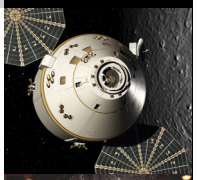








NESC tech bulletin









Capability Demonstrations for Penetrant Nondestructive Evaluation (NDE) of Metallic Tanks and Composite Overwrapped Pressure Vessel (COPV) Liners

As the desired crack detection size is decreased and approaches the physical limitations of liquid penetrant inspection techniques, the approach of performing a probability of detection (POD) validation test at a single aspect ratio, and then extending the results to other aspect ratios based on equivalent area predictions may not be valid. POD testing for penetrant inspection of metallic pressure vessels and COPV liners should be performed at the bounds of the required range of crack aspect ratios.

Applicability

Penetrant NDE of metallic aerospace pressure vessels and COPV liners.

Background

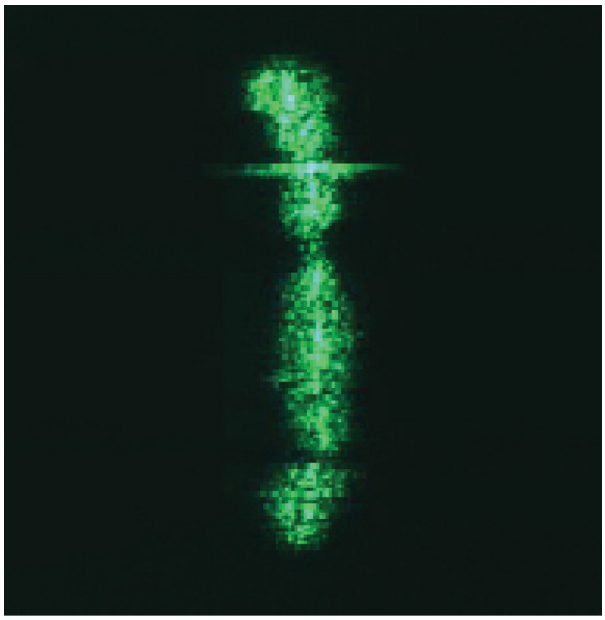
To minimize mass, designers of aerospace systems are reducing the wall thickness for metallic pressure vessels, such as the Mars Science Laboratory (MSL) propellant tank and COPV liners that will be used in future Constellation Program vehicles. This reduction in wall thickness produces higher net section stresses, for a given internal pressure, resulting in smaller critical initial flaw size (CIFS). These smaller crack sizes are approaching the limitations of penetrant NDE. Failure to adequately demonstrate the capabilities of penetrant inspection methods over the required range of crack aspect ratios may lead to the failure to detect a critical flaw resulting in a catastrophic tank failure.

Data and Analysis

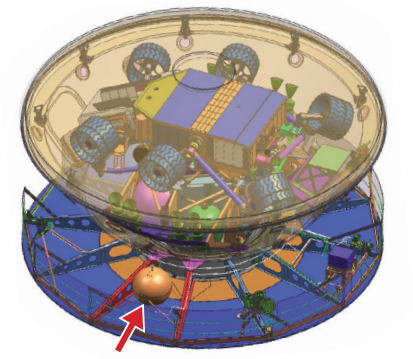
The current standards governing aerospace metallic pressure vessels (AIAA S-080) and COPV liners (AIAA S-081) require that fracture analysis be performed to determine the CIFS for cracks having an aspect ratio ranging from 0.1 to 0.5. They further require that NDE methods have a demonstrated capability of 90 percent probability of detection with a 95 percent confidence (90/95 POD) for the CIFS determined by this analysis. Previously, NASA demonstrated this capability by testing at only a single aspect ratio and then used an equivalent area approach to extend the results to the required range of aspect ratios. However, there is insufficient data to support this approach and it may break down for smaller CIFS. Testing is needed to demonstrate the capability of penetrant inspection for smaller CIFS over the full aspect ratio range, or it may be necessary to demonstrate and implement alternative inspection techniques.

References

AIAA S-080 - Space Systems Metallic Pressure Vessels, Pressurized Structures, and Pressure Components; AIAA S-081 - Space Systems Composite Overwrapped Pressure Vessels (COPVs); NASA-STD-5009 – Nondestructive Evaluation Requirements for Fracture-Critical Metallic Components; Orbiter Fracture Control Program



Penetrant Indication for Tightly Closed (0.088 inch) Fatigue Crack



MSL Cruise Stage Propellant Tank

For information contact the NESC at www.nesc.nasa.gov

NESC tech bulletin









Self-Contained Oxygen Generator: Effects of Organic Contamination, Briquette Fracturing, Pressure Containment, and Variations in Chemical Composition

A Self-Contained Oxygen Generator (SCOG) produces breathable oxygen (O_2) by using chemically-reactive briquettes that begin producing O_2 when mechanically ignited. Contamination with organic material of, or manufacturing defects in, the briquettes have been shown to lead to conditions that can cause an explosive failure

Applicability

This information is applicable to military and aerospace SCOGs.

Background

SCOG failures were recently investigated by the NASA Engineering and Safety Center (NESC) as a result of an SCOG explosion aboard the United Kingdom's Royal Navy submarine *HMS Tireless*. The root cause identified during this investigation was contamination of the internal briquette. When the briquette is contaminated, it can result in a runaway pressure event, which can lead to an SCOG explosion.

Findings and Conclusions

Liquid organic (oil) contamination can cause excessive heating and an increased burn rate in SCOGs. Contamination also contributes to an accelerated pressure increase, which does not allow the containment system to vent the accelerated pressure increase effectively.

A history of overheating and faster burn rate areas attributed to uneven mixing of the chemicals in the briquette was identified in SCOGs. The chemical mixture in the briquette contains iron filings that act as an accelerant for the SCOG reaction. When the iron is not uniformly distributed in the briquette mixture, the result will be locally enriched "hot spots" with faster burn rates.

An additional area of concern with the design of the SCOG containment system was identified. Systems that have an undersized venting mechanism could fail as a result of pressure runaway. This pressure runaway is caused when the gas is generated in the SCOG faster than it can be vented from the containment system.

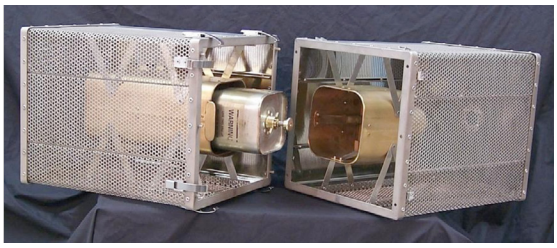
Corrective actions were identified for the safe operation of SCOGs, one of which was to prevent organic material/fuel contamination. Contamination should be prevented by maintaining the briquette seals and storing away from organic materials. The briquette should be tested for uneven mixing of iron additives. Another corrective action was to design the containment system in a manner that allows the pressure to escape during the chemical reaction. There are a variety of possibilities for the containment system for a SCOG. The United States Navy uses an open containment system for their SCOGs and this system has been working successfully.

Reference

Self-Contained Oxygen Generator Safety Assessment: Effects of Organics Contamination, Briquette Fracturing, Pressure Containment and Variations in Chemical Composition. NESC Assessment Number: 07-051-E, October 2008

WSTF-IR-1120-001-08 Self-contained Oxygen Generator Investigation, Analysis and Testing

This work was led by Henry Rotter and John Graf, Johnson Space Flight Center, and by Jon Haas, White Sands Test Facility.



Space Station Backup Oxygen Candle System (4" x 4" square candle)





(Far left) Test cell candle initiation in 8' x 8' test cell with Lexan flexible sheets

(Left) Duplication of explosion on the Royal Navy submarine (Note: destroyed Lexan sheets)

For information contact the NESC at www.nesc.nasa.gov

NESC tech bulletin

Power MOSFET Thermal Instability

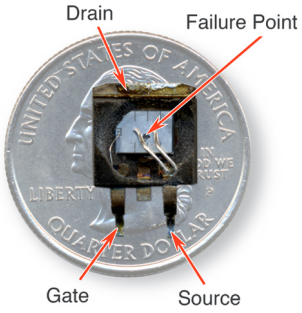
In the quest for faster switching times and lower "on resistance" the Metal-Oxide Semiconductor Field-Effect Transistor (MOSFET), produced since 1998, has achieved most intended goals. Unfortunately, lower "on resistance" and higher switching speeds in the designs now being produced allow the charge carrier dominated region to develop conditions that could lead to thermal runaway. Temperatures above 450º C on any location within the part can cause the metals to begin migrating causing a fatal short circuit.

Applicability

Any power MOSFET that is used with a low gate voltage (not switched mode) for periods of time greater than 10 microseconds. The problem is more pronounced with parts produced since 1998.

Background

Based on recent testing and failure investigations, it appears that the "old" manufacturer application curves are inaccurate with regard to application of some MOSFET parts. These parts may be used extensively in flight hardware and ground support equipment.



Failed Field-Effect Transistor

The push for faster switching and lower "on resistance" power MOSFETs resulted in an unintended consequence similar to the secondary voltage breakdown effect that has not been seen since the prime of the bipolar transistor. When MOSFETs are in the charge carrier dominated region (low gate to source voltage, Vgs) the device allows more current to flow as the temperature increases causing a thermal runaway. It was discovered that the safe operating area (SOA) curves provided by the manufacturers were lacking in describing the region of thermal instability. The problem was identified during a test of a protection circuit that provided a low voltage on the gate of a MOSFET, which failed within seconds. The MOSFET was replaced and a new corrected test was performed. The outcome of the second test was the failure of the second MOSFET. Examination of the de-lidded part revealed a "bulls-eye" heating pattern and aluminum spheres. The failure mode for the two MOSFETs was determined to be common and was the result of the MOSFETs being placed in a thermal runaway condition when the gate voltage was low, but well within the SOA for the MOSFET. This problem, known as "thermal instability" in the industry, has been experienced in the automotive industry since 1997 when advanced, very fast, switching MOSFET devices became available and found wide usage.

MOSFET Failures inside the Advertised SOA

Thermal runaway is a problem affecting a wide range of modern MOSFETs from more than one manufacturer. Older parts can also display thermal runaway, usually well outside the SOA.

Therefore, one may experience other problems first with those older parts. Thermal runaway is caused at low gate to source voltages when the drain current increases at higher temperatures causing a positive feedback effect. Thermal runaway is currently over a larger area of the Vds-Id plane and inside the advertised SOA. The recommended new limit for the SOA can be determined using the Spirito stability formula where Stability (S) is less than one. When S equals one, the calculated temperature approaches an infinite value theoretically. A proper derating is necessary to bring the temperature down to a value below the MOSFET failure temperature. As found in testing, the leakage current of a MOSFET starts to become uncontrollable at about 250º C, so the standard temperature limit of 175º C is recommended. However, the dynamic temperature at the hottest point within the device must be constrained to safe limits.

References

1) IRF510 Data Sheet: 5.6A, 100V, 0.540 Ohm, N-Channel Power MOSFET'; Fairchild Semiconductor; January 2002.

2) Marie Denison, Martin Pfost, Klaus-Willi Pieper, Stefan Märkl, Dieter Metzner, Matthias Stecher; Influence of Inhomogeneous Current Distribution on the Thermal SOA of Integrated DMOS Transistors; Proceedings of 2004 International Symposium on Power Semiconductor Devices & ICs; Kitakyushu; pp. 409–412.

3) P.L.Hower and P.K.Govil; IEEE Transactions on Electron Devices; Volume ED-21, Number 10; October 1974, pp. 617–623.

4) P. Spirito, G. Breglio, V. d'Alessandro, N. Rinaldi; Analytical Model for Thermal Instability Of Low Voltage Power MOS and S.O.A. In Pulse Operation; 14th International Symposium on Power Semiconductor Devices & ICS; Santa Fe, NM; 4–7 June 2002; pp. 269–272.

For information contact the NESC at: www.nesc.nasa.gov









NESC tech bulletin









Potential Failure of Dual Simultaneously Initiated Pyrotechnic Operated Valves

The NASA Engineering and Safety Center (NESC) Technical Bulletin No. 09-01 reported an independent investigation of four pyrovalve failures that occurred while using aluminum (Al) pyrovalve primer chamber assemblies (PCAs) during ground testing. The investigation revealed that simultaneous firing (within a few microseconds) of the NASA Standard Initiators (NSIs) was the primary reason why the booster charge failed to ignite and the pyrovalves subsequently failed to operate. A second investigation of a new stainless steel (SS) PCA design with separate flame channels was completed in 2010. The new SS configuration was found to be improved in most respects; however, no improvement was noted in the temperature delivered to ignite the booster during dual simultaneous NSI firings. Simultaneous firings should be avoided when using either the Al or the SS PCA design.

Applicability

NASA and industry frequently use pyrovalves in propulsion systems and other types of applications.

Background

In 2008, the NESC investigated four instances when normally closed pyrovalves did not actuate after simultaneous firing of dual NSIs failed to ignite the booster charge. In each anomaly, an Al PCA with NSI flame channels in a Y configuration (Y-PCA) was used to direct the output energy to the booster charge. The booster charge generates most of the force to actuate the ram and open the pyrovalve. Based on assessment findings that the Al PCA channels eroded during firings, reducing energy for booster initiation, and that the "Y" flow passage had potential flow issues, the Mars Science Laboratory propulsion system team chose a new SS PCA with independent V-shaped flow passages (see figure). The NESC conducted an additional independent assessment to compare the booster interface temperature for the two configurations and quantify the improvements.

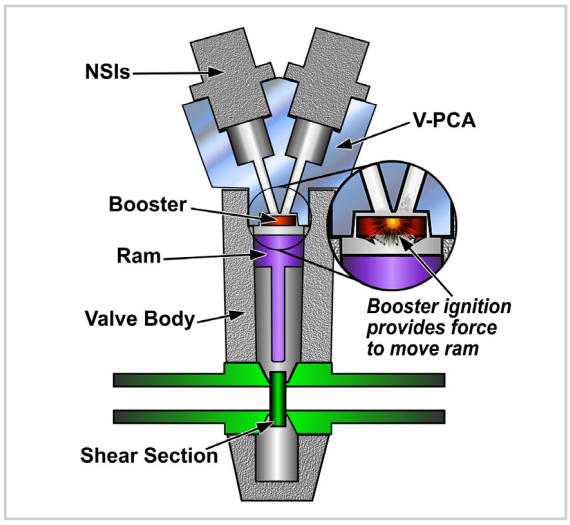


Diagram of a Normally Closed (NC) Pyrovalve Block

Findings and Conclusions

Based on testing to date, the SS V-PCA produced an average temperature of 2300°F at the booster interface versus 1400°F for the legacy Al Y-PCA during a single initiator firing indicating that both are reliable in this firing mode. However, the SS V-PCA did not improve the pyrovalve performance during simultaneous firings (skew within 5 microseconds). Although the NSI firings were nominal, neither configuration produced a temperature at the booster that was significantly above the auto-ignition temperature of the booster propellant. Doubling the diameter of the flow passages in the SS V-PCA above the standard diameter (four times the cross-sectional area) was also evaluated and did not eliminate the simultaneous firing anomaly.

As in the legacy Al Y-PCA, test results for the SS V-PCA indicated firing commands for the two initiators should be separated by at least 2 milliseconds (ms) to guard against potential operational failure. When separated by 2 ms or more, both the legacy Al design and the new SS design produced booster interface temperatures adequate for reliable booster ignition.

References

NESC Technical Bulletin No. 09-01, Failure of Pyrotechnic Operated Valves with Dual Initiators. NASA Engineering and Safety Center.

Jet Propulsion Laboratory, Disclosure for the Steel Primer Chamber Assemblies for Dual Initiated Pyrovalves. New Technology Report #46302, California Institute of Technology, July 7, 2008.

CONAX Y-PCA Booster Anomaly Investigation Report, NESC Document Number RP-08-111, NASA Technical Memorandum (TM) Number TM-2008-215548.

For more information contact the NESC at www.nesc.nasa.gov

NESC tech bulletin









Nickel-Hydrogen (NiH_2) Common Pressure Vessel (CPV) Cell Capacity Loss and Voltage Collapse

During an investigation of anomalous voltages during a NASA scientific mission, a NASA Engineering and Safety Center (NESC) team discovered that the design of NiH_2 CPV batteries may be susceptible to a unique electrolyte bridging between the two internal cells resulting in undesired ionic current flow. This condition can lead to depletion of the capacity within one of the two cells.

Applicability

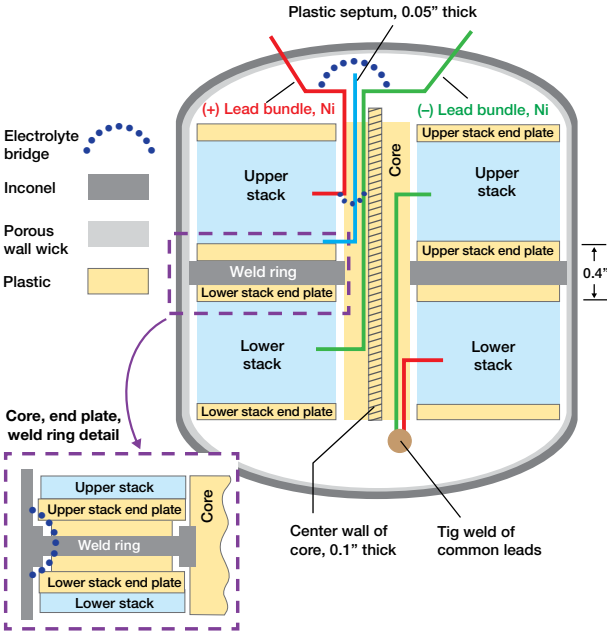
All NiH_2 battery applications utilizing CPVs.

Background

The Wilkinson Microwave Anisotropy Probe (WMAP) was launched in 2001 and outfitted with an 11 cell CPV NiH_2 battery. WMAP was designed to operate in full sun conditions. An unexpected series of discrete voltage drops began in August 2009 that were clearly traceable to the loss of one of the two individual cells contained within multiple battery CPVs. An examination of the limited telemetry available provided confirmation that each event was associated with a transient thermal load increase that occurred in conjunction with each step loss of voltage. Battery differential voltage telemetry indicated the events were apparently occurring randomly throughout the battery with no evidence that both cells within any given CPV were being affected. An NESC team was quickly assembled to evaluate the conditions and provide recommendations to arrest or reverse the degradation characteristics in order to complete the scheduled extended mission.

Potential NiH_2 Battery CPV Issue

As a result of the investigation into the anomalous battery behavior, analysis and testing determined NiH_2 CPV battery cell designs are susceptible to a unique electrolyte bridging between the two internal cells that can potentially result in undesired ionic current flow, which can ultimately deplete the capacity within one of the two cells. The internal design configuration of a normal CPV allows free material transport between cells as both cells within a CPV are intended to share the hydrogen gas necessary for NiH_2 cell functionality. Two conditions were identified where it is possible for free potassium hydroxide (KOH) electrolyte to creep between the cell stacks and to establish an undesirable conductive ionic pathway that effectively shorts out one of the two cells within the CPV. Those conditions are: 1) activating the NiH_2 CPV cells with excess electrolyte present or 2) allowing the cells to reach very low states of charge during operation. Based on observations and available data, once the electrolyte bridge is established there are no effective means to eliminate the problem with the possible exception of fully reconditioning the battery cell, or at least extended operation (up to a few weeks) in an open circuit condition. The application of periodic high rate charge pulses (between C/10 and C/4) was observed to be effective in at least temporarily stemming the continued voltage degradation of the WMAP battery and in a similar laboratory test battery. However, careful consideration to avoid high temperatures (above +10°C) needed to be in place to reduce the possibility of thermal runaway.



Simple Illustration of Ni-H2 Common Pressure Vessel Design and Identified Possible Electrolyte Bridging Locations

References

Wilkinson Microwave Anisotropy Probe (WMAP) Battery Operations Problem Resolution Team (PRT), NESC Document Number: RP-10-00608, NASA TM Number: TM-2010-216840

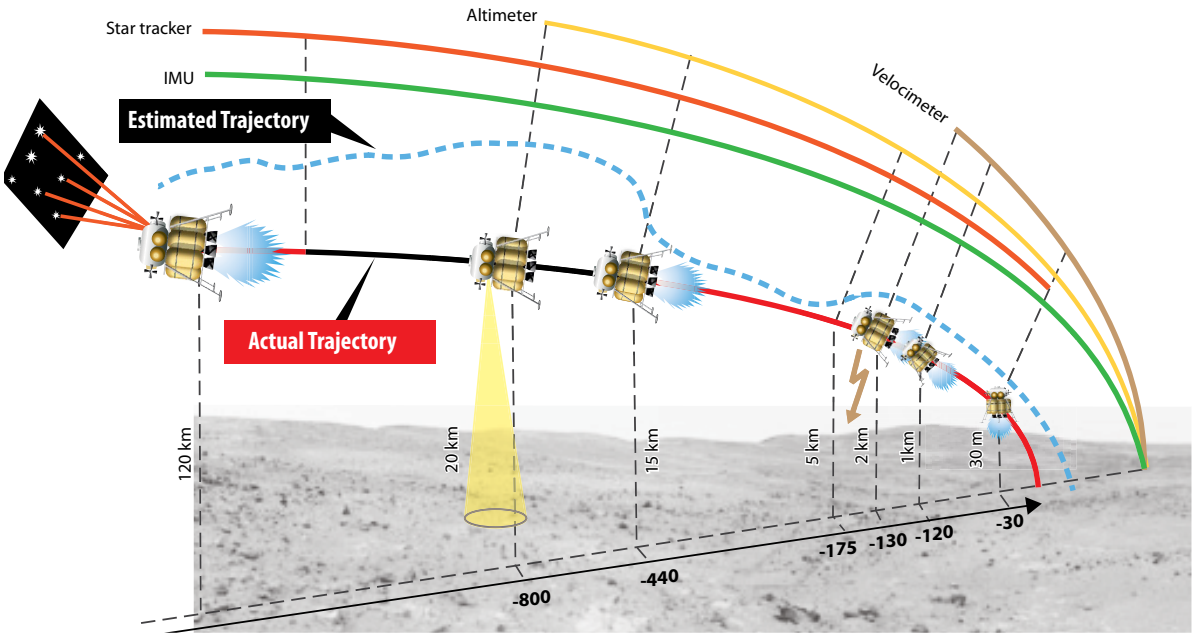
Effects of a Simulated Electrolyte Bridge in a Common Pressure Vessel (CPV) Nickel Hydrogen Cell, Aerospace Report Number: ATR-2010 (5175)-1

For information contact the NESC at www.nesc.nasa.gov

NESC tech bulletin

Simulation Framework for Rapid Entry, Descent, and Landing Analysis

The NASA Engineering and Safety Center has archived a number of key historic Entry, Descent, and Landing (EDL) simulation models and developed several new models to enhance the capability of the Agency to evaluate a wide range of EDL systems for system analysis studies, preliminary design, mission development and execution, and time-critical assessments. The simulation models developed in this activity can be used to help define the required architectures and investment strategies for future robotic and human exploration missions.



Applicability

All Entry, Descent, and Landing systems and missions.

Simulation Framework and Models

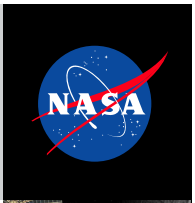
EDL flight simulations are typically developed for specific missions or analysis tasks. In many cases, once the effort is completed, the simulation models are not adequately documented or retained. Because many projects or studies requiring EDL would benefit from high-fidelity simulations with a library of validated and documented models, an NESC team converted and archived current and historic EDL models and scripts into a secure user library with appropriate user documentation and test cases. The team also developed several new models currently of interest in the EDL community. All of these models are implemented in a simulation framework utilizing the Program to Optimize Simulated Trajectories II (POST2). As a whole, the models include aerodynamic and mass models of entry vehicles, atmospheric and gravity models of planets and moons, guidance and control algorithms, a multimode Kalman Navigation Filter for onboard state estimation, aerodynamic uncertainties for dispersion analyses, guidance models for aerocapture and aerobraking, and several basic attitude-control models. A set of test cases is included to confirm the proper functioning of these models when incorporated into future simulations. The details and user guides for the models, scripts, and test cases have been published (see references below). Request for access to the simulation framework and models can be made at http://post2.larc.nasa.gov

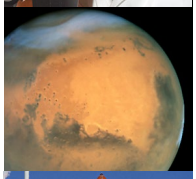
References

Murri, Daniel G.: Simulation Framework for Rapid Entry, Descent, and Landing (EDL) Analysis. NASA TM-2010-216867, Volumes I and II. November 2010

Murri, Daniel G.: Simulation Framework for Rapid Entry, Descent, and Landing (EDL) Analysis, Phase 2 Results. NASA TM-2011-217063. February 2011

For more information, contact the NESC at www.nesc.nasa.gov




NESC tech bulletin

Structural Analyses and Margins of Safety

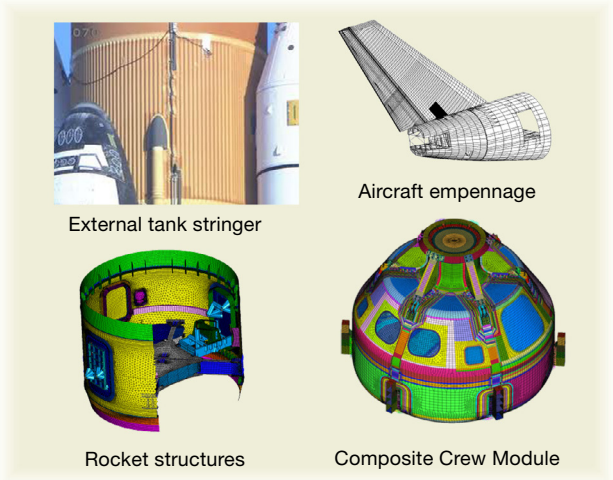
There is an increasing reliance on modeling and simulation to verify, quantify, and certify designs of complex structures. The availability of a range of commercial modeling and simulations tools and packages with a variety of capabilities, in conjunction with increased computational resources, is allowing analysts to rapidly perform detailed analyses. However, care should be taken to understand specific tool limitations, assumptions, and boundary conditions as erroneous results can be generated without being recognized by the analysts. In addition, the reported margins of safety should be carefully interrogated to identify any false positive or negative margins and highlight any areas for structural concern.

Applicability

Structural analysis Agency-wide.

Background

Advances in modeling and simulation, new finite element software packages, modern computing platforms, computing engines, and powerful computers are providing opportunities to interrogate complex designs in a very different manner and in a more detailed approach than ever before. The current trend in the structural design process is increasing reliance on modeling and simulation to assess local stress states and evaluate margins of safety. In addition, there is also a tendency to perform three-dimensional (3D) analyses under the assumption that detailed 3D models inherently provide higher fidelity and more accuracy than two-dimensional (2D) and shell models. Furthermore, aerospace structural components are inherently complex; typically local stress concentrations, free edges, skin-stiffeners, varying thickness shells, etc. are par for the course. Global- or system-level structural models of these components often include connections between and among finite elements of different dimensionality (e.g., beam element connected to a plate/shell/solid element). Quite often negative stress margins are calculated and reported from these analyses. The reported negative margins raise questions about the adequacy of the structural design and may, in fact, initiate separate independent assessments of the design, a redesign of the component(s), or both. Alternatively, in many instances these stress values may be prescribed as input to a life-prediction analysis and tools, and the predicted outcome may be an inadequate design life, driven in part by these artificially high local stress values. As a consequence, schedule delays may result and costs may increase due to perceived necessity to redesign.



Examples of complex structural analysis models

Findings and Conclusions:

Recent studies show that in some, but not all cases, these negative stress margins computed using local stresses are inaccurate and are artifacts of modeling and analysis. The areas where negative margins are frequently encountered are often near stress concentrations; point loads and load discontinuities; near locations of stress singularities; in areas having large gradients but with insufficient mesh density; in areas with modeling issues and modeling errors; in areas with connections and interfaces; in areas of 2D-3D transitions; near bolts, due to details of bolt modeling; and near areas of complex boundary conditions. Now, more than ever, structural analysts need to examine, interrogate, and interpret their analysis results and perform basic "sanity checks" to determine if these negative margins are, in fact, real or they are just artifacts of modeling and analyses. Knowledge of the behavior of structures and the theory of elasticity, the ability to formulate an estimate of expected results before they are obtained, the awareness of consequences of modeling assumptions, etc. are essential to interpret the numerical results.

Another disturbing aspect noted in the recent past is the inability to prescribe appropriate boundary conditions by widely available desktop software packages. The reported positive margins by these software packages may, in fact, be false positive. These packages are inexpensive and may not have all the analysis options and capabilities that the widely used general-purpose software packages (such as NASTRAN, ANSYS, ABAQUS, etc.) offer. The margins evaluated with these desktop packages need to be confirmed by performing a reanalysis with the widely used packages and also ensuring that proper boundary conditions are prescribed.

References

Raju, I. S.; Lee, D. S.; and Mohaghegh, M.: "Negative Stress Margins – Are They Real?", AIAA-2011-1808-588, Paper Presented at the 52nd AIAA SDM conference, Denver, Colorado, April 4-7, 2011.

For more information, contact the NESC at www.nesc.nasa.gov



NESC tech bulletin

Designing for Flight Through Periods of Instability

For completeness, it is imperative that Flight Control System (FCS) designers use both complementary time and frequency domain techniques to address periods of instability. Use of standard frequency domain synthesis techniques alone may not always yield an FCS design with sufficient gain and phase stability robustness margins while simultaneously satisfying performance requirements.

Instability Cause and Consequence

Analysis and evaluation must be performed of any potential source of instability (e.g., propellant slosh, flexible structure, or aerodynamics), while flying through periods of rapidly changing dynamics. A large body of experience has been accumulated regarding successfully flying through not only degraded margins, but also relatively brief periods of linearized model instability. These instabilities occur as the flight environment and vehicle dynamics undergo rapid changes. When linearized stability robustness margin requirements cannot be satisfied, alternative methods are then needed to ensure that deficient stability margins do not present a high risk of losing control during the mission.



The Orion launch abort system successfully flew through brief periods of instability. Known instabilities and risks were evaluated prior to flight using best practices.

Best Practices for Flight Control System Design

FCS designers should consider employing non-linear system requirements that capture both stability and performance aspects. Occasionally, it may be necessary to set aside the traditional frequency domain gain and phase stability robustness margins in favor of another technique. The tried-and-true guideline that stability always comes before performance in the design process remains the same. However, since real flight systems behave in a non-linear manner, "stability" should be understood as control of the vehicle never being lost while simultaneously achieving attitude control performance requirements.

Consider four complementary recommendations for certifying FCS designs with deficient stability margins:

1) Accept some Relaxed or even Negative Stability Margins: additional analysis may not be required if a stability margin fails the requirement for only a brief time. Seek out prior experience with similar configurations and conditions.

2) Evaluation of Uncertainties: reassess whether the uncertainties input into the analysis are realistic. In certain cases, the effects of correlated variables can be taken into account to reduce the level of uncertainties used in the analysis.

3) Checking the Time to Double Amplitude: determine if the vehicle will fly through the region of concern before the oscillations reach unacceptable amplitudes, in which case a relaxed or even negative margin may be acceptable.

4) Use of Non-Linear Time-Domain Simulations: exploit the complete non-linear time-domain models to prove that the vehicle exhibits acceptable behavior, even with programmed test inputs to excite oscillations. Additionally, the loop gains and/or time lags can be adjusted in the simulation to evaluate the gain and phase stability margins remaining from a non-linear perspective.

Historically, some launch vehicles have been successfully flown with the known threat of slosh instabilities. The Atlas-II was successfully flown with linearly unstable (as viewed from a purely linear frequency-domain perspective) slosh modes.

An FCS designer should question the application of linear stability requirements and not rely exclusively on the frequency domain approaches to verify stable flight. The use and application of the frequency-domain synthesis and analysis tools must be balanced with the non-linear time-domain performance simulation tools and the Time to Double Amplitude criteria.

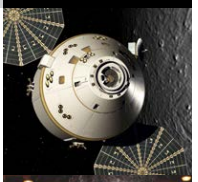
References

1. NASA/TM-2011-217183, NESC-RP-09-00602 v2.0, Independent Review of the Ares-I Control Sensitivity to Orion Service Module Tank Slosh Dynamics, Oct. 2011

2. NASA Document Number: EAM-CEV-09-001, Shuttle Ascent and Entry GN&C Stability Verification, Edgar Medina (PA-1 Flight Dynamics Team), Jan. 23, 2009

3. NASA/SP–2010–3408, Space Shuttle Entry Digital Autopilot, Section 9.0 Lessons Learned, Larry McWhorter and Milt Reed, Feb. 2010

For information contact the NESC at nesc.nasa.gov









NESC tech bulletin

Aerodynamic Reaction Control System (RCS) Orientation and Jet Interaction (JI) Model Validation

Careful consideration should be given to placement and orientation of RCS jet thrusters on hypersonic entry vehicles in order to minimize adverse RCS JI. Modern state-of-the-art computational fluid dynamics (CFD) tools should be able to predict the RCS effectiveness and JI accurately when coupled with verification and validation studies, including the use of appropriately designed experimental wind tunnel testing.

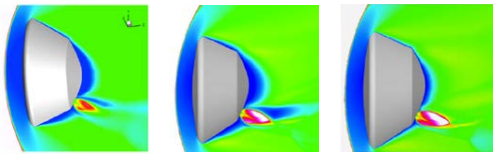
Applicability

Development of experimental techniques and CFD predictive capabilities to determine proper placement and orientation of RCS jet thrusters on hypersonic entry vehicles to minimize adverse RCS JI.

Historical JI Prediction Issues

Historically, the prediction of hypersonic entry RCS effectiveness and associated JIs with surrounding flowfields has been a challenging CFD problem. For example, during the bank maneuvers of the first space shuttle orbiter reentry, the rolling moment that occurred when the forward yaw thrusters were fired was less than expected, resulting in greater RCS fuel usage than anticipated. The cause of this discrepancy was attributed to improper scaling of wind tunnel derived RCS interaction correlations to the flight condition.[1] In a more recent example, CFD analyses of the RCS JI on the Mars Phoenix entry vehicle indicated the possibility of uncontrollable adverse JI, enough so that the project chose to not use the RCS during portions of the entry phase, increasing the landing footprint and the overall mission risk.[2]

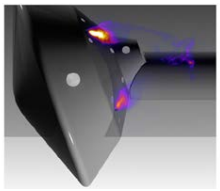
The Mars Science Laboratory (MSL) mission was plagued by similar issues in the early design phases. The entry vehicle aerodynamics was based on a combination of experimental results, CFD calculations, and comparisons with estimates of flight aerodynamics from previous Mars missions. Estimates of the RCS effectiveness and RCS JI with the aftbody flow-field were originally developed based primarily on CFD calculations, indicating the potential for large, undesirable RCS JI. Recommendations were made to change the RCS jet locations and orientations in an attempt to reduce plume impingement on the spacecraft, jet-to-jet plume interactions, and to minimize undesirable interaction torques. Given the uncertainties associated with the wake flow predictive capabilities of current CFD codes, a wind tunnel test was designed and executed in the Langley Research Center 31-Inch Mach 10 Wind Tunnel to provide experimental data for the new MSL RCS thruster configuration design.[3] This data served to provide validation results specific to MSL and, at the same time, the experimental test techniques developed would potentially be of benefit to other projects and programs employing blunt body entry aeroshell designs with aftbody RCS jet thrusters (e.g., Orion/Multi-Purpose Crew Vehicle or commercial crew vehicle designs). Additional CFD calculations were made on the new thruster configuration to assess effects of the aerodynamics and RCS interactions.[4] Results indicated generally good agreement between the experimental data and CFD predictions of the RCS JI. This, along with recommended conservative uncertainty values for RCS JI, provided an appropriate degree of confidence to the MSL Project on the adequacy of the new thruster configuration and overall robustness of the entry flight control system.



Comparison of MSL Aero/RCS interaction using 3 different CFD codes.



MSL model in LaRC 31-Inch Mach 10 Wind Tunnel.



Experimental flow image of MSL RCS jets.

Conclusions and Guidance

Appropriate consideration must be given to RCS thruster locations and orientations to minimize impingements and interactions. Modern CFD tools should be used in conjunction with well-designed experimental testing early in development to accurately predict the RCS JI and overall control effectiveness.

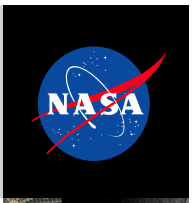
References

1. Scallion, W.I., Compton, H.R., Suit, W.T., Powell, R.W., Blackstock, T.A., and Bates, B.L.: "Space Shuttle Third Flight (STS-3) Entry RCS Analysis," AIAA Paper 83-0116.

2. Dyakonov, A. A., Glass, C. E., Desai, P. N., and Van Norman, J. W.: "Analysis of Effectiveness of Phoenix Reaction Control System," AIAA Paper 2008-7220.

3. NASA/TM-2013-218023, NESC-RP-10-00613 Mars Science Laboratory (MSL) Reaction Control System (RCS) Jet Interactions (JI) Testing and Analysis, July 2013

4. Schoenenberger, M., Van Norman, J. V., Rhode, M., and Paulson, J.: "Characterization of Aerodynamic Interactions with the Mars Science Laboratory Reaction Control System Using Computation and Experiment," AIAA Paper 2013-097.











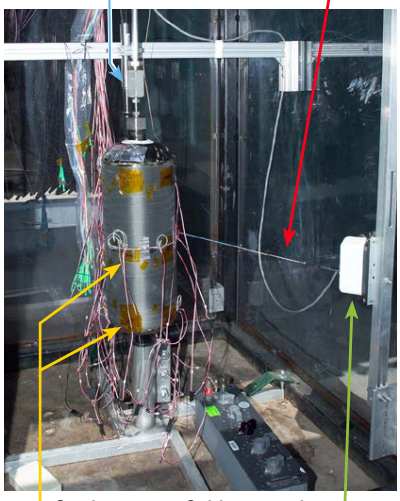
NESC tech bulletin

COPV Mechanical Model Validation

Global and local deformation measurements should be incorporated into the composite overwrapped pressure vessel (COPV) design and analysis process to allow correlation of these measurements with finite element analysis (FEA) models. This correlation improves understanding of liner, liner/overwrap interface, and composite deformation response in COPVs. The improved accuracy reduces error in subsequent analyses, such as fracture, fatigue, and stress rupture that are critical for COPV qualification.

Current Obstacles to COPV Mechanical Model Validation

Mechanics models and FEA of COPVs developed by manufacturers have not always been adequate to provide accurate general deformation response and to pinpoint areas of stress concentration in the composite shell and liner. This lack of accuracy has been an obstacle to determining risks associated with failure modes, such as stress rupture and fatigue crack growth. Key phenomena in the understanding of COPV liner and composite response include overwrap stress-deformation states, liner mechanics, and liner/overwrap interface mechanics. Accurate quantification of the interference strain between the liner and overwrap is difficult to capture without measurement and model correlation.



Model correlation study test fixture.

While closed-form solutions and FEA models with simple liner-overwrap interface assumptions may be calibrated to conservatively bound hoop strain response, they cannot accurately capture the complete multi-axial stress and deformation state to simultaneously correlate with all axial, circumferential, and volumetric deformation measurements, especially in the presence of an interface gap. The cited reference identifies ways in which measurements and model correlation can be performed. Global measurements taken from axial linear variable differential transducers (LVDTs), belly bands, and volumetric measurements, along with local measurements of axial and hoop strain from strain gages and laser profilometry measurements, were all demonstrated to be helpful in understanding the complex mechanical response of the COPV. COPVs are classified into 3 levels, and guidelines for measurements are suggested.

Best Practices for Validation of COPV Models

Three levels of measurements are recommended based on design burst safety factors and are intended to serve as guidelines for measurements on flight pressure vessels.

Level 1: Burst factor > 3.0

Determine composite and liner response based on analysis of the vessel per the as-built specifications and demonstrated burst pressure. Alternatively, determine composite and liner response based on closed-form analysis of a measured fiber strain response (nominal or local) as a function of pressure to burst.

Level 2: 2.0 < Burst factor < 3.0

Determine composite and liner response based on fully verified FEA. Measurements needed as a function of applied internal pressure include:

1. Global measurements: Axial elongation by LVDT and internal volume growth.

2. Local measurements: Hoop and axial strain at equator and other carefully referenced positions by foil strain gages and/or full-field methods of optical metrology.

Level 3: Burst factor < 2.0

Determine composite and liner response based on fully verified finite element model. Measurements needed:

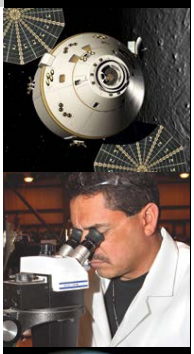
1. Global measurements: Axial elongation by LVDT and internal volume growth.

2. Local measurements: Hoop and axial strain at equator and other carefully referenced positions by foil strain gages and/or full-field methods of optical metrology.

3. Interior Laser Profilometry: Unwound liner, wound liners prior to overwrap cure, wound liner post-overwrap cure prior to autofrettage, and cured COPV post autofrettage.

References

Thesken, J.C., et. al., Composite Pressure Vessel Working Group (CPVWG) Task 4: A Theoretical and Experimental Investigation of Composite Overwrapped Pressure Vessel (COPV) Autofrettage, December 19, 2013. TM-2014-218260.







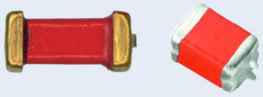
NESC tech bulletin

Preventing Incorrect Installation of Polarized Capacitors

Even though NASA's Lessons Learned Information System has an entry on the reverse installation of polarized capacitors, this error keeps reoccurring and is a "lesson not learned." The purpose of this bulletin is to discuss some of the reasons this keeps happening as well as offer best practices to prevent this error in the future.

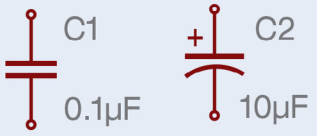
Examples of polarity marking methods for tantalum capacitors.





- CWR09 & CWR11 capacitors identify polarity by a beveled edge in the case and/or a polarity bar marked on the case ("+" or a stripe adjacent to the anode termination).
- CWR06 capacitors typically identify polarity by a small projection "nub" in the center of the anode termination.
- Exceptions or variations to these conventions may exist.

Conventional schematic capture symbols for capacitors.



Non-polarized Polarized

Polarized capacitors continue to be installed incorrectly

So why does reverse installation continue to happen even though we've had hard lessons in the past? Probably the most significant reason is that NASA's parts derating policy masks the problem. NASA usually puts a part in an application that has significant margin on its forward operating voltage rating vs. the application forward voltage. When such a derated part is installed in reverse that large margin often results in no immediate indication or failure. This is in stark contrast to commercial terrestrial designs where applications with much smaller margin can result in immediate energetic failure. A second significant factor in all of this is the polarity marking standards in surface mount capacitors aren't "standardized" and are often at odds with one another. Does the black band mean positive or negative? Depending on the marking convention, it could be either.

One way a reverse installation error can be introduced as the design evolves is if a part, such as a capacitor, is changed from non-polarized to polarized without a proper update of the schematic and assembly drawings. In a recent occurrence, the failure of the power supply in a ground hardware simulator was the result of an abnormal voltage caused by leakage in two polarized capacitors installed in reverse polarity. Similar capacitors in the flight units on the ISS are also installed in reverse polarity but have not yet resulted in failure.

The capacitor components, which are polarized tantalum devices, were erroneously specified on the schematic with a generic, non-polarized capacitor symbol. These capacitors, originally 0.1 microfarad (µF), were later changed to 10 µF, which necessitated a change from a non-polarized to a polarized part. The capacitor value was changed in the schematic and in the parts list without changing the part symbol. Accordingly, the translation from schematic to assembly drawing arbitrarily designated the improper polarity.

In another recent instance (different hardware), an on-orbit failure was experienced due to a reverse polarity solid tantalum capacitor. Possible confusion due to differences in part polarity marking conventions may have contributed.

Best Practices for avoiding reverse installation

1. Ensure there is a procedure to review the parts list and verify in the various drawings that the polarized parts are installed or represented with the correct polarity.

2. Account for changes from non-polarized to polarized parts: review and change schematic drawings as required to ensure proper part polarity.

3. Never use non-polarized symbols to represent polarized components in drawings.

4. Recognize that the potential exists for certain components to be changed from non-polarized to polarized during design evolution.

5. Ensure assembly and inspection personnel are cognizant of the allowable variations of polarity markings for polarized capacitors.

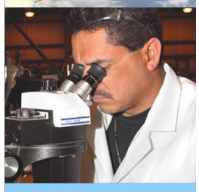
References

NESC-RP-13-00874, Reverse Polarity Capacitor Installation Anomaly on the International Space Station (ISS) Expedite the Processing of Experiments to the Space Station (ExPRESS) Logistics Carrier (ELC) Simulator, Jan. 2015.

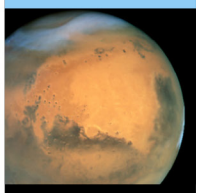
NASA Lesson Learned 981 "Reverse Polarity Concerns With Tantalum Capacitors," June 12, 2000.

For information contact the NESC at www.nesc.nasa.gov









NESC tech bulletin









Best Practices for Use of Sine Burst Testing

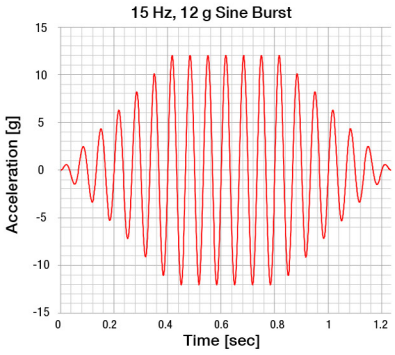
Sine Burst (SB) Testing is used for strength testing of aerospace hardware as an alternate to static pull and centrifuge tests. The main advantage is that testing can be implemented while hardware is on the shaker for other tests. It also imposes a lower number of cycles on the hardware compared with a sine dwell or sweep, and is particularly suitable for relatively stiff components or electronics boxes, instruments, or spacecraft. Identified risks can be mitigated by best practices.

Background of SB Testing

In the late 1980's, the SB method was used as a means to impart a static load into a component, instrument, or relatively small/stiff spacecraft. The shaker controller is used to apply an enveloped sinusoidal base drive acceleration to the item at a fixed frequency with 5-10 cycles at peak level as shown in the Figure. The test frequency is such that the item response would be pre-resonant or as close as possible to the rigid body mode, usually being no more than 1/3 of the first mode frequency of the test article. Because the test article is being accelerated as a rigid body, a uniform inertial body load is generated in the test article.

Limitations and Risk of SB Testing

To achieve the target stresses in some areas of the hardware, an over-test may need to be imparted in other areas. Therefore, pre-test analysis is required to verify the stress targets can be achieved within acceptable levels of over-test. Also, if the required load case is unidirectional (say compression), there will be a reversal load (tension) imparted on the article or vice-versa. This is a single axis test so different orientations of the test article may be required to achieve strength qualification. There is a need to monitor the test article for any unexpected dynamic amplification, especially if the applied frequency does not meet the 1/3 of natural frequency guideline.



SB Testing Risks can include:

- Impacting the shaker stops by exceeding the shaker maximum displacement or stroke.
- Shaker stiction: The controller computes a linear transfer function of acceleration to update the drive for the next level. If the shaker has any stiction (non-linear behavior) at the targeted test levels, the updated drive may be higher than required and impart an unintended over-test.
- An unintended operator action or controller setting, which drives the amplifier to an over-test.
- Drive signal adjustments: If the test procedure is such that intermediate levels require engineering adjustments to the drive signal, the risk is a wrong calculation of this adjustment and would lead to an unintended over-test.
- Lack of independent test over-protection system.
- Incorrect software version in the drive controller.

For information contact the NESC at www.nesc.nasa.gov

Best Practices for SB Testing

Consider these best practices during the planning and execution phases:

1) Given the impulsive nature of SB testing, do not count on the shaker displacement soft shut down (SSD) switch and set a proper SB frequency high enough not to exceed the displacement that triggers the SSD.

2) Drive adjustments made by engineering personnel should be independently checked and the test sequence should be restarted from the lower levels.

3) Avoid using SB testing at high levels of assembly or on a complete flight unit. The preference is to use the method with engineering test units, which usually comprise the structure under test with mass simulators.

4) Develop metrics for routinely assessing the mechanical "health" of the shaker and slip table systems.

5) Evaluate the drive signal magnitude and the coherence function estimate between the drive and control accelerometer prior to test continuation. Coherence in the frequency band close to the SB frequency should not be lower than 0.9.

6) Perform a checkout with a mass mockup and compare recorded drive signal voltages at each level during the actual test. Ensure adequate test planning between the analysts, the test engineers, and operators.

7) Review and understand the time history acceleration and or force data collected after each test run, including the controller drive voltage and amplifier output time histories.

8) Reconsider testing via SB any hardware that is inherently non-linear, unless the non-linear nature is understood and accounted for in the pre-test analysis.

9) If any of the risk mitigations fail or a new flaw is discovered, the final defense resides in the use of an independent over-test protection system along with hardware positive margin of safety for the abort setting.

References

1) NASA Report on High Energy Solar Spectroscopic Imager (HESSI) Test Mishap, (Washington, D.C.: NASA Headquarters, Code S, May 2000)

2) LADEE Spacecraft, Type C Mishap, IRIS Case Number: S–2012–124–00008

Best Practices for Use of Sine Vibration Testing

Sine Vibration (SV) Testing involves subjecting the test article to a swept sine input over a frequency range (typically 5-100 Hz) to replicate the low-frequency launch environment. This test method is used for various purposes on a structural model but mainly on flight articles. The SV levels are derived from measured flight data or based on interface acceleration levels from coupled loads analysis (CLA). A logarithmic sweep rate is typically used to excite a constant time interval per bandwidth for the test (e.g., 2 or 4 octave/min), which is intended to simulate sustained sine and transient events that occur during launch. Risks can be mitigated through best practices.

Background of SV Testing

SV testing is required by NASA-STD-7002 and most launch vehicle organizations as a final dynamic qualification of the payload to demonstrate acceptability for flight. NASA requirements differ however between the SV testing requirements provided in Air Force Standard SMC-S-016, Test Requirements for Launch, Upper-Stage and Space Vehicles, and The European Space Agency (ESA) Space Engineering Testing Standard ECSS-E-ST-10-03C.

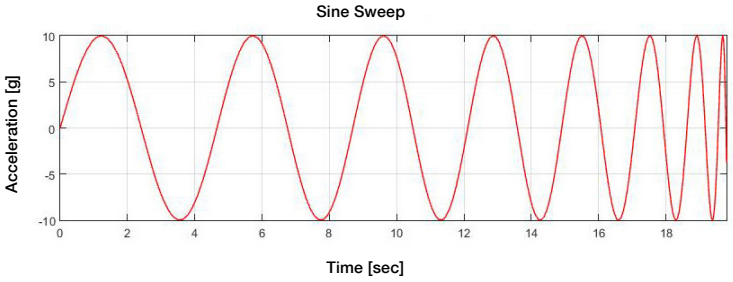
SV Testing Risks

Test incidents and mishaps have happened associated with the risk of testing an article through resonance. The following is a list of identified risks:

- Testing in a frequency range beyond the CLA validity or cut-off frequency, or beyond the range of model test correlation.
- Lack of definition of test abort settings criteria and workable margin between limit and abort levels.
- A hard shut down can happen either due to loss of electrical power and/or exceeding amplifier capability.
- Lack of sufficient pre-test analysis and non-linear response in the structure.
- Lack of sufficient instrumentation to adequately monitor hardware responses and protect from over-test.
- Unpredicted interactions between the shaker and test article.
- Incorrect software version in the drive controller.

Best Practices for SV Testing

- Perform sufficient pre-test analysis to determine instrumentation locations and response limits which can be used to protect the hardware from over-test.
- Prior to running a full-level test, lower levels of input with proportional limits should be run to verify the behavior of the test article and control system. After completion of each low-level run, the response should be compared with analysis predictions and prior runs to verify that the test article is behaving as expected.
- Structural response in this test is through resonance, thus the limit and abort levels need to be properly defined.
- Clearly define and implement response abort levels for which positive margin of safety can be demonstrated for the hardware.
- Do not test beyond the model correlation frequency range and/or the CLA range as margins cannot be relied upon because responses in that range are not available.
- Even if the test item is expected to have rigid body behavior, define and implement response aborts. This prevents frequency shifts and unexpected resonance build-up, and to prevent the unexpected.
- At the beginning of the test, check and compare the unfiltered or raw time histories and the controller spectra. Expect some differences in response limits and aborts and adjust accordingly.



- Consider non-proportional limits at the lower levels of excitation to allow for additional response to understand lightly damped responses; use proportional limits from there onwards to verify controller performance.
- The team should define in advance the control strategy that best suits the objectives. This is related to average, weighted average, or extremal control use.

References

1) National Aeronautics and Space Administration, Payload Test Requirements, NASA Technical Standard NASA-STD-7002, September 10, 2004.

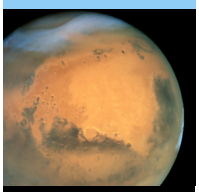
2) Air Force Space Command Space and Missile Systems Center, Test Requirements for Launch, Upper-Stage and Space Vehicles, SMC Standard SMC-S-016, September 5, 2014.

3) ESA Space Engineering Testing Standard, ECSS-E-ST-10-03C, June 1, 2012.









Buckling Knockdown Factors for Composite Cylinders

The buckling performance of thin-walled cylindrical shells is well known to be sensitive to small geometric and loading imperfections. During design, this sensitivity is typically accounted for by multiplying the predicted buckling load of a geometrically perfect structure by an empirical design factor known as a buckling knockdown factor (KDF). The most widely used source of KDFs for cylindrical launch-vehicle structures is NASA SP-8007. However, general composite shells are outside the original scope of SP-8007, and a universal KDF of 0.65 for all composite shell designs has been used in several recent NASA studies, though the technical justification is unclear. If the NASA SP-8007 is used to calculate KDFs for composite cylinders, the original assumptions and limitations should be understood and care must be taken. Additionally, the universal KDF of 0.65 is thought to be *unconservative for certain designs and is therefore not recommended.*

Background

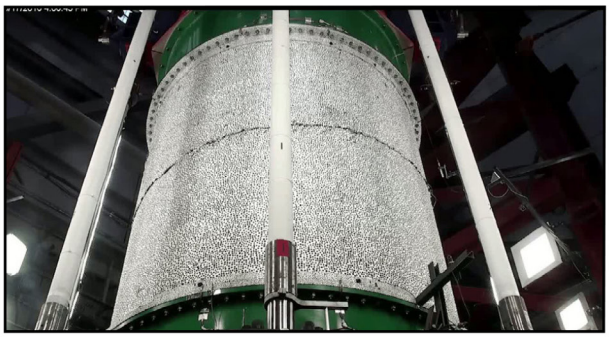
Thin-walled composite shell structures have been used in launch vehicles for many years. Additionally, NASA is increasingly considering composite structures for use in launch vehicles. For many such launch-vehicle shell structures, composite structures are chosen for structural efficiency and reasonable manufacturing considerations. However, it is well known that thin-walled shell structures can be very imperfection sensitive when subjected to destabilizing loads. That is, small geometric or loading imperfections can cause the actual buckling loads of the as-built shells to be significantly lower than the theoretical predictions, which are based on simplified linear bifurcation buckling analyses of geometrically perfect shells. Therefore, it is important to understand the structural response and imperfection sensitivity of such shell structures.

To account for the imperfection sensitivity during design of a thin-walled shell, the theoretical buckling load of the perfect structure is typically multiplied by a buckling KDF to determine a safe design load level. Hence, the guidelines for determining these KDFs can be very important for the design of structurally efficient shells. The most widely used source for KDFs for cylindrical shells is the NASA SP-8007 [1], which has recommendations that were developed based on experimental buckling tests from the 1930s-1960s. However, SP-8007 has not been updated since the late 1960s and few, if any, composite shells were tested in the development. Consequently, the SP-8007 guidelines may not be applicable to shells constructed from modern materials, improved manufacturing processes, and new structural concepts. Several recent NASA studies have used 0.65 as a universal buckling KDF for cylindrical composite shells regardless of the structural concept (sandwich, stiffened shell, etc.) and the design details (thicknesses, stiffener dimensions, layup, etc.).

The NASA Engineering and Safety Center (NESC) is currently assessing the NASA SP-8007 guidelines with the intent of revising these guidelines for selected metallic and composite cylindrical structures. The purpose of this Technical Bulletin is to provide guidance on the KDFs that should be used for composite structures until the new guidelines are developed and published.

Findings and Conclusions

It is unclear from where the universal 0.65 KDF for composite shell structures came, or if it is always conservative. In particular, when applied to anisotropic composite sandwich shells, the SP-8007-recommended KDFs for orthotropic cylinders and isotropic sandwich cylinders can be significantly lower than 0.65. Nonlinear finite-element analysis to date however suggests that these SP-8007 KDFs are conservative for all the sandwich composite cylinders considered. Because the SP-8007 KDFs for many composite shells are less than 0.65, 0.65 should not be used as a universal KDF for composite cylinders unless there is other appropriate rationale.



Sandwich composite test article showing material failure that occurred as a result of global buckling.

If SP-8007 is used to calculate KDFs for composite cylinders, the original assumptions and limitations must be understood and caution should be used if the recommendations are extended outside their original scope. Particular caution should be used when applying SP-8007 recommendations to composite cylinders that do not consist of orthotropic layers aligned with the axial and circumferential directions of the cylinder (cross-ply laminates), those with extreme stiffness tailoring, or those with significant contributions from the extension-shear, extension-bend, or bend-twist terms. Additional consideration must be made for cylindrical shells with low transverse shear stiffness (such as some sandwich shells) because they can have significantly lower predicted buckling loads than similar shells with high transverse shear stiffness. More detailed recommendations will be made by the NESC when the new guidelines are published.

References

1. Anonymous, "Buckling of Thin-Walled Circular Cylinders," NASA SP-8007, 1965, revised 1968.

For information contact the NESC at www.nesc.nasa.gov



NESC tech bulletin

Damage Tolerance Life Issues in COPVs with Thin Liners

During composite overwrapped pressure vessel (COPV) qualification, damage tolerance life analysis and/or tests may not adequately address crack growth for COPVs with thin liners, and additional qualification tests beyond those in current requirements documents may be needed to quantify crack growth.

Background

Damage tolerance life (safe-life) is a fracture control approach that assumes the existence of cracks of a size that can be reliably detected by an established nondestructive evaluation (NDE) method used to inspect the COPV liner prior to service. The intent of damage tolerance life is to demonstrate that cracks at or below this size will not grow to a depth equal to the thickness of the liner (leak) or to a length that is predicted to become unstable. ANSI/AIAA S-081A1 requires that metallic COPV liners possess adequate damage tolerance life that is demonstrated by analysis or test. Details on testing and analysis are specified in S-081A.[1]



Typical spherical COPV

Issue

Many COPVs are designed with a liner that responds elastically for all pressure and combined load conditions after autofrettage. For these elastically responding liners, S-081A allows demonstration of damage tolerance life based on linear elastic fracture mechanics (LEFM).

However, the use of LEFM methods may not be appropriate if the liner is relatively thin compared to the inspectable crack depth (for example, a detectable crack depth of 0.025 inch in a liner that is only 0.04-inch thick, resulting in a ligament that is 0.015 inch). The crack growth rate through the ligament may be faster than that predicted by LEFM for two reasons:

- **Plasticity:** Even though far-field analysis shows that thin liners are responding elastically, local plasticity in the ligament must be considered. LEFM assumes that the crack-tip plastic zone is small relative to the size of the crack. Regions of local yielding (remaining ligament or local stress concentrations) adjacent to cracks may create plasticity that renders LEFM analysis inappropriate. For example, liner embossing (plastically straining the liner into the overwrap during autofrettage) could lead to highly localized strain concentrations, affecting the growth of cracks in the remaining ligament.

- **Microstructure:** When the remaining ligament is relatively small, the ligament thickness may be on the same order as microstructural features, such as grain size. The use of crack growth rate data obtained from standardized tests (such as that supplied in NASGRO) may not be representative of crack growth in the ligament. Instead, tests based on ASTM Standard E-647 (Appendix X3) guidelines that address the measurement of small fatigue crack growth rates may be more appropriate. [2]

These "small-scale" effects could result in the inappropriate use of LEFM methods and existing crack growth rate data resulting in an unconservative estimate of damage tolerance life.

Path Forward

Additional understanding will be required to establish limitations on the use of LEFM-based analysis and test methods for elastically responding COPV liners. This effort will require a better understanding of localized strain fields and microstructural considerations for applicable combinations of material, material processing, autofrettage and subsequent response characteristics, NDE method, and crack depth for each aspect ratio. Evaluation of these parameters and their relative importance to damage tolerance life would allow guidelines for the appropriate use of LEFM for thin liners.

Small-scale effects are not limited only to elastically responding liners. For COPVs with far-field plastic response, coupon or vessel testing is required per S-081A. Such tests may be adequate to address small scale effects by test if the test captures the effects of plasticity and microstructure in the remaining ligament; however, test methods and guidance for ensuring that worst-case conditions were present during coupon or full-scale tests would need to be developed.

The NESC will be developing specific guidelines for damage tolerance life analysis and test that addresses crack growth in these small uncracked ligaments that include localized plasticity and microstructure effects. This may result in the need for additional qualification tests to quantify crack growth in flight COPVs with thin liners.

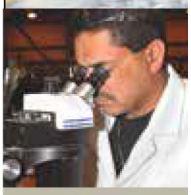
References

1. ANSI/AIAA S-081A-2006, Space Systems-Composite Overwrapped Pressure Vessels (COPVs), American Institute of Aeronautics and Astronautics, VA.

2. ASTM Standard E647-15, Standard Test Method for Measurement of Fatigue Crack Growth Rates, ASTM International, West Conshohocken, PA.

For information contact the NESC at www.nesc.nasa.gov









NESC tech bulletin

Development of NASA Standards for Enabling Certification of Additively Manufactured Parts

There are currently no NASA standards providing specific design and construction requirements for certification of additively manufactured parts. Several international standards organizations are developing standards for additive manufacturing; however, NASA mission schedules preclude the Agency from relying on these organizations to develop standards that are both timely and applicable. NASA and its partners in human spaceflight (Commercial Crew, Space Launch System, and Orion Multi-Purpose Crew Vehicle Programs) are actively developing additively manufactured parts for flight as early as 2018. To bridge this gap, NASA Marshall Space Flight Center (MSFC) is authoring a Center-level standard (MSFC-STD-3716)[1] to establish standard practices for the Laser Powder Bed Fusion (L-PBF) process. In its draft form, the MSFC standard has been used as a basis for L-PBF process implementation for each of the human spaceflight programs. The development of an Agency-level standard is proposed, based upon the principles of MSFC-STD-3716, which would have application to multiple additive manufacturing processes and be readily adaptable to all NASA programs.

Background

Additive manufacturing (AM) has rapidly become prevalent in aerospace applications. AM offers the ability to rapidly manufacture complex part designs at a reduced cost; however, the extreme pace of AM implementation introduces risks to the safe adoption of this developing technology. The development of aerospace quality standards and specifications is required to properly balance the benefits of AM technologies with the inherent risks. NASA design and construction standards do not yet include specific requirements for controlling the unique aspects of the AM process and resulting hardware. While a significant national effort is now focused on creating standards for AM, the content and scheduled release of these consensus standards do not support the near-term programmatic needs of NASA.



Aerojet-Rocketdyne

RS-25 Engine



SpaceX

SuperDraco Engine

MSFC Standard and Application to Human Spaceflight Hardware

NASA MSFC has led with the development of a Center-level standard, MSFC-STD-3716, to aid in the development of standard practices for L-PBF processes. This standard and its companion specification[2], MSFC-SPEC-3717, will now provide a consistent framework for the development, production, and evaluation of additively manufactured parts for spaceflight applications. The standard contains requirements addressing material property development, part classification, part process control, part inspection, and acceptance. The companion specification provides requirements for qualification of L-PBF metallurgical processes, equipment process control, and personnel training. Engineers from the three active human spaceflight programs have used the MSFC standard as a guideline for implementation of AM parts, assuring partners establish reliable AM processes and meet the intent of all NASA standards in materials, fracture control, nondestructive evaluation, and propulsion structures.

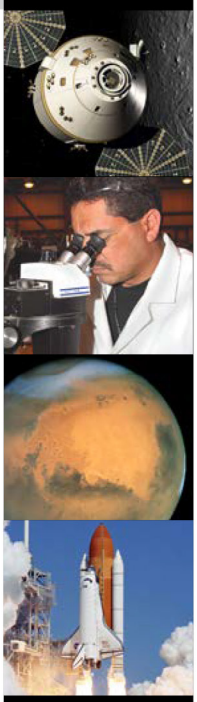
Path Forward to an AM Standard

In addition to human spaceflight, standards for appropriate application of AM to other NASA missions such as science and aeronautics require consideration. Full embrace of AM technologies requires standardization beyond the Powder Bed Fusion process. A planned Agency standard applicable to all NASA programs and most AM technologies is currently being explored. Proper standardization is the key to enabling the innovative promise of AM, while ensuring safe, functional, and reliable AM parts.

References

1. MSFC-STD-3716 "Standard for Additively Manufactured Spaceflight Hardware by Laser Powder Bed Fusion in Metals," October, 18, 2017.

2. MSFC-SPEC-3717, "Specification for Control and Qualification of Laser Powder Bed Fusion Metallurgical Processes," October 18, 2017.



National Aeronautics and Space Administration

NASA Engineering and Safety Center Technical Bulletin No. 19-01-1

Mitigating Risks of Single-Event Effects in Space Applications

Since most Electrical, Electronic, and Electromechanical (EEE) parts are intended for terrestrial applications, they are susceptible to a range of radiation threats in the space environment if the resulting effects are not properly characterized and mitigated. Even specially designed radiation-hardened parts may not be tolerant to all types of radiation effects. Radiation hardness is a multi-dimensional property of any part that describes intrinsic abilities to tolerate various radiation environments [1,2]. Effects to be concerned with include total ionizing dose, total non-ionizing dose, and single-event effects (SEE) – all of which depend on the mission, environment, application, and lifetime. Radiation effects concerns may be the same whether a EEE part is Commercial-Off-The-Shelf (COTS), MIL-SPEC, or some other variant, all of which are susceptible to the same radiation threats [3]. SEE consequences range from recoverable faults to catastrophic failure. Like other random faults, SEE can be mitigated with informed circuit design practices at the device, card, and/or system level.

Background

Good fault-tolerant design practices, broad use of radiation-hardened and minimally-radiation-susceptible parts, determined through radiation characterization in applicable environments, and sufficient shielding have minimized severe radiation-induced effects in NASA missions over the years. Unfortunately, the difficulty, cost, and time-consuming nature of radiation testing has often meant that knowledge of radiation susceptibility of the parts or circuits was not available until late in the design process. As such, modeling, earlier testing, and analysis at the part, board, and box level are increasingly important so that SEE induced failures can be included in reliability models and all of their consequences assessed. The illustration depicts how irreparable and reparable (recoverable) errors factor into a notional reliability calculation. Radiation-induced SEE that fall into these categories can be accounted for in such calculations assuming that failure rates and repair times can be accurately determined.

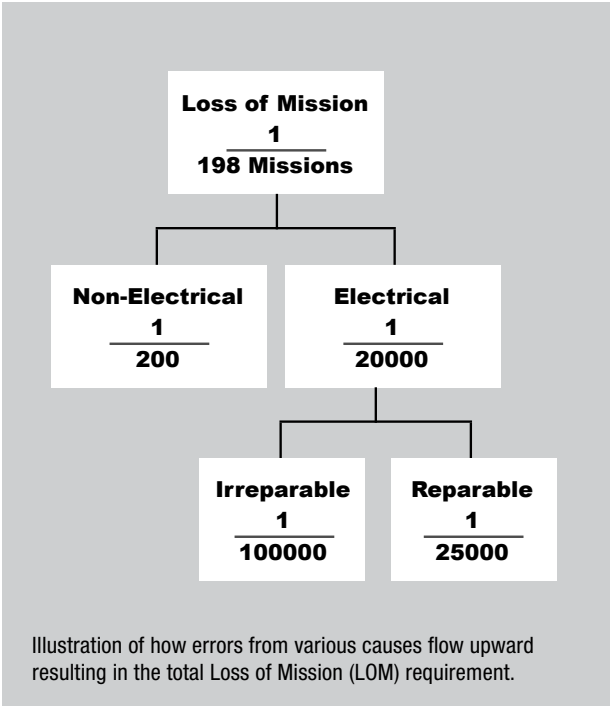


Illustration of how errors from various causes flow upward resulting in the total Loss of Mission (LOM) requirement.

Best Practices

In systems using redundant mitigation, system failure rates scale nonlinearly with unit failure rates, so limiting SEE rates is important. In particular, destructive SEE can cause failure rates to increase with time. To prevent SEE-induced failures from overwhelming system-level redundancy, it is recommended that:

1. Irreparable and reparable SEE rates should be included in system models.
   a. Include irreparable SEE rates in reliability models with other hard failures.
   b. Include reparable SEE rates in system availability models.
   c. Explore model parametric sensitivities (e.g., SEE rates, repair times, etc.) over a range of values to establish where system performance degrades unacceptably.
2. SEE testing and analysis should be prioritized based on expected benefit according to such system modeling, and function criticality.
3. System redundancy may be used for multiple purposes (e.g., a 3-unit redundant element can ensure availability if at least 1 unit remains functional, or a voting system to correct unit errors if ≥2 of 3 units remain functional). In addition, a mission may have several phases with different risk postures. System reliability and availability models should be detailed enough to assess the system risk for all the different mission phases or modes.
4. To minimize design process disruption, work-around or redesign strategies should be developed for use if parts selected for test exhibit unacceptable SEE performance.
5. For SEE susceptible functions, ensure through design, test, and analysis that devices are protected from SEE-induced transient effects and have sufficient margin to account for bounding conditions defined by the mission, environment, application criticality, and lifetime requirements.

References

1. NASA/TM-2019220269, Radiation Single Event Effects Impact on Complex Avionics Architecture Reliability, April 2019
2. NASA/TM-20210018053, Avionics Radiation Hardness Assurance (RHA) Guidelines, July 2021
3. NASA/TM-20205011579, Recommendations on Use of Commercial-Off-The-Shelf (COTS) Electrical, Electronic, and Electromechanical (EEE) Parts for NASA Missions, June 2021

90/95 POD Radiography Concern for COPVs and Metal Tank Welds

Radiographic inspections of welds in all-metal tanks and composite overwrapped pressure vessel (COPV) liners that are used to establish initial crack size in damage tolerance assessments are not as rigorous as previously understood. As a result, the 90/95 percent probability of detection (POD) requirements in S-080[1] and S-081[2] are not met when this inspection method is used. Development of new inspection methods will require about three years. During that time, additional review and assessment of the fracture margin may be needed to support waivers and provide a better understanding of weld cracking risk associated with an individual tank design.

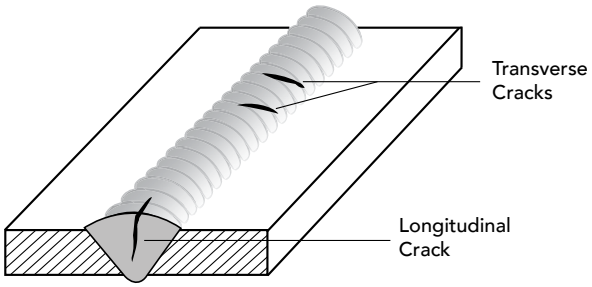


Illustration of metal weld cracks

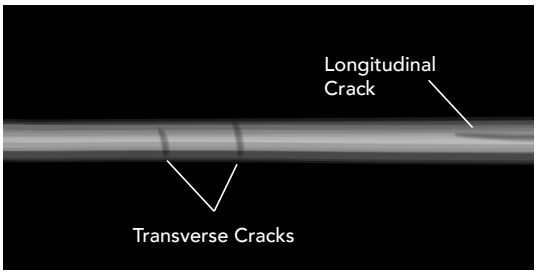


Illustration of notional radiographic inspection of metal weld cracks

Discussion

Damage tolerance life (safe-life) for COPVs and metallic tanks is a deterministic damage tolerance approach required by S-081 and S-080. It assumes the existence of cracks of a size that can be reliably detected by an established nondestructive evaluation (NDE) method used to inspect the liner/tank prior to service. The intent of damage tolerance life is to demonstrate that cracks at or below this size will not grow to failure during the service life. S-081 and S-080 require that this initial crack size be determined from the sensitivity limit of the 90% POD at a 95% confidence level.

For volumetric inspections of tank welds and domes, tank manufacturers typically use radiography. The majority use a crack depth of 60% of the thickness (0.6t, identified as special radiography) and specific inspectors and processes have been certified by NASA to be able to detect cracks of that size with POD of 90/95 in accordance with NASA-STD 5009[3]. The larger, 0.7t crack depth is occasionally used and requires less rigor under NASA-STD 5009.

Recent radiography studies have concluded that 0.6t and 0.7t cracks are not as consistently detectable as previously understood. Detectability of cracks on the film (or digital radiography) is sensitive to several parameters: the need for double-wall inspection on close-out welds, separation distance of the tank walls, incidence angle, wall thickness, and exposure time. These parameters have not been included in certification tests in the past, but were found to be important in crack detection. Implementation of more stringent certification tests that capture these parameters will take about three years since new image quality aids will need to be developed, qualified, and implemented. It is understood that these planned improved double-wall radiography methods may not be achievable in all tank designs. In the near term, certifications will continue in the current protocol to establish that heritage capability has not changed.

As a result, manufacturers that are currently certified to 0.6t or 0.7t radiography may not be able to detect cracks of that size with 90/95 POD, so the risk of missing a crack larger than 0.6t or 0.7t is higher than previously understood. This risk has been present in previous flights, but was not appreciated until recent studies of radiography techniques were completed.

Since the damage tolerance analysis or test assumes crack sizes associated with radiography, additional analysis and tests may be needed to understand fracture risks associated with cyclic and sustained load crack growth. Tests of larger initial crack sizes or better understanding of analytically-derived fracture margin and critical initial flaw size analysis may be needed to support waivers against the 90/95 POD requirements in S-081 and S-080 and provide a better understanding of the risks associated with individual tank designs.

References

1. American Institute of Aeronautics and Astronautics (AIAA) S-080 Space Systems - Metallic Pressure Vessels, Pressurized Structures, and Pressure Components
2. AIAA S-081, Pressure Vessel Standards Implementation Guidelines
3. NASA-STD-5009 Nondestructive Evaluation Requirements for Fracture-Critical Metallic Components

For information contact Dr. Grimes-Ledesma at
lorie.r.grimes-ledesma@jpl.nasa.gov

Latching Safety Critical Signals in Pyrotechnic Circuits

In recent designs of safety-critical pyro control circuitry, latching circuits, used to store the state of control signals, have been found to have sensitivity to noise that could lead to inadvertent firing. This technical bulletin describes the sensitive circuit, and provides best practice recommendations to improve the design.

Background

Recent designs of pyro control circuits utilized D Flip-Flops (F/Fs) to latch critical signals that must persist after loss of main power. These F/Fs and subsequent logic, control the MOSFETs used to fire the pyro initiator. These designs used discrete D-type F/Fs in the configuration shown in Fig. 1 to latch the incoming signal that was applied to the clock line (CP) input.

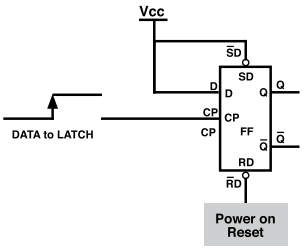


Fig. 1: Sensitive Latching Circuit

One circuit inadvertently fired a pyro during a pyro shock test and the sensitivity of this configuration was deemed to be a contributor to root cause.

The circuit used to capture the state of fire control signals in Fig. 1 sets the F/F on the positive edge of the clock line. Clock inputs on F/Fs are edge-triggered and can respond to very fast pulses. The problem with this design approach is that noise on the clock line can set the F/F. The design has three undesirable features: (1) the D input is preloaded by connecting it directly to Vcc, (2) there is susceptibility to high frequency noise as the CP input can respond to nanosecond pulses, and (3) there is no mechanism to limit or qualify the clock input to reduce the window of when noise could affect the circuit. Alternate design approaches can reduce the sensitivity of this circuit.

Recommended Design Best Practices

A number of simple enhancements can be made to improve this design. The preferred method would be to qualify the data signal. This is possible if the source of the signal is coming from a circuit that can also produce a qualifying data strobe indicating that the data is valid. For example, if the signals come from a micro-controller (as was the case with the system that misfired) two output ports could be used in the configuration as shown in Fig. 2.

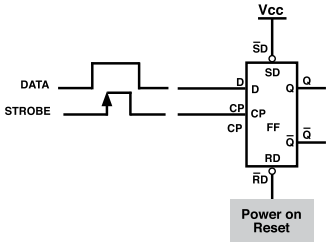


Fig. 2: Improved Latching Circuit

This circuit has the advantage that the F/F will only be set when DATA is coincident with the positive edge of the STROBE; at other times the F/F will be immune to noise. In pyro control systems that use a 2-phase ARM and FIRE control approach, the ARM control can potentially be used on the DATA input and the FIRE control can be used to latch the DATA on the STROBE input. When a DATA/STROBE configuration is not possible other techniques can be used to improve noise immunity.

A simple RC low pass filter shown in Fig. 3 can be added to the clock line in Fig. 1. This will attenuate noise above the cutoff frequency (fc) where fc=1/ (2πRC). A word of caution with this approach, some F/Fs will not operate properly if the clock edge transitions too slowly. One should use a F/F (i.e. 74LVC1G74) with a Schmitt trigger on the clock input that can tolerate a slow clock rise time, or the design should include an external Schmitt trigger.

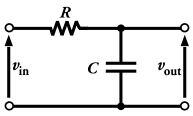


Fig. 3: Low-Pass Filter

Alternately, a debouncer (i.e. LCT6994) shown in Fig. 4 can be used as a low-pass filter. A delay value can be set with an external resistor network as shown.

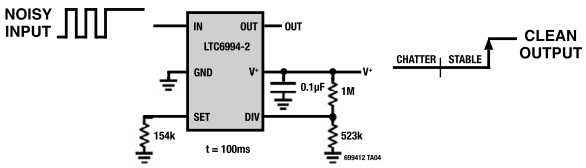


Fig. 4: Debouncer

In this configuration, the input signal must be stable for 100ms before the output changes; short pulses are ignored (filtered). For this to be effective, the debouncer and F/F of Fig.1 should be located near each other to minimize the signal path. It is also possible to apply a combination of techniques to ensure correct data latching. Lastly, confirming the design noise margin, either by test or via analysis when test is impractical, to inadvertent firing is important in a system where an inadvertent fire is catastrophic. This margin should be on critical control inputs in thresholding logic ahead of the fire control inhibit semiconductor switches. Per specifications that date back to MIL-STD-1576, the noise floor during tests should not reach ½ the threshold voltage (6 dB) required to activate the devices.

References

1. LTC6994 Datasheet, Linear Technologies
2. 74LVC1G74-Q100 Datasheet, Nexperia

For information contact Dr. Robert F. Hodson, robert.f.hodson@nasa.gov.

Effective and Environmentally Compliant Cleaner - Solstice® Performance Fluid

On January 1, 2015, the United States Environmental Protection Agency identified exemptions on the continued use of the hydrochlorofluorocarbon (HCFC)-225ca and -225cb. As these solvents are commonly used in cleaning and verification of aerospace propulsion systems using liquid and gaseous oxygen, the NESC supported the Agency initiative to identify and characterize acceptable alternate fluids. Honeywell's Solstice® Performance Fluid (PF), PF-high purity (HP), and PF-HP spray are an effective nonflammable cleaning solution system, with a favorable toxicity profile and low environmental impact. Solstice PF is suitable for electronics, metal, and precision cleaning. It can be used in vapor degreasing equipment and may be dispensed with a propellant to create an aerosol contact cleaner. Solstice PF has been shown to have negligible ozone depletion and a global warming potential of 1. With these characterized environmental and solvency properties, Solstice PF, PF-HP, or PF-HP spray may be an excellent choice for a variety of cleaning applications.

Cleaning Capabilities: The solubility characteristics allow for Solstice PF (NVR < 10 PPM) and PF-HP (NVR< 2 PPM) to be used to dissolve a number of typical soils that are encountered in military and aerospace cleaning operations.

Non-Flammable: Solstice PF does not exhibit flashpoint or vapor flame limits. It was determined not to have vapor flame limits at temperatures to 100°C (212°F) using an ASTM E 681 apparatus.

Oxygen System Cleaning: Solstice PF, PF-HP, and PF-HP spray are well suited for oxygen line cleaning as they effectively remove contamination and then can be completely dried. Solstice PF-HP and PF-HP spray passed the mechanical impact tests per ASTM D 2512- 82, has an oxygen-enriched autoignition temperature of 182°C (360°F) at 13.8 MPa (2,000 psig) per ASTM G 72, and Heat of Combustion of 2,448 kcal/kg (4,403 BTU/lb) per ASTM D240.

Compatibility: Solstice PF is compatible with metals commonly used in aerospace and military, and in all cases the metals tested per ASTM F483 indicated no solvent breakdown or acid formation.

Implementation Consideration: Solstice PF characteristics compared to other currently available cleaning solutions:

- Low solvent loss due to:
  - High heat of vaporization, and low surface tension - improved wetting characteristics and reduced drag-out loss
  - Recovery potential - distillation and carbon recovery
- Reduced energy requirements for processing
- High solvency, not a high-cost filler - reduces or eliminates blending
- High wetting index for removal of particulate matter from complex parts
- No post-process residue removal
- Potential drop-in alternative in aerosol cleaners

The unique solubility characteristics, high performance, nonflammability, stability, low toxicity, and environmental compliant properties of Solstice PF and PF-HP allow for use in a wide variety of applications from oxygen line cleaning to degreasing. NASA Cleaning Facility Conversion: Cleaning facilities at SSC and MSFC have converted to Solstice PF with minimal issues. Points of contact at these facilities are Rick Ross (harold.r.ross@nasa.gov, 228-688-2353) and Mark Mitchell (mark.a.mitchell@nasa.gov, 256-544-5860).

References

1. Replacement of Hydrochlorofluorocarbon-225 Solvent for Cleaning and Verification Sampling of NASA Propulsion Oxygen Systems Hardware, Ground Support Equipment, and Associated Test Systems, NASA/TP-2015-218207

2. Solvent Replacement for Hydrochlorofluorocarbon-225 for Cleaning Oxygen System Components, NASA/TM-2017-219687

3. ASTM STP 1596, "Flammability and Sensitivity of Materials in Oxygen-Enriched Atmospheres, 14th Volume. (West Conshohocken, PA: ASTM International, 2016)



Solstice® Performance Fluid

Environmental and Safety Properties

Flash Point	None
Lower/Upper Flame Limit (volume %)	None
Occupational Exposure Limit (PPM)	800
Global Warming Potential (100-year)	1
Volatile Organic Compound (U.S. and California South Coast Air Quality Management District)	Exempt

Physical Properties

Property	Solstice PF
Chemical Name	trans-1-chloro-3,3,3 trifluoropropene
Molecular Formula	CF3-CH=CCIH
Molecular Weight	130
Boiling Point	19°C (66°F)
Latent Heat of Vaporization at Boiling Point	194 kJ/kg (83.4 BTU/lb)
Freezing Point	-107°C (-161°F)
Vapor Pressure at 20°C (68°F)	109 kPa (15.8 psia)
Liquid Density at 20°C (68°F)	1.27 gm/mL (10.6 lb/gal)
Surface Tension at 20°C (68°F)	12.7 dyne/cm
Liquid Viscosity at 20°C (68°F)	0.503 cP
Solubility of Water in Solvent at 25°C (77°F)	460 ppm
KB Value	25



For information, contact Steven J. Gentz at steven.j.gentz@nasa.gov.

Navigation Filter Design Best Practices

Onboard navigation and attitude estimation systems are at the heart of almost all of NASA's missions, either on launch vehicles, robotic science spacecraft, or on crewed human exploration vehicles. Best practices for attitude estimation systems/filters are scattered throughout open literature, however, even within NASA there has been no previous attempt to codify this knowledge into a readily available design handbook. Without such a document, it is possible for isolated practitioners to lack understanding and appreciation of many tried and true approaches to successful and robust filter design, including the implied cost/benefit trades associated with them. To aid designers of current and future missions, a handbook of navigation filter best practices has been developed and is introduced here [1]. The development of this document is also an outgrowth of a recommendation made in an NESC summary of lessons learned from the DARPA Orbital Express mission to utilize best practices for rendezvous navigation filter design [3]. With this handbook, future designers have a reference that establishes NASA's best practices.

Background

Safe and reliably-performing navigation systems are essential elements for a wide variety of missions. These include routine low-Earth orbiting science missions, rendezvous and proximity operation missions or precision-formation flying missions (where relative navigation is a necessity), navigation through the solar system, precision landing on planets/small bodies, and many more mission types.

NASA pioneered the use of the Extended Kalman Filter (EKF) for onboard navigation of the Apollo missions' lunar rendezvous. The story of the development of the EKF has been well-chronicled [2]. However, the accumulated art and lore, tips and tricks, and other institutional knowledge that NASA navigators have employed to design and operate EKFs is much less well-known. This body of knowledge has been used to support dozens of missions in the Gemini/Apollo era, well over one hundred Space Shuttle missions, and numerous robotic missions, without a failure ever attributed to an EKF.

Summary of Navigation Filter Best Practices

This bulletin presents a few of the onboard navigation filter best practices and sets the stage for the reader to delve into a more comprehensive set in the reference below.

a. Maintain an accurate representation of the target-chaser relative state estimation errors, including an accurate variance-covariance matrix. This allows the filter to compute an appropriate gain matrix. It also aids the filter in appropriately editing unsuitable measurements.

b. Provide a capability for measurement underweighting that adapts to the current uncertainty in the filters state estimation error, as required to be consistent with the suboptimality of the navigation filters measurement update. Multiplicative adjustment of the measurement noise covariance matrix within the computation of the residual covariance has been found to be less effective and is not recommended unless other methods are not feasible.

c. Estimate states that model biases in sensor measurements and account for unmodeled accelerations. Gauss-Markov models for these biases have been found to be more effective than random-constant or random walk models. Random-constant models can become stale, and random walk models can overflow during long periods without measurement updates.

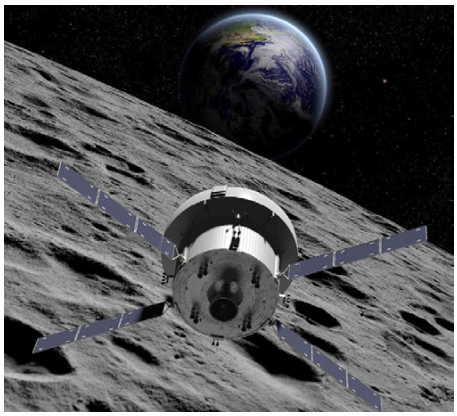


Illustration of Orion spacecraft in lunar orbit

d. Provide commands that allow for selective processing of individual measurement types. If the filter utilizes an automated residual-edit process, then the recommended command capability should be able to override the residual-edit test.

e. Maintain a backup ephemeris, unaltered by measurement updates since initialization, which can be used to restart the filter without uplink of a new state vector.

f. Provide a capability for reinitializing the covariance matrix without altering the current state estimate.

g. Ensure tuning parameters can be uplinked to the spacecraft and are capable of being introduced to the filter without loss of onboard-navigation data.

h. Provide flexibility to take advantage of sensors and sensor suites full capability over all operating ranges.

References

1. Navigation Filter Best Practices, J.R. Carpenter and C.N. D'Souza Eds., 2018, NASA/TP-2018-219822, https://ntrs.nasa.gov/archive/nasa/casi.ntrs.nasa.gov/20180003657.pdf.
2. S.F. Schmidt. The Kalman Filter - Its Recognition and Development for Aerospace Applications. Journal of Guidance, Control, and Dynamics, 4(1):4–7, 2016/01/09 1981.
3. C.J. Dennehy and J.R. Carpenter. A Summary Of The Rendezvous, Proximity Operations, Docking, And Undocking (RPODU) Lessons Learned From The Defense Advanced Research Project Agency (DARPA) Orbital Express (OE) Demonstration System Mission. NASA/TM-2011-217088, NASA Engineering and Safety Center, 2011.

For information, contact Neil Dennehy at cornelius.j.dennehy@nasa.gov.

Alternative O-Rings for Hypergolic Propellant Systems

O-rings are used in many NASA propulsion systems to seal high pressure lines that contain liquid engine propellants and gases. Production of a widely-used commercial O-ring, compatible with these liquids and gases, was discontinued due to lack of a key compound ingredient. The NESC engaged O-ring and material manufacturers and performed extensive materials compatibility testing to find suitable replacements. These replacement candidates are still awaiting qualification to NASA design and construction standards (e.g., NASA-STD-6016, etc.).

Background

Parker-Hannifin has stopped making O-rings with E0515-80, an ethylene propylene diene monomer (EPDM) material often used in hypergolic propellant systems. Production was halted due to a supplier of an E0515 compound ingredient unexpectedly and suddenly ceasing operations in late 2018. The O-rings are used in many NASA programs. An NESC assessment team was formed and planned to test several candidate replacement materials to avoid future dependence on a single material. While the E0515 O-rings are used in multiple applications across NASA, the use of the rings in hypergolic propellants is of particular interest. Parker-Hannifin suggested another in-house material, EM163, as the replacement for E0515. EM163 is a Shore M 80-durometer EPDM material, certified to NAS1613 Rev. 6, a specification for use in hydraulic fluid systems. Note that E0515 was certified to NAS1613 Rev. 2. The main difference between Rev. 2 and Rev. 6 is the requirement to be compatible with additional hydraulic fluids. Parker-Hannifin expects EM163 to perform similarly to E0515 but did not perform testing for hypergolic propellant compatibility.

Replacement Materials Testing and Results

The NESC assessment team chose six candidate materials for testing as possible E0515 replacements. The assessment team also contacted several material compounding firms in the event none of the six candidate materials were found to be compatible. Short and long-duration tests were performed in accordance with standard testing procedures. Figure 1 shows unexposed and exposed Park-Hannifin E0515 O-rings from the short-duration testing. Two of the candidate materials, including the EM163 material suggested by Parker-Hannifin, were eliminated from consideration after short-duration testing.

Three materials, Parker E0540, Precix E152, and Parco 5778-80, successfully completed short- and long-duration testing and are considered compatible replacements for Parker E0515 in hypergolic propellant applications. One material, Freudenberg-NOK E458, gave mixed results during the short- and long-duration testing and is considered a compatible replacement for Parker E0515 in limited hypergolic propellant applications.

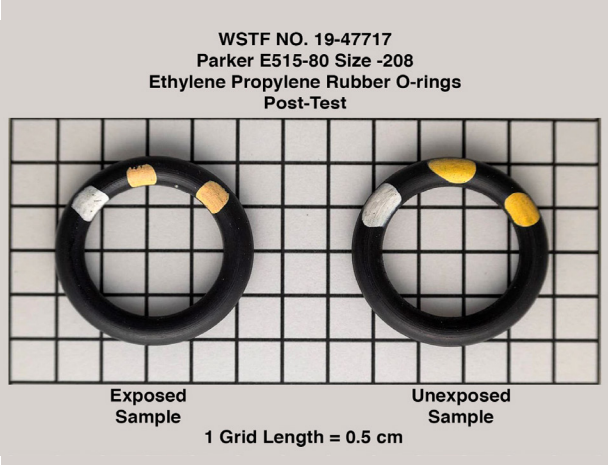


Figure 1. Unexposed and exposed Parker-Hannifin E0515 O-Rings.

References

1. ASTM D395, Standard Test Methods for Rubber Property—Compression Set.
2. NASA-STD-6001B, Flammability, Offgassing, and Compatibility Requirements and Test Procedures, April 21, 2016.
3. Parker O-Ring Handbook, ORD-5700, Parker Hannifin Corporation, Cleveland, OH, 2018.

For information, contact Daniel J. Dorney at daniel.j.dorney@nasa.gov.

National Aeronautics and Space Administration

NASA Engineering and Safety Center Technical Bulletin No. 20-05

Determination of Autogenous Ignition Temperature of Isopropyl Alcohol and Ethanol

The NESC performed tests to measure the autogenous ignition temperature (AIT) of isopropyl alcohol (IPA) and ethanol in a pressurized, pure oxygen environment. The available data were for lower pressures than required and the majority of the data were for air rather than oxygen. Test results showed the average AITs for IPA in gaseous oxygen at 10.3 megapascals (MPa) (1,500 psi) and 15.2 MPa (2,200 psi) were 199.3 degrees Celsius (°C) (390.8 degrees Fahrenheit (°F)) and 201.6°C (394.8°F), respectively. The average AITs for ethanol in gaseous oxygen at 10.3 MPa (1,500 psi) and 15.2 MPa (2,200 psi) were 193.2°C (379.8°F) and 198.2°C (388.8°F), respectively.

Background

A request was recently made to NASA to provide the autogenous ignition temperature (AIT) of isopropyl alcohol (IPA) in a pressurized, pure oxygen environment. NASA provided the available data, but there was significant variability between data sources. The available data were for much lower pressures than required, and the majority of the data were for air rather than oxygen. The scatter seen in previous tests was likely due to test configuration and experimental technique differences, as well as inherent variability in the AIT response itself. NASA was requested to experimentally determine the AIT of both IPA and ethanol, both of which are extensively applied as cleaners and solvents in propulsion systems.

Test Procedures

The AIT testing of IPA and ethanol was performed at White Sands Test Facility (WSTF) for pressures representative of those found in spacecraft and launch vehicle propulsion systems. The WSTF standard test method was performed as follows. A sample holding assembly, contained within a reaction vessel pressurized with 100% oxygen to the required test pressure, was heated in an electric furnace at a rate of 5 ± 1°C (9 ± 1°F)/min from 60 to 260°C (140 to 500°F). Heating of the vessel was continued at an uncontrolled rate to a maximum temperature of 450 °C (842°F). Temperatures were monitored as a function of time by means of a thermocouple and data acquisition system. During testing, pressure was monitored but not maintained. Ignition of the test sample was indicated by a rapid temperature rise of at least 20°C (36°F) and was confirmed post-test by the destruction of the sample.

The tests used Sigma-Aldrich anhydrous 2-propanol (IPA), part number 278475, 99.5% purity, and Sigma-Aldrich ethyl alcohol (ethanol), pure, part number 459844, minimum 99.5% purity, American Chemical Society reagent. Both the IPA and ethanol were used as received without further purification. Testing was performed for the IPA and the ethanol at both 10.3 MPa (1,500 psi) and 15.2 MPa (2,200 psi). Five tests were run at each pressure using ~200 mg each of the IPA and ethanol. An additional test was run using 500 mg of IPA at 1,500 psi.

Results

The results are tabulated in Tables 1 and 2.

20-47851 - IPA

Sample Number	Test Pressure		Sample Weight	AIT		Pressure at Ignition		Δ Temp Rise on Ignition		Δ Press Rise on Ignition	
	MPa	(psia)	g	°C	(°F)	MPa	(psia)	°C	(°F)	MPa	(psia)
1	10	1500	0.217	196	385	16	2393	81	145	4	545
2			0.22	198	388	16	2354	111	200	3	468
3			0.225	203	397	17	2400	124	223	3	418
4			0.222	189	373	15	2247	105	189	5	702
5			0.213	211	411	16	2384	56	101	3	405
Average			0.2194	199.3	390.8	16.2	2355.6	95.3	171.6	3.5	507.6
1	10	1500	0.521	208	407	17	2424	311	559	14	1979
1	15	2200	0.221	202	396	24	3445	144	259	5	706
2			0.22	194	381	24	3526	88	159	4	595
3			0.218	201	394	19	2753	89	161	4	645
4			0.212	205	401	25	3664	77	138	4	629
5			0.226	206	402	24	3435	106	191	6	933
Average			0.2194	201.6	394.8	23.2	3364.6	100.9	181.6	4.8	701.6

Table 1. Autogenous ignition temperatures for IPA.

20-47852 - Ethanol

Sample Number	Test Pressure		Sample Weight	AIT		Pressure at Ignition		Δ Temp Rise on Ignition		Δ Press Rise on Ignition	
	MPa	(psia)	g	°C	(°F)	MPa	(psia)	°C	(°F)	MPa	(psia)
1	10	1500	0.224	184	364	15	2173	114	205	2	339
2			0.231	198	389	16	2336	102	183	2	324
3			0.224	204	400	17	2494	76	136	4	618
4			0.221	191	375	16	2366	97	175	3	448
5			0.223	188	371	16	2328	97	175	3	394
Average			0.2246	193.2	379.8	16.1	2339.4	97.1	174.8	2.9	424.6
1	15	2200	0.218	201	393	26	3717	64	115	4	634
2			0.216	202	396	24	3547	78	140	4	536
3			0.217	202	396	25	3621	67	121	4	621
4			0.218	200	392	25	3636	76	136	3	470
5			0.219	186	367	25	3615	81	146	5	653
Average			0.2176	198.2	388.8	25.0	3627.2	73.1	131.6	4.0	582.8

Table 2. Autogenous ignition temperatures for ethanol.

References

1. Dorney, D.; Harper, S.; Reys, I.; Wentzel, D.; McClure, M.; Juarez, A.: Determination of Autogenous Ignition Temperature for Isopropyl Alcohol and Ethanol. NASA/TM-2020-5004683.
2. ASTM G72/G72M-15, Standard Test Method for Autogenous Ignition Temperatu re of Liquids and Solids in a High-Pressure Oxygen-Enriched Environment, ASTM International, West Conshohocken, Pennsylvania.
3. Wegener, W.; Binder, C.; Hengstenberg, P.; Herrmann, K.-P.; and Weinert, D.' "Tests to Evaluate the Suitability of Materials for Oxygen Service," Flammability and Sensitivity of Materials in Oxygen-Enriched Atmospheres: Third Volume, ASTM STP 986, D. W. Schroll, Ed., ASTM, Philadelphia, 1988, pp. 268-278.

For information, contact Daniel J. Dorney at daniel.j.dorney@nasa.gov.

National Aeronautics and Space Administration

NASA Engineering and Safety Center Technical Bulletin No. 20-06

Material Compatibility Assessment of Spacecraft Oxidizer Systems

Recently designed oxidizer systems used in spacecraft propulsion are pushing the limits of materials and operating conditions. As a result, nitrogen tetroxide (NTO) oxidizer systems are exhibiting failures driven by ignition mechanisms similar to oxygen systems. Oxidizer systems (e.g., O_2, N_2O_4, N_2O, H_2O_2) have generally been designed and operated within industry experience for material corrosion concerns without a thorough understanding of potential material ignition and burning. To compound the problem, the effects of varying parameters on ignition and the kindling chain have not been studied, and there is a very limited amount of published data to help with the understanding. NASA-sponsored testing is actively researching ignition mechanisms, determining thresholds, and defining operating envelopes to inform the aerospace community.

Applicability

The information in this technical bulletin is applicable to spacecraft oxidizer systems found to be situationally flammable with oxidizers. Titanium was the focus of recent work in the presence of NTO, but other metals such as certain thicknesses of stainless steel and also soft goods may be susceptible as well in the right configuration.

Background

Recent testing found that traditionally acceptable materials of construction (titanium and certain thicknesses of stainless steel) are flammable and ignitable in NTO. Literature searches, flammability testing, and ignition testing confirmed that these materials are sensitive to ignition in much the same way as they are in oxygen systems. Flammability and ignition susceptibility have traditionally not been evaluated for these types of propulsion oxidizer systems other than oxygen.

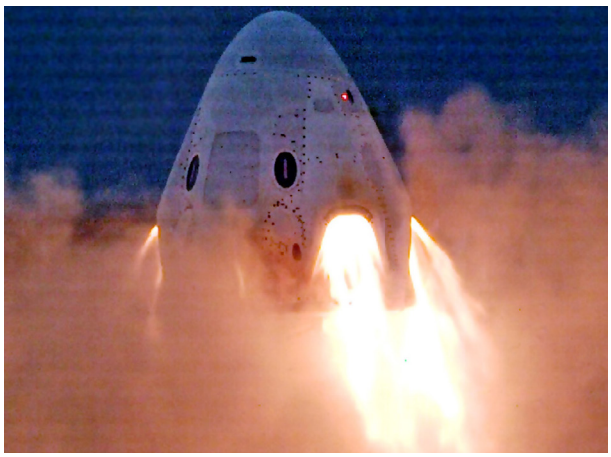
Discussion

Recent testing has identified the need for compatibility assessments in all oxidizer systems consistent with oxygen systems per NASA-STD-6016A. As a result, NASA-STD-6016A has been updated with this requirement. The recommended oxidizer compatibility evaluation process for NTO and other oxidizers is based on the existing oxygen compatibility assessment process per NASA/TM-2007-213740. Materials evaluation testing is performed per NASA-STD-6001B.

The intent of the oxidizer compatibility assessment process is to identify the likelihood of ignition for flammable materials through system interrogation. High probability ignition sources can be further assessed through targeted testing at the material, component, or system level. The process also identifies potential hazard controls through material change, system configuration, or operation.

Path Forward

NASA-STD-6016B now requires all spacecraft oxidizer systems to be evaluated per NASA/TM-2007-213740. NASA-sponsored testing is actively researching ignition mechanisms, determining thresholds, and defining operating envelopes to inform the aerospace community.



Successful static fire test with incorporated lessons learned

References

1. NASA-STD-6016B Standard Materials and Processes Requirements for Spacecraft
2. NASA/TM-2007-213740 Guide for Oxygen Compatibility Assessments on Oxygen Components and Systems
3. NASA-STD-6001B Flammability, Offgassing, and Compatibility Requirements and Test Procedures

For information, contact Gregory J. Harrigan at gregory.j.harrigan@nasa.gov.

National Aeronautics and Space Administration

NASA Engineering and Safety Center Technical Bulletin No. 20-07

Evaluating and Mitigating Liner Strain Spikes in COPVs

Unexpected cracking and leaking in bonded composite overwrapped pressure vessel (COPV) liners occurring in recent test programs have been attributed to liner strain spikes observed through measurement and predicted by analysis. Diminished load transfer between the liner and composite overwrap can lead to localized excessive liner yielding in the dome section. This diminished constraint can occur due to yielding of the adhesive or a manufacturing unbond defect. COPVs should be assessed for susceptibility to this new failure mode.

Background

COPVs are often designed with a bond between the liner and composite. The purpose of the bondline is to provide load transfer continuity between the liner and overwrap during pressurization and depressurization cycles throughout the lifetime of a COPV. In the cylinder region the liner and overwrap longitudinal strains are often similar; therefore, the bondline is not highly strained in shear. However, longitudinal strains are not similar in the dome, leading to development of bondline shear stress. This shear stress can concentrate in the liner at geometric transitions such as at a liner thickness taper near the boss.

Bondline Strain Mechanisms

If the liner taper does not smoothly transfer load into the overwrap from the liner, stress concentrations can result in both the liner and the bondline. For example, if the taper is too short, then geometric stress concentrations in the liner occur near the thin end of the liner taper along with an abrupt increase of adhesive shear stress between the liner and overwrap as the liner thickness increases. These stress concentrations can result in larger plastic strains than intended in both the liner and adhesive and when these large plastic strains occur at the same location in the liner and the adhesive, the liner deforms independently from the overwrap. This allows the plastic strain in the liner to localize and the resulting strain spike can increase quickly with additional deformation. The figure shows large plastic strains in the adhesive associated with the strain spike in the liner can lead to failure of the adhesive, increasing the independence of the liner. A similar plastic strain concentration in the liner can occur in regions where the composite and liner are unbonded due to a manufacturing error.

Recommendations to Mitigate Bondline Strain Spikes

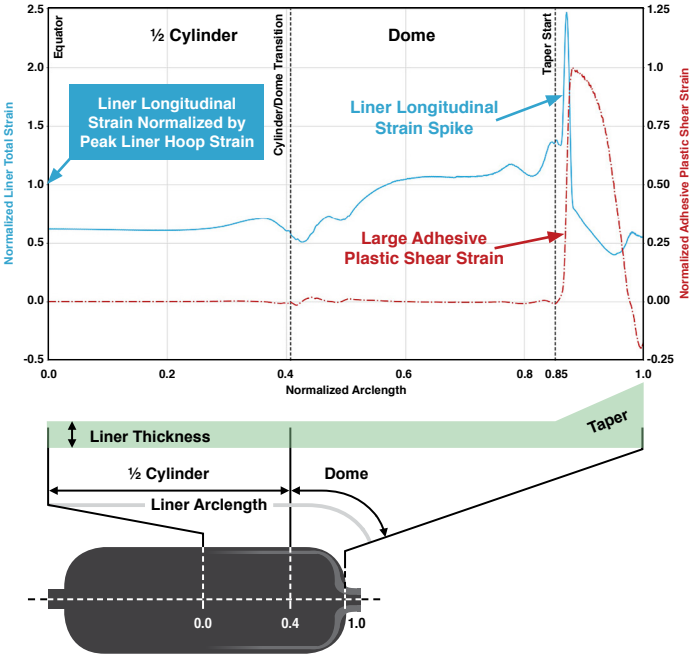
Liner strain concentrations from adhesive and liner yield interaction or manufacturing defects can lead to crack nucleation and growth or development of a liner buckle. To evaluate the risk, the margin of safety should be determined at design burst. If it is positive, then examine strain distributions for evidence of alignment of adhesive and liner yield. If the adhesive is predicted to yield or disbond at a location concurrent with net section liner yielding, perform one of the following:

1. Explicitly model the bondline with elastic-plastic properties and re-evaluate the development of the liner strain spike. Determine the magnitude of any strain spike that develops in this new model. If adhesive strains approach the shear failure criterion of the bondline, then a local disbond should be modeled and strain spikes re-evaluated.
2. Add a disbond only at the location where the adhesive exceeds yield and determine the magnitude of any strain spike that develops in the liner.

Note that simulating a disbond over the entire bondline either by releasing nodes or diminishing shear modulus is not necessarily conservative. To evaluate the significance of the strain spike for all pressure conditions of the COPV, include the magnitude of the strain spike in all required verification activities associated with crack nucleation, crack growth, and liner buckling failure modes in ANSI/AIAA S-081B Space Systems-Composite Overwrapped Pressure Vessels (sections 5.2.13 Fracture Control Design, 5.2.14 Fatigue Life Design, 5.2.6 Negative Pressure Differential Design, and 5.2.10 Stability Design). The potential for local normal deflection reversals (oil-canning) at a disbond should be considered in crack nucleation and growth failure modes.

If the magnitude of the liner strain spike is too large to be robust to these failure modes, then the design can be modified to reduce the shear stress in the adhesive below yield. For example, increasing the taper length could be considered. In addition, process control measures should be implemented to ensure that the risk of unbonds is acceptably low.

Analytical Results: Explicitly Modeled Elastic-Plastic Adhesive, Disbond Not Included



www.nasa.gov *For information contact Dr. Grimes-Ledesma at lorie.r.grimes-ledesma@jpl.nasa.gov*

NESC tech bulletin

National Aeronautics and Space Administration

NASA Engineering and Safety Center Technical Bulletin No. 20-08

Assessment of Ketazine Derived High Purity Hydrazine for Spacecraft Propellant Systems

Hydrazine and its derivatives have dominated the class of hypergolic liquid propellants for bipropellant propulsion systems in rockets such as the Titan, MX Missile, and Ariane; it has also been widely utilized as a monopropellant in auxiliary power units and in thrusters for altitude and in-orbit control of satellites and spacecraft. With continued use of hydrazine in current and future spacecraft and payloads, it is necessary to understand the historical and current states of synthesis for the commodity and possible implications that may arise from changes in production processes for the United States stock.

Background

A particular concern with newer methodologies for synthesizing high purity hydrazine (HPH) is the presence of extraneous unknown carbonaceous materials. These are organic byproducts from the synthesis processes, which may or may not have serious effects on the long-term storage of the commodity or on propulsion performance of the material. Further, changes in process methods could also alter the residual content levels of other components (e.g., cadmium, tin, or silicon). Traditionally, only iron (Fe) content has a limit in military specification MIL-PRF-26536G HPH; however, with different processes now being utilized for production, not only is a comprehensive analysis of elemental content required to determine what different constituents are present, but the question also remains whether iron should still be the only metal/element monitored on a regular basis.

Arch Chemicals (now Lonza Group) were the pioneers of hydrazine production in the United States using the Olin Raschig Process based on the oxidation of ammonia using alkaline hypochlorite. The development of the Military Specification, MIL-PRF-26536G, for certification of hydrazine, focused on inclusion of contaminants related to this specific production process. While Lonza maintains operation of a blending/purification facility at their plant, they no longer produce hydrazine via the Raschig method. Instead, hydrazine hydrate is purchased from an external, non-U.S., entity and purified to high purity requirements by Lonza. The common newer methods used worldwide for hydrazine synthesis are ketazine-based processes where the oxidation of ammonia occurs in the presence of aliphatic ketones to yield a ketazine intermediate. The intermediate is then subsequently hydrolyzed to form hydrazine. With the introduction of organic species in the synthesis, numerous byproducts can be produced and possibly present in the final product that were not previously a concern and are not identified for monitoring in the procurement specification. Beyond organic impurities, these new processes may also cause other constituents such as metals to be retained in the final product.

Current Results from Hydrazine Sample Testing

Recent testing of HPH samples at Kennedy Space Center (KSC) yielded extraneous, unidentified peaks in the carbonaceous assay when analyzing HPH made from this newer ketazine method. In 2017, Revision G of MIL-PRF-26536 was adapted to include other carbonaceous materials (OCM) - anything that produced a positive FID response – in addition to "other volatile carbonaceous materials, UDMH, MMH, and isopropanol" as part of the total carbonaceous measurement. However, actual identification of these OCM peaks has not been explored until now (See Figure 1). Data for a comprehensive elemental analysis for the HPH material is also lacking for baseline data collection and evaluation. New analytical methods via GC-MS and ICP-OES have been developed to resolve these shortcomings in data for ketazine-derived HPH. With different vendors and processes now being utilized for production, a comprehensive analysis of elemental content is required to determine what different constituents are present. The NESC will soon release a review of synthesis methodologies along with results from current analytical work at KSC for the identification of the aforementioned carbonaceous species and elemental profiling in recent lots of ketazine-derived HPH.

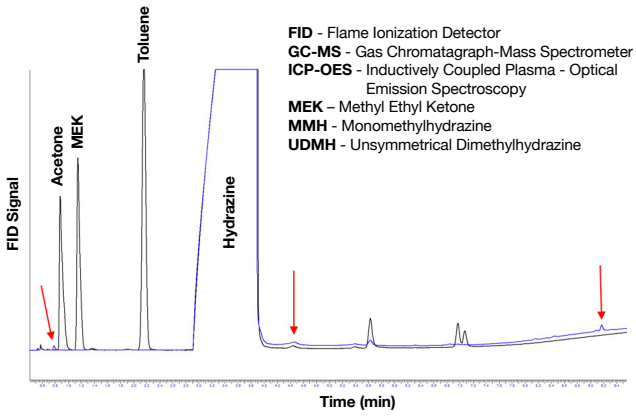


Figure 1. Overlay of 100-ppm Acetone-MEK-Toluene standard (Black) and Ketazine HPH sample (Blue). Red arrows show contaminants not yet elucidated.

Path Forward

NASA programs and other HPH users should evaluate their mission portfolio for hydrazine thruster use to identify potential material incompatibilities based on the results of this on-going work and if appropriate, coordinate any future testing needed by projects. Possible mitigation techniques to remove carbonaceous contamination may be required. Round Robin test results have provided insight into optimal laboratory methodologies for analyzing HPH for elements beyond Fe and recommendations will be made to Air Force owners of MIL-PRF-26536G for possible incorporation into a future revision.

References

1. Hydrazine and Its Derivatives Kirk-Othmer Encyclopedia of Chemical Technology, 5th Ed., Wiley, Vol 13 (2004).
2. Schmidt, E. Hydrazine and Its Derivatives – Preparation, Properties, Applications, 2nd Ed. Wiley (2001).
3. Schirmann, J.; Bourdauducq, P. Hydrazine Ullmann's Encyclopedia of Industrial Chemistry, Wiley (2012).
4. Lonza "A History of Innovation and Excellence" https://www.hydrazine.com/history
5. Performance Specification – Propellant, Hydrazine, MIL-PRF-26536G, Department of Defense, (July 11, 2017).

For information, contact Donald Parker at donald.s.parker@nasa.gov.

Experimental and Computational Study of Cavitation in Hydrogen Peroxide

Cavitation in liquid propulsion systems can lead to performance degradation and hardware failures. The NESC sponsored an investigation to measure and model cavitation in pressurized hydrogen peroxide flow. The experimentally measured and computationally predicted cavitation lengths were compared as a function of cavitation number. The measured and predicted data exhibited close agreement over the range of pressures and temperatures studied, and no calibration of the cavitation model coefficients was needed.

Background

Cavitation is a flow phenomenon that can occur in a liquid system when the local pressure drops below the vapor pressure. In propulsion systems, cavitation can then lead to performance degradation and hardware failures. In order to design robust propulsion systems, a thorough understanding of cavitation is necessary. There is little cavitation data in the available literature for hydrogen peroxide (H_2O_2), so an NESC-sponsored investigation was undertaken to determine the cavitation characteristics of 90% H_2O_2 at several pressures and temperatures. The results of the experiments, which were performed at Purdue University, were compared with simulations using the Loci-CHEM [1] computational fluid dynamics (CFD) code and the cavitation model developed by Merkle et al. [2].

Test Configuration

This test campaign targeted H_2O_2 flowing through a test article with upstream pressures of up to 2.75 MPa. The test section contained polycarbonate windows, Viton O-rings for compatibility with the H_2O_2, and simple sharp-edged inserts to form a rectangular channel test section (see Figure 1). T-type thermocouples (±1° C) were used for temperature measurements and 3.45 MPa UNIK-5000 series pressure transducers (±1.38 kPa) were used to minimize analog data uncertainties. The temperature and pressure measurements were taken immediately upstream and downstream of the test article to get the most representative measurements. The pressure drops through the test article inlet and outlet were calculated to be insignificant as compared to the pressure drop in the test section, affirming that the pressure transducer locations were adequate. A control valve on the downstream side of the test section was used to vary the downstream pressure and the mass flow rate. A high-speed camera (5 kHz frame rate) was used to record the cavitation in the test section and the instantaneous cavitation length was synchronized with the pressure and mass flow measurements.

Results

Tests were run for upstream pressures of 1.37 and 2.75 MPa at H_2O_2 temperatures ranging from 5° to 40° C. Figure 1 shows a sample of the cavitating flow in the test section. In Figure 1, the flow moves from top to bottom in the video frame, and cavitation appears as the darker regions in the channel. The experimentally measured and computationally predicted cavitation lengths were compared as a function of cavitation number. The cavitation number is defined by:

$$K = \frac{P_1 - P_{vap}}{P_1 - P_2}$$

where K is the cavitation number, P_1 is the inlet pressure, P_2 is exit pressure and P_{vap} is the vapor pressure of H_2O_2. The measured and predicted cavitation lengths exhibited close agreement over the range of pressures and temperatures studied, and no calibration of the cavitation model coefficients was needed. Prospective users of these data should contact Dr. Daniel Dorney at the address given below.

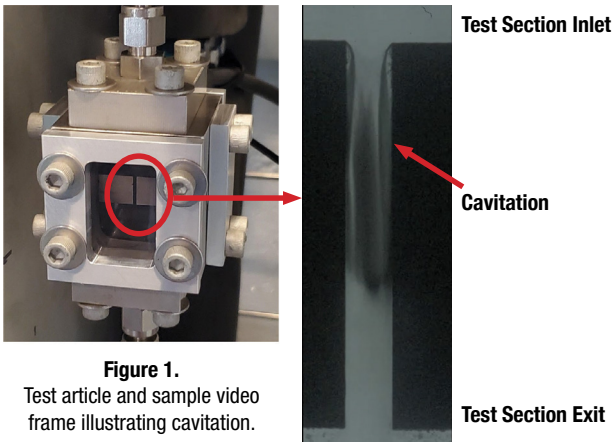


Figure 1.
Test article and sample video frame illustrating cavitation.

References

1. Westra, D.; Lin, J.; West, J.; and Tucker, K.: "Use, Assessment, and Improvement of the Loci-CHEM CFD Code for Simulation of Combustion in a Single Element GO2/GH2 Injector and Chamber," NASA Thermal & Fluids Analysis Workshop (TFAWS), Goddard Space Flight Center, August 7-11, 2006.
2. Merkle, C. L.; Feng, J. Z.; Buelow, P. E. O.: "Computational Modeling of the Dynamics of Sheet Cavitation", Proceedings of the 3rd International Symposium on Cavitation, Grenoble, France, 1998, pp. 307-311.

For information, contact Daniel J. Dorney at daniel.j.dorney@nasa.gov.

Genesis Flight Mechanics Simulation

The NASA Engineering and Safety Center (NESC) consolidated and modernized a suite of legacy flight mechanics simulations, including the Flight Analysis and Simulation Tool (FAST), resulting in Genesis, a generic, multi-vehicle, variable-degree-of-freedom flight mechanics simulation for ascent, aerocapture, entry, descent, and landing (A^2EDL) trajectory design.

Genesis is more flexible, capable, and performant than FAST. It enables trajectory optimization and interactive trajectory generation. Its interoperability with Copernicus, an exo-atmospheric and interplanetary trajectory design tool, facilitates end-to-end trajectory optimization across all mission phases. Genesis is implemented in Julia, a new language for technical computing that combines the ease of use of scripting languages with the run-time performance of compiled languages.

Background

Flight mechanics simulations are used throughout a program's life cycle for tasks such as developing Design Reference Mission (DRM) trajectories for conceptual vehicle designs, evaluating or prototyping guidance algorithms, designing and reconstructing test flights, evaluating vehicle performance, and designing trajectories for operational missions. The JSC flight mechanics community relied on a suite of legacy flight mechanics simulations for these tasks. To simplify maintenance, improve on-boarding of new users, and better leverage modern high-performance computing (HPC) environments, the NESC consolidated the legacy simulations to create Genesis.

Benefits for the A^2EDL Engineer

Julia is approachable to engineers without formal computer science training, which makes it easier for them to modify existing models or add new models. Julia does the heavy lifting to support multiple operating systems, including Windows, macOS, and Linux. Julia has a built-in package manager and a rich ecosystem of third-party packages, including optimizers, which can be used with Genesis. Julia has built-in support for linear algebra and Unicode variable names, which means that Julia code can closely resemble the textbook equation it implements.

Documentation: $\ddot{x} = u + R^T\left[\ddot{s} + 2\tilde{\omega}\dot{s} + \left(\dot{\tilde{\omega}} + \tilde{\omega}\tilde{\omega}\right)s\right]$

```
Julia: ẍ = u + R' * (s̈ + 2*ω̃*ṡ + (ω̇̃ + ω̃*ω̃)*s)
```

Figure 1: Julia code corresponds closely to the way an equation is documented.

Julia can be used in notebook programming environments that allow engineers to mix expository text, executable code blocks, and inline code outputs. This enables engineers to turn their Genesis analysis into an interactive document.

Genesis and Copernicus can be used in conjunction to enable end-to-end trajectory optimization. With the Copernicus plug-in capability, Genesis can generate segments of the overall trajectory. Copernicus can pass optimization variables to Genesis, allowing Copernicus to optimize the entire trajectory at once.

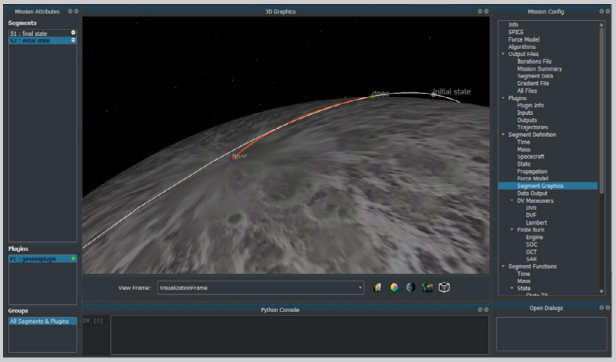


Figure 2: Copernicus and Genesis can be used together to enable end-to-end trajectory optimization. Here, the white trajectory is propagated by Copernicus, and the red trajectory is propagated by Genesis for a lunar descent and landing.

References

1. NASA/TM-20210014622, Improvements to the FAST and Initial Development of the Genesis Flight Mechanics Simulation for A^2EDL Trajectory Design, April 2021
2. The Genesis GitLab page: https://gitlab-fsl.jsc.nasa.gov/Genesis/Genesis.jl (NASA-Only)
3. Julia main page: https://julialang.org

For information, contact Daniel G. Murri at daniel.g.murri@nasa.gov or Daniel A. Matz at daniel.a.matz@nasa.gov.

National Aeronautics and Space Administration

NASA Engineering and Safety Center Technical Bulletin No. 21-03-1

Best Practices for the Elemental Profiling of High-Purity Hydrazine

Trace contaminants in high-purity hydrazine (HPH) propellant impact a wide variety of commercial, Department of Defense (DoD), and NASA missions. Depending on thruster design, elemental contaminants must be kept at extremely low levels and are verified as such by routine analysis. A number of these contaminants have recently undergone an assessment to shed light on their quantities present following changes in the HPH supply chain. A round robin analysis utilizing four separate laboratories resulted in unacceptably high variability in the quantification of these contaminants. The principal objective of this technical bulletin is to signal the availability of a new analysis methodology which yields accurate and repeatable quantification by providing best practices for both quantitation methodology and strategies for avoiding sample contamination during analysis.

Background:

Hypergolic propellants (e.g., hydrazine (N2H4)) are used to power monopropellant and bipropellant propulsion systems. Investigations to better understand HPH manufacturing processes and the associated introduction of contaminants have been a priority for the HPH user community after the chemical reaction scheme employed to produce a precursor to HPH, which is used as the feedstock by the Defense Logistics Agency's sole source HPH provider, changed in mid-2018.

Particular concern arose regarding the possible introduction of organic species (e.g., carbonaceous compounds) and elemental content (e.g., cadmium (Cd)) to the final HPH product, as this carries an increased risk of performance degradation and/or flow-path blockage to thruster system valves, softgoods and catalyst beds.

Analysis was completed to identify extraneous unknown carbonaceous materials present in current HPH in addition to comprehensive elemental profiling by four laboratories to develop a full elemental profile of the commodity in relation to heritage HPH stocks.

The elemental laboratory data revealed varying and/or high levels of multiple elements outside of nominal laboratory-to-laboratory variation, and sample-to-sample variation was independently confirmed. The NESC concluded that, while there was variation in the elemental content of the samples, there was also an apparent inconsistent handling of samples within each of the four laboratories that, in some cases, led to widely varying elemental assay results.

Causes of Analysis Variability:

There was an unexpectedly wide variation in elemental assay results from the analysis of single batch-sourced samples from four laboratories. Further analysis revealed that the provided samples themselves exhibited variation, possibly as a result of pre-laboratory handling. However, in some cases, large discrepancies were determined to have been caused by differences in analytical procedures and methods at the laboratories themselves. Refinement of analytical methodology for HPH, other hydrazine derivative sample handling and processing, as well as the instrumental analysis methodology for extended elemental content, are essential to gaining accurate and equivalent results from multiple laboratories performing this type of analysis.

Best Practices for HPH Elemental Analysis:

The detailed best practice recommendations for conducting the elemental analysis process are described in [1]. Briefly:

A. Glassware usage should be minimized in all steps of the analytical process to minimize sample contamination.

B. Blanks for water and acid stock solutions used in sample preparation should be prepared alongside, and analyzed with, each batch of samples analyzed to ensure any contamination is accounted for from the process.

C. When using platinum evaporation dishes, adequate cleaning between samples should be ensured.

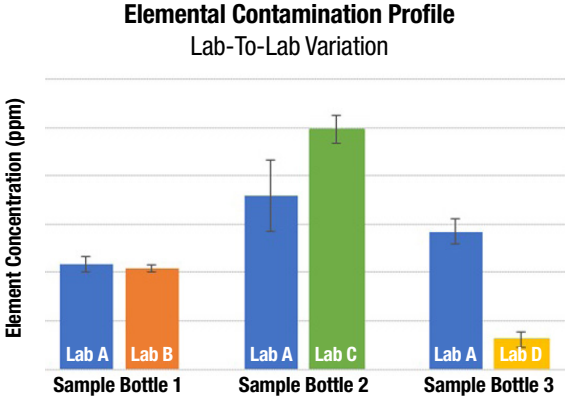
D. Method detection limits and reporting limits should be established for all elements in analysis for proper reporting of trace elemental levels.

E. For ICP-OES (Inductively Coupled Plasma - Optical Emission Spectrometry) or ICP-MS (Inductively Coupled Plasma - Mass Spectrometry) analysis, survey the elements that are to be analyzed and determine what possible interferences may exist for those elements, which should be addressed prior to analysis.

F. Samples should be analyzed in duplicate or triplicate, when possible.

References:

1. NASA Lesson Learned Information System entry No. 29801. Available from https://llis.nasa.gov/lesson/29801



Lab-to-lab variation in analysis of exemplar elemental content across multiple sample bottles of single-source commodity.

For information, contact Donald Parker at donald.s.parker@nasa.gov and Janelle Coutts at janelle.coutts@nasa.gov.

National Aeronautics and Space Administration

NASA Engineering and Safety Center Technical Bulletin No. 21-04

Evaluating Appropriateness of LEFM Tools for COPV and Metal Pressure Vessel Damage Tolerance Life Verification

Human spaceflight composite overwrapped pressure vessels (COPVs) and metal pressure vessels can use linear elastic fracture mechanics (LEFM) analysis to demonstrate damage tolerance life in some cases per ANSI/AIAA-S-081 for COPVs and ANSI/AIAA-S-080 for metal pressure vessels. LEFM analysis assumptions require that the crack tip plastic zone is small relative to the crack size and is completely surrounded by elastically responding material. Test and analysis have shown that LEFM tools (e.g., NASGRO*) can provide unconservative crack growth predictions for cracks in COPV liners that violate LEFM assumptions. COPV and metal pressure vessel designers should evaluate and address the violation of LEFM plasticity assumptions before using LEFM analysis tools for damage tolerance life verification.

Background

LEFM methods have traditionally been used to successfully characterize the damage tolerance life of elastically responding components that contain cracks that are small relative to the thickness or other structural features. However, prediction of part-through cracks in thin metallic materials, where break-through is an end-of-life condition (e.g., COPV liners or thin metal pressure vessels), presents a unique problem. For example, traditional plastic zone limits that bound the use of LEFM (e.g., Irwin plastic zone model) are based on cracks in semi-infinite bodies and can be unconservative for a part-through crack approaching the back surface of a thin component. Furthermore, existing standards (e.g., ANSI/AIAA S-081 and S-080) do not provide guidelines for end-of-life limits in damage tolerance life analysis with LEFM tools such as NASGRO.

Discussion

In addressing the impact of LEFM plasticity assumptions on conservatism of damage tolerance life predictions, the NESC assessment team:

- Performed testing to generate crack growth and crack mouth opening displacement (CMOD) data.
- Performed LEFM analyses using NASGRO v8.2 as an exemplar LEFM tool to compare against crack growth test data.
- Developed a validated finite element model (FEM) to compare predicted crack behavior using elastic and elastic-plastic material models (Figure 1).
- Experimentally and numerically demonstrated that the divergence between elastic and elastic-plastic predictions is gradual.

The validated FEM considered various crack sizes, liner thicknesses, stress levels, and materials. Analysis data demonstrated a gradual divergence in predicted elastic-plastic and elastic crack behavior. As a result, the NESC assessment team:

- Developed criteria that expands on the concepts developed in ASTM E2899 to determine when LEFM plasticity assumptions are invalid (i.e., LEFM limit, a_L).
- Provided a modified failure criterion, a_i*, to be considered when LEFM analyses are used beyond the LEFM limit.

As illustrated in Figure 2, a_i* is a knockdown on the LEFM damage tolerance life state-of-practice limit (i.e., the Irwin plastic zone limit, a_i), meaning a_i* is as or more conservative than a_i. To account for the aforementioned gradual divergence between elastic and elastic-plastic predictions, the knockdown is only applied when the analysis shows exceedance of the LEFM limit, a_L. The magnitude of the knockdown depends on the degree of exceedance, elastic-plastic finite element analysis, and applicable test data.

LEFM Evaluation Approach

When LEFM-based fatigue crack growth predictions are made for damage tolerance life (e.g., with a LEFM tool such as NASGRO), COPV and metal pressure vessel designers should use the following analysis procedure to address the potential violation of LEFM plasticity assumptions:

- Simulate crack growth to failure (i.e., breakthrough).
- Identify the predicted crack depth after 4-lifetimes, a_F.
- Identify the limits a_i, a_L, and a_i*.
- Verify that $a_F < a_i$*, otherwise the design does not meet recommended requirement for damage tolerance life by analysis.
- Report a_F, a_i, a_L, and a_i* to fracture control engineering technical authority.

References

1. ANSI/AIAA-S-081 and ANSI/AIAA-S-080, Space Systems – Composite Overwrapped Pressure Vessels, Metallic Pressure Vessels, Pressurized Structures, and Pressure Components
2. COPV Damage Tolerance Life Analysis and Test Best Practices, NASA/TM-2020-5006765
3. Damage Tolerance Life Issues in COPVs with Thin Liners, NESC-TB-16-02

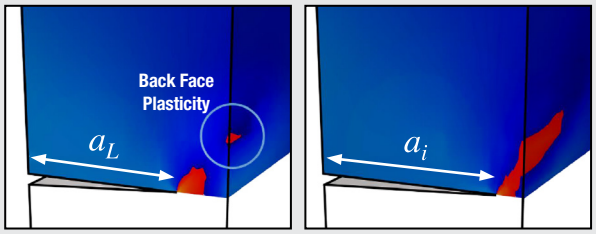


Figure 1. Plastic zone size from FEM comparing LEFM limit calculated according to ASTM E2899-15 and the Irwin limit. The crack tip plastic zone is highlighted in red.

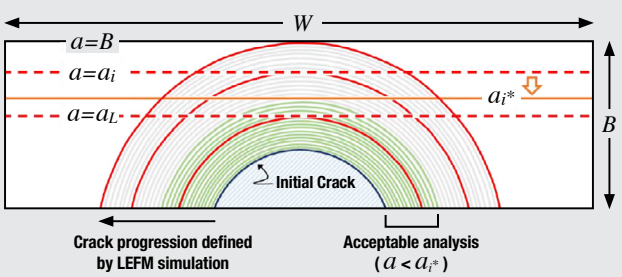


Figure 2. Schematic of a surface crack growth simulation and applicable limits on a, including the Irwin limit, a_i, the LEFM limit, a_L, and the modification limit, a_i*.

*NASA retains a royalty-free license to use NASGRO for NASA purposes, including use by NASA contractors on NASA projects.

For information, contact Heather Hickman at heather.k.hickman@nasa.gov.

NESC tech bulletin

National Aeronautics and Space Administration

NASA Engineering and Safety Center Technical Bulletin No. 21-05

Industry Recommendations from Arecibo Observatory Zinc Spelter Socket Joint Failure Analysis

A structural analysis and forensic investigation concluded that the Arecibo Observatory M4N socket joint failure in August 2020 was primarily due to cumulative damage caused by initially low structural design margins and a high percentage of sustained load, resulting in zinc creep deformation, progressive internal socket wire damage, and eventual loss of joint capacity. Open spelter sockets of this type are used throughout industry in stay cables. Recommendations are proposed to prevent failures of similar socket joints, including verification of positive stress margins in socket joint wires for all failure modes, periodic visual inspections with pass/fail criteria for zinc extrusion that are tied to structural qualification, and revisiting codes/industry standards to capture lessons learned.

Background

The Arecibo Observatory's telescope consisted of an instrument platform suspended above the dish by stay cables connected to three towers. In August 2020, an auxiliary cable slipped from its socket joint on one of the towers, eventually leading to the total collapse of the observatory in December 2020.

NASA structural analysis and forensic investigation concluded that the M4N Arecibo socket joint failure was primarily due to cumulative damage caused by initially low structural design margins and a high percentage of sustained load, leading to zinc creep deformation, progressive internal socket wire damage, and eventual loss of joint capacity. Visual inspections identified progressive zinc extrusion, which in hindsight was evidence of cumulative damage due to creep [1].

Socket Termination Overview and Mechanics

Zinc spelter socket joints are terminations in stay cables used throughout industry that transfer loads between adjacent structures. The socket termination comprises stay cable wires that are unraveled, broomed, and then embedded/bonded into a zinc casting inside a conical volume. Cable tension wedges the zinc material against the slanted conical surface, so that a large compression zone develops within the zinc such that failure occurs outside the socket joint in the cable span. Stay cables in the United States are regulated by ASCE 19-10 and 19-96 [2].

Findings

Finite element analysis and forensic investigation of an open conical zinc spelter socket with 1x127 cable strand showed non-uniform stress distribution across wires at half the cable breaking load, with outer wires stressed near ultimate strength but with residual elongation capability.

Traditional design/build verification methodologies for similar socket terminations may not adequately consider constituent stresses and localized stress concentrations in demonstrating positive structural margins; consequently, these socket terminations may be vulnerable to time-dependent cumulative damage from fatigue and creep.

Analysis also showed that in applications with a high percentage of sustained (dead) load and a design factor of safety of approximately 2, there is a greater potential for zinc creep. Creep will visually manifest as zinc extrusion from the socket and was shown to further reduce wire capacity at the socket termination.

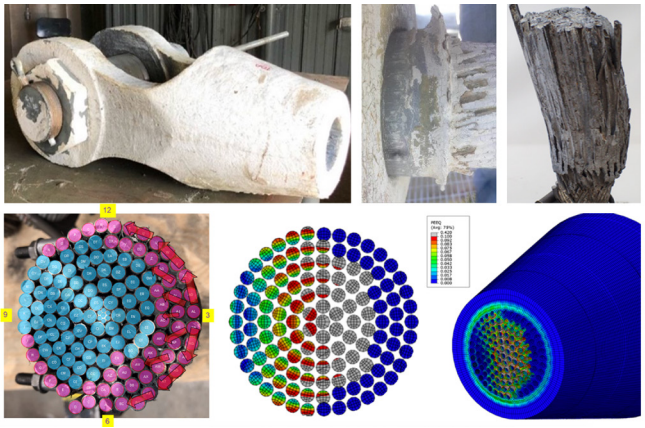


Figure 1: NASA Investigation of failed Arecibo Aux M4N cable. Top: socket (left); zinc extrusion (center); pulled out cable (right). Bottom: forensic and finite element model recreation of M4N failure progression.

Forensic investigation also found internal damage due to environmental conditions, which in combination with wire defects may have further degraded capacity of the socket joint without clear external indication.

Recommendations

1. Socket joint constituents should be verified to have positive structural margins for strength, fatigue, and creep failure modes for the service life of the socket for all design load combinations.
2. Periodic visual inspection of socket joints should include pass/fail criteria for zinc extrusion tied to a structural qualification test program that verifies the creep failure mode. Qualified processes such as cable replacement and socket joint refurbishment should then be defined to restore joint capacity in the event of failed inspection.
3. ASCE 19-10 and 19-96 codes should be revisited to ensure that the design factors consider time-dependent creep effects in dead load dominated structures, environmental conditions, and workmanship sensitivity to wire defects or brooming.

References

1. "Arecibo Observatory Auxiliary M4N Socket Termination Failure Investigation," 30 June 2021, NASA/TM-20210017934.
2. American Society of Civil Engineers (ASCE) 19-10/ASCE 19-96 "Structural Applications of Steel Cables for Buildings."

www.nasa.gov

For information, contact greg.harrigan@nasa.gov or vinay.k.goyal@aero.org.

Detecting Flow-Induced Vibration in Bellows

The NESC performed testing to determine if high-speed video techniques can be used to predict the onset of flow-induced vibrations (FIV) in bellows. A comprehensive test matrix was established to determine if Motion Magnification (MM) and Digital Image Correlation (DIC) can be used to determine the onset of FIV in straight and gimbaled bellows. Several of the tests were intended to determine if MM and DIC can establish the resonant frequencies of the bellows with no a priori knowledge. The results of the MM and DIC were compared with data from strain gages and microphones. Although the testing was limited to one single-ply unshielded bellows, this effort provided the proof-of-concept that MM and DIC are feasible methods for determining the onset of FIV in bellows.

Background

Bellows (see Figure 1) are used to connect systems/components in rocket engines while allowing for expansion or contraction associated with temperature variations and articulation due to engine gimbaling. FIV are caused by resonance generated through the coupling of vortex shedding from bellows convolutions with the flexible line natural structural frequencies. FIV have caused the failure of bellows and flex hoses in several rocket engines [ref. 1]. Most NASA programs use analytical techniques instead of testing to predict the onset of FIV. However, these techniques do not account for bends in the bellows/flex hoses due to engine gimbaling [ref. 2]. In addition, the characterization of FIV through testing with strain gages is difficult for straight and gimbaled bellows (e.g., accessibility, durability, temperature range, etc.). Thus, FIV behavior during engine gimbal can only be estimated.

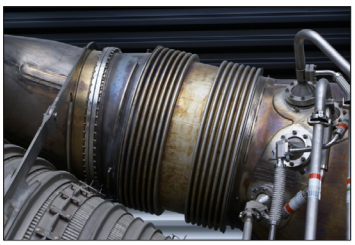


Figure 1: Example Rocket Engine Bellows

MM is the process by which small, imperceptible motions in an image series are visualized by manipulating each image in a digital video series [refs. 3-4]. MM works by decomposing each image in a time series into its local spatial amplitude and phase. By assessing how the local spatial phase changes from image to image within the series, and magnifying those small phase changes, the minute motions may be visualized and measured.

DIC is an optical, non-contacting method for extracting full-field displacements, full-field strains, velocities, and accelerations [refs. 5-6]. This technique requires a pair of digital cameras that are focused on the same area but viewing the structure from different angles. The surface of the structure is painted with a high-contrast (e.g., black/white) random speckle pattern. DIC uses pattern recognition on small subsets of the speckle pattern to determine the translations and distortions. A comparison is made of the position of the speckles in the deformed state to that of the undeformed state.

MM and DIC were chosen for this investigation because they are non-intrusive optical methods that produce significantly more information than a limited number of strain gages and/or microphones.

Testing

The testing was performed at the NASA Marshall Space Flight Center (MSFC) Component Development Area (CDA) water flow loop using a bellows from previous testing. This facility uses an electric motor-driven pump with a variable frequency drive and turbine flow meter to precisely establish and control the desired flow rate. More than 40 tests were performed to determine the ability of MM and DIC to predict the onset of FIV in bellows. Figures 2a, 2b, and 2c show strain gauge data, microphone data, and the results from MM for one of the tests. The three measurement techniques show the same dominant frequency for the onset of FIV. The difference in the amplitudes of the harmonics is due to the locations of the strain gage and microphone. The MM and DIC techniques produced similar accurate predictions for the onset of FIV in all test cases investigated.

References

1. *J-2 Engine AS-502 (Apollo 6) Flight Report – S-II and S-IVB Stages, Volume 2: S-II Stage Failure Analysis,* Contract NAS8-19, R-7450-2, NASA-CR-61992, Rocketdyne, June 17, 1968.
2. *Assessment of Flexible Lines for Flow Induced Vibration*, MSFC-DWG-20M02540, Rev. E, December 19, 1991.
3. Liu, C.; Torralba, A. B.; Freeman, W. T.; Durand, F.; and Adelson, E. H.: *"Motion Magnification,"* ACM Transactions on Graphics (SIGGRAPH), 24(3): 519-526, 2005.
4. Chen, J. G.; Wadhwa, N.; Durand, F.; Freeman, W. T.; and Buyukozturk, O.: *"Developments with Motion Magnification for Structural Modal Identification through Camera Video,"* (eds) Dynamics of Civil Structures, Volume 2, Conference Proceedings of the Society for Experimental Mechanics Series, Springer, Cham., 2015. https://doi.org/10.1007/978-3-319-15248-6_5
5. Sutton, M. A.; Orteu, J. J.; and Schreier, H. W.: *"Image Correlation for Shape, Motion, and Deformation Measurements,"* Springer Science and Business Media, 2009.
6. *A Good Practices Guide for Digital Image Correlation*, International Digital Image Correlation Society - Standardization, Good Practices, And Uncertainty Quantification Committee, October 2018.

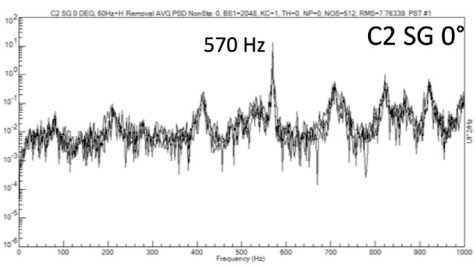


Figure 2a: Bellows Strain Gage Data

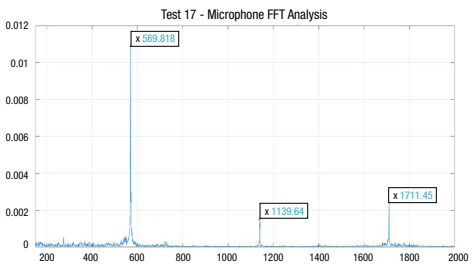


Figure 2b: Bellows Microphone Data

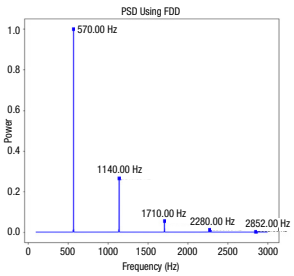


Figure 2c: Bellows MM Data

For information, contact Daniel J. Dorney daniel.j.dorney@nasa.gov
03/17/22 DOC ID: 20220004162

National Aeronautics and Space Administration

NASA Engineering and Safety Center Technical Bulletin No. 22-02

Revisiting Filtration Standards and Definitions for Spaceflight Propulsion and Pressurant Systems

The NESC performed an assessment of existing filtration standards and guidance documents for propellant and pressurant systems. The assessment included a vendor survey to better understand concerns about filtration systems, defined a common set of filtration and contamination-related terms, and developed guidelines for system filtration design and implementation.

Background

Contamination has been accepted as the root cause of many spaceflight system anomalies. Some of these could have been prevented if an appropriate filtration approach had been specified and implemented. No standards exist for sizing, building, and verifying the performance of spaceflight propulsion/pressurant filters. Component and system cleanliness standards exist, but the interpretation of cleanliness level applicability varies widely. There is no standard technique to determine how cleanliness levels are applied at a system level and how they correlate to filtration requirements. Basic filtration terms, such as "nominal" and "absolute" filter ratings, have different meanings from vendor to vendor.

The NESC assessment, which focused on particulate contamination, was undertaken to define a common approach to filtration terminology, suggested guidelines, design, and verification for spaceflight propulsion and pressurant systems. The guidance for the design of a filter element, such as filtration rating, contamination capacity, flow rate vs. pressure drop, and differential collapse pressure, was evaluated along with filter housing performance (i.e., proof and burst).



Space Launch System Core Stage RS-25 Engine Testing

Sources of Particulate Contamination

The assessment determined there are only four sources of particulate contamination:

1. Particulate loaded with the fluid or gaseous media.
2. Particulate built into parts and components at the vendor.
3. Particulate introduced by manufacturing processes, including welding and cutting at the sub-assembly and final assembly levels.
4. Self-generated particulate produced by moving parts and soft-good/material degradation within the system.

Filtration System Design Process

The filtration system design guidelines outline seven steps:

1. List the individual elements and their cleanliness level upstream of the filter.
   - Include all units and sub-assemblies ("elements"). The list should include the highest-level assembly that was verified clean to a specification.
2. Determine the multiplying factor for lifetime.
   - This is the total fluid that will flow through the element. Include pyrovalve actuation counts and weld repair counts.
3. Determine the particle decay rate.
   - Repeated flushing of an element will decrease the particle count within each size range. Omitting the decay rate will increase conservatism.
4. Total the particle counts.
   - Total across elements, which provides the total count within each particle size range.
5. Convert to test dust.
   - The Jet Propulsion Laboratory determined a correlation for the number of particles within each size range for a mass of air cleaner test dust [refs. 1-2].
6. Determine the necessary dirt holding capacity.
   - This is the largest mass value across the appropriate particle size ranges.
7. Specify the margin.
   - Factors of 2x to 4x are typical. The process recommends adding margin, but not the amount of margin.

The process was demonstrated on an example hydrazine propulsion system [ref. 3]. The guidelines developed in the NESC assessment are recommended for all launch vehicle and spacecraft propulsion systems and may be applicable to a range of other systems.

References

1. Jan, D., and Guernsey, C., "A Procedure for Sizing Propulsion System Filter Capacity," AIAA-92-3535, AIAA/SAE/ASME/ASEE 28th Joint Propulsion Conference and Exhibit, Nashville, TN, July 6-8, 1992.
2. "Road Vehicles - Test Dust for Filter Evaluation," ISO 12103-1, International Organization for Standardization, 1997.
3. *Filtration of Spaceflight Propulsion and Pressurant Systems*, NESC RP-19-01498, February 17, 2022.



For information, contact Daniel J. Dorney daniel.j.dorney@nasa.gov

03/17/22 DOC ID: 20220004167

Treatment of Transient Pressure Events in Space Flight Pressurized Systems

Analytical and experimental evidence shows that fast-moving dynamic pressure fluctuations caused by valve actuation, fluid-system priming, fluid discharge, vibration, and flow disturbances can elicit adverse structural response and must be considered in the space flight pressure system design and verification process.

Background

Transient pressure events are fast-moving dynamic fluctuations due to disruptions within the pressurized systems, Figure 1. Since numerous factors influence pressure transients, a comprehensive approach to treating these is absent. Vague or contradictory requirements have led hardware developers to bypass this assessment. Structural failures have occurred in aerospace applications from overloads or fatigue from transients.

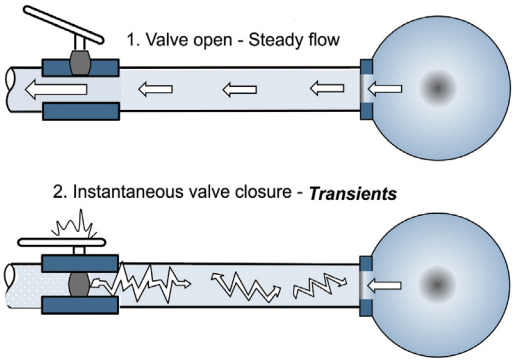


Figure 1: Illustrations of Pressure Transients

Guidelines

Accounting for pressure transients is a multi-disciplinary activity involving Fluids, Dynamics, and Structures. The NESC paper [1] brings clarity to the understanding of transients caused by flow disturbances and documents best practices with case studies and roadmap. A 6-step process (Figure 2) highlights, 1) Pressure System design establishing nominal operating pressure and initial steps to minimize transients, 2) Assessment of pressure transients via fluids analysis or test, 3) Classification of pressure system components, 4) Dynamic response of structure, 5) Establishing Maximum Expected Operating Pressure (MEOP), which includes transient response, 6) Structural verification.

Pressure transients are characterized via simple fluids analyses using the Joukowsky equation or 1D fluid models using coupled first-order partial differential equations involving continuity and momentum equations. Detailed test-validated 2D or 3D models can capture losses and geometric effects. Transients can also be measured via instrumented subsystem tests.

Fast-moving transients induce a dynamic structural response. Localized stress peaks are created whose magnitudes are influenced by the component geometry, material properties, and pressure wave (velocity, amplitude, and shape). A ratio called Dynamic Amplification Factor (DAF) provides a quantitative measure of structural response via structural dynamics analysis. A parametric study performed by varying the mean radius (r), wall thickness (t), modulus of elasticity (E), and density (ρ) of a pipe subjected to a half-sine traveling pressure wave showed that the ratio (ω^*) of pressure wave frequency (ω) to the ring natural frequency (ω_n) of the pipe was a key parameter in DAF calculations.

$$\omega^* = \omega/\omega_n = r\omega/\sqrt{E/\rho} \quad (rad/s)$$

Three outcomes are possible:

$\omega^* << 1 \rightarrow$ similar to static pressure load, DAF = 1
$\omega^* = 1 \rightarrow$ resonance, response is amplified, DAF ~ 3
$\omega^* >> 1 \rightarrow$ structure responds slower than the load, DAF ~ 0

Pressure Vessels vs. Pressure System Components

The transient pressure wave entering fluid storage vessels, such as tanks and pressurized structures, dissipates due to relatively large volume compared to that of the connecting pipe. In these cases, DAF is zero and the magnitude of the pressure transient is added to the steady state pressure to define MEOP. Pressurized components, such as pipes and valves, may show a minimal dynamic response (DAF~0.0), a quasi-static response (0.0 < DAF < 1.0), or an amplified response (DAF ≥ 1.0).

Verification Process

Establish a MEOP that mimics a localized maximum stress at the critical location, which is equivalent to that of steady state pressure plus pressure transient. A damage tolerance approach with lower proof and burst factors can result in weight-savings, especially when pressure transient magnitudes are significant.

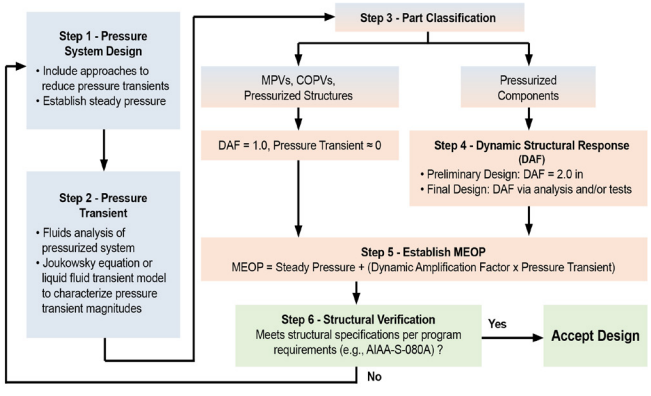


Figure 2: Workflow for Transient Pressure Evaluation

References

1. K. Imtiaz, V. Goyal, P. Babuska, E. Barbour, and J. Smith, *Treatment of Transient Pressure Events in Space Flight Pressurized Systems* NASA Engineering and Safety Center, NESC, NASA/TM 2021-0022275, https://ntrs.nasa.gov/citations/20210022275, 2021.

For information, contact Kauser Imtiaz, kauser.s.imtiaz@nasa.gov

05/20/22 DOC ID:20220006583

Uncertainty Quantification of Reduced Order Structural Dynamic Models

Uncertainty quantification (UQ) provides statistical bounds on prediction accuracy based on finite element model (FEM) uncertainty. An alternate method for UQ, called the Hybrid Parametric Variation (HPV) combines a parametric variation of the Hurty/Craig-Bampton (HCB) fixed-interface (FI) modal frequencies with a nonparametric variation (NPV) method. This provides a UQ method that can be traced to test data, which can be updated as additional data and improved correlated models become available.

Background

The purpose of uncertainty quantification (UQ) is to provide statistical bounds on prediction accuracy based on model uncertainty. This is distinct from model updating, which attempts to modify models to improve their accuracy. UQ does not improve the accuracy of models but accepts that the models are inherently inaccurate and attempts to quantify the impact of that inaccuracy on predicted results. The most common method for modeling uncertainty in the structural dynamics community is a parametric approach, which varies physical parameters in the model. However, there are several disadvantages associated with the parametric method. Determining a reduced set of parameters that have a significant impact on the system response can be time consuming, and the selected parameter probability distributions are rarely reliably known. Model-form uncertainty cannot be directly represented by FEM input parameters nor included in a parametric approach. However, model-form uncertainty can be modeled using random matrix theory (RMT), where a probability distribution is developed for the matrix ensemble of interest.

The HPV Method for UQ

An alternate method that has the potential to improve for UQ, called the HPV method, has been summarized in [ref 1]. The HPV method combines a parametric variation of the HCB FI modal frequencies with a NPV method that randomly varies the HCB mass and stiffness matrices as Wishart [ref. 2] random matrix distributions using RMT.

The basis for the NPV component of the HPV method is to replace the HCB matrices representing each system component with an ensemble of random matrices, based on RMT. Each matrix in the ensemble must be close to the nominal matrix in the sense of some matrix norm and must meet certain requirements (e.g., symmetry and correct sign definiteness). However, the matrices are otherwise free and are not tied to any particular set of parameters in the FEM. Soize [ref. 3] used the maximum entropy principle to derive the positive definite and positive semidefinite ensembles SE ^+ and SE ^(+0) that follow the matrix variate gamma distribution and are capable of representing random structural matrices. This means the matrices in the ensembles are real, symmetric, and possess the appropriate sign definiteness to represent structural mass, stiffness, or damping matrices. As the dimension of the random matrix n increases, the matrix variate gamma distribution converges to a matrix variate Wishart distribution.

The HPV method uses uncertainty models for HCB components based on component modal test/analysis correlation results. The NPV based dispersion of the HCB mass matrix is derived from the test self-orthogonality matrix. Two different test self-orthogonality metrics were considered, the root mean square (RMS) value of the off-diagonal terms, and the mean absolute value of the off-diagonal terms. FI mode eigenvalue uncertainty within the HCB stiffness matrix is based on frequency error between matching HCB FI modes and test modes. The NPV method is then applied to the HCB stiffness matrix by layering it on top of the FI eigenvalue variation. The stiffness matrix dispersion level is based upon the FEM/test XO matrix using the diagonal cross-generalized mass (DCGM) metric, which is the RMS value of the diagonal terms. The basis for the HCB component uncertainty model is shown in Figure 1.

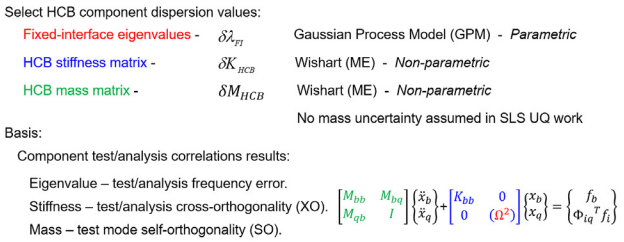


Figure 1. Basis for HCB Component Uncertainty Model

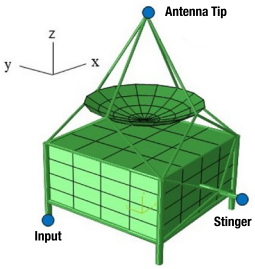


Figure 2. GSC Frequency Response Input and Output Locations

The validity and efficacy of the HPV method and corresponding component uncertainty model development procedure is examined by applying the approach to two examples in [ref 1]. The General Spacecraft (GSC) example (Figure 2) provides a representation where the test model was known. The uncertainty model developed for the GSC HCB component based on the test-configuration modal correlation results show the flight-configuration test frequencies and frequency response with the P98/90 probability enclosure coverage (Figure 3).

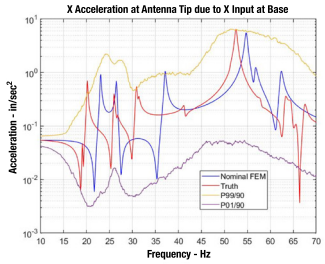


Figure 3. GSC Flight-Configuration

Based on this work and other assessments [refs. 4-7], the HPV method adds another device to the toolset used for complex system UQ analysis that accounts for both parametric and model-form uncertainty and is based on test data. From experience gathered to date using the HPV method, additional design specific applications must be investigated to determine which self-orthogonality metric provides the best mass matrix dispersion results, and to provide further confidence in the validity of the HPV method of UQ analysis.

References

1. Johnson, D.; Kammer, D.; Blelloch, P.; and Sills J.: "Uncertainty Models for the Hybrid Parametric Variation Method of Uncertainty Quantification," NASA/TM-20220010939, July 2022.
2. A Wishart, J.: "Generalized Product Moment Distribution in Samples," Biometrika, vol. 20A, no. 1-2, pp. 32-52, 1928.
3. Soize, C.:"A Nonparametric Model of Random Uncertainties for Reduced Matrix Models in Structural Dynamics,"Probabilistic Engineering Mechanics, vol.15, no. 3, pp.277-294, 2000.
4. Kammer, D.; Blelloch, P.; and Sills, J.: "Test-Based Uncertainty Quantification and Propagation Using Hurty/Craig-Bampton Substructure Representations," in IMAC, Orlando, FL, 2019.
5. Kammer, D.; Blelloch, P.; and Sills, J.: "Variational Coupled Loads Analysis using the Hybrid Parametric Variation Method," in IMAC, Houston, TX, 2020.
6. Kammer, D.; Blelloch, P.; and Sills, J.: "SLS Integrated Modal Test Uncertainty Quantification using the Hybrid Parametric Variation Method," in IMAC, 2021.
7. Kammer, D.; Blelloch, P.; and Sills, J.: "Probability Bounds Analysis Applied to Multi-Purpose Crew Vehicle Nonlinearity," in IMAC, Orlando, FL, 2022.

Contact Joel Sills, joel.w.sills@nasa.gov and Dan Kammer, dan.kammer@ata-e.com

NESC tech bulletin

National Aeronautics and Space Administration

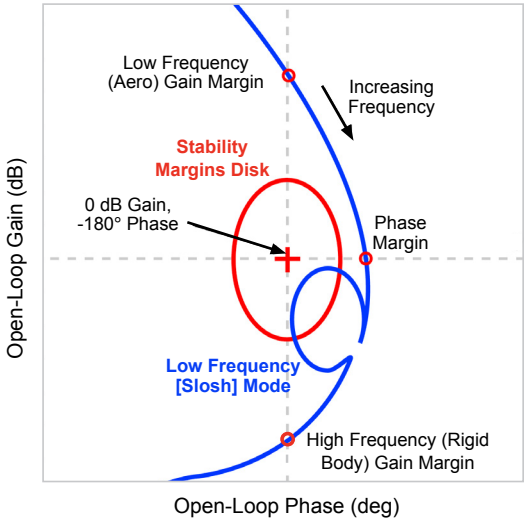
NASA Engineering and Safety Center Technical Bulletin No. 22-05

Launch Vehicle Flight Control Stability Margin Reduction Considerations

Launch vehicle ascent stability analyses typically rely on a combination of frequency and time domain analyses. Frequency domain analysis uses a sequence of high-fidelity linear models with constant parameters spanning the ascent trajectory. Complementary time domain analysis is performed using high-fidelity, nonlinear 6-DOF simulations. Analyses are typically dispersed to verify robustness to parameter variations by showing the vehicle meets frequency domain stability margin requirements and time domain performance metrics. This Technical Bulletin outlines standard stability margin best practices and provides recommendations for treatment of deviations from industry-standard launch vehicle stability margins due to vehicle flexibility, slosh dynamics, aerodynamics, other offending dynamics, or coupling thereof.

Stability Margin Best Practices

Current best practices for launch vehicle flight control design target 6 dB/30 degrees undispersed rigid body gain/phase margins and 12 dB amplitude margin for gain-stabilized flexible body modes. Well-characterized fundamental (low-frequency) flexible body modes can potentially be phase-stabilized to maintain 45 degrees of undispersed phase margins. Best practices for dispersed analysis ensure 3 dB/20 degrees on the rigid body gain/phase margin, 6 dB amplitude margin for gain-stabilized flexible body modes, and 30 degrees for phase-stabilized flexible body modes. All relevant dynamics, including engine inertial coupling, bending, and slosh dynamics, are included in the linear plant model and should respect the same stability margin requirements. Due to the nonlinear and uncertain characteristics of propellant slosh modes in the absence of passive damping devices (e.g., ring baffles), analysis beyond that of the standard frequency and time domain analyses may be needed to address the effects of sloshing propellant for bare-walled tanks. Any other vehicle dynamics exhibiting significant nonlinearities or complex coupling, or where the available model representation is of low fidelity and/or not anchored to test data, may similarly necessitate an extended treatment.



Notional Nichols Plot with Adversely Phased Propellant Slosh Mode

Recommended Treatment for Deviations from Standard Launch Vehicle Stability Margin Requirements

Stability margins should be reported with the inclusion of all relevant dynamics (i.e., rigid body, slosh, flexible body, and aerodynamics). If the resulting stability margins deviate from industry standards, the routine analysis approach should be augmented by an adequately extensive treatment, including:

- Analysis of the **fundamental physics** involved, with applicable simulation tool verification. Verify consistency among rules of thumb, linear analyses, nonlinear analyses, and flight data.
- **Sensitivity studies** in frequency and time domains to analyze effects of possible parameter and system variations.
- Assessment of the **consequences of potential instability** associated with offending modes by evaluating stressing cases in the time domain.
- **Assessment of alternative flight control designs** to demonstrate, in the context of risk/consequence, that the baseline design appropriately balances overall launch vehicle risk. Appropriate risk management trades may vary depending on the program's development/operational stage. Lower margins (i.e., larger deviations from industry standards) may be considered following successful flight demonstration and test-validated model analysis.

Regardless of the margin posture, sensitivity studies and stress cases can be automated and evaluated as a standard practice to establish high confidence in the design and its robustness.

References

1. NESC Technical Bulletin No. 14-01, "Designing for Flight Through Periods of Instability," September 2014. https://www.nasa.gov/nesc/technicalbulletins.
2. NESC Report "Treatment of Launch Vehicle Flight Control Stability Margin Reductions for Crewed Missions with Emphasis on Slosh Dynamics," June 2022. https://ntrs.nasa.gov/citations/20220009857.
3. NESC Technical Bulletin No. 22-06, "Treatment of Slosh Stability Margin Reductions for Human-Rated Launch Vehicles," August 2022. https://www.nasa.gov/nesc/technicalbulletins.

For information, contact Dr. Tannen S. VanZwieten tannen.vanzwieten@nasa.gov and Cornelius J. Dennehy cornelius.j.dennehy@nasa.gov and John H. Wall, john.w.wall@nasa.gov.

National Aeronautics and Space Administration

NASA Engineering and Safety Center Technical Bulletin No. 22-06

Treatment of Slosh Stability Margin Reductions for Human-Rated Launch Vehicles

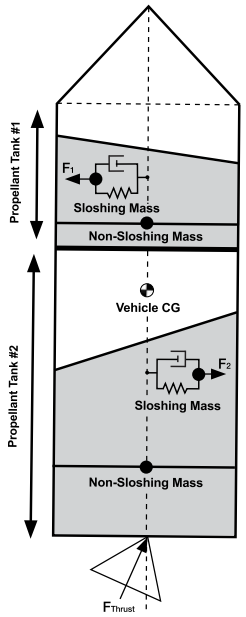
Slosh dynamics pose a stability concern for human-rated launch vehicles during ascent. Historical perspectives on the treatment of slosh dynamics, newly developed rules of thumb, the utility of flight data, and methods for analyzing and dispositioning slosh instability risks should be considered when linear stability margins are lower than typically accepted for human-rated systems.

Historical Perspective on Slosh Treatment for Human Space Flight (Ascent)

No conclusive example has been found in Space Shuttle or Saturn Program crewed flight history in which transient negative linear slosh stability margins were permitted. The uncrewed Saturn 1 S-IV had low-to-negative slosh margins, but tank baffles and a slosh deflector were added to gain-stabilize slosh prior to human-rating the S-IVB vehicle. Precedent exists in Saturn and Shuttle to rely on time domain performance metrics to accept reduced slosh margins. Time domain simulations included external forcing functions to quantify impacts (e.g., gimbal oscillations, attitude error, crew acceleration) associated with worst-case slosh excitation due to disturbances (e.g., staging and guidance command transients).

Slosh Fundamentals

Each slosh mode can be accurately modeled as a linear mass-spring-damper or spherical pendulum with two degrees of freedom. The mechanical model parameters are scheduled as a function of flight condition (e.g., propellant liquid level, acceleration) based on test-correlated analytical and empirical relationships. This mechanical analog provides insight into the basic nature of slosh response. Analysis of fundamental physics involved in sloshing propellants can demonstrate the nature of the slosh response and serve as a foundation for understanding and verifying responses from more complex vehicle simulations. A rule of thumb known as the slosh "danger zone" was established in the Saturn era for a single tank. This zone predicts poor phasing of slosh dynamics will occur when the slosh mode location falls below the center of percussion and above a location near the vehicle center of gravity (CG). An advanced analytical technique was recently developed to determine the propensity for unfavorable phasing with dual-tank sloshing modes that would be undetected by the single-tank danger zone criteria. Slosh interactions with flexible structural dynamics can also impact vehicle stability. Analysts should verify consistency between rules of thumb, linear analyses, nonlinear analyses, and flight data.



Typical Slosh Model

Utility of Flight Data for Slosh Stability Model Validation

Flight data is typically inconclusive regarding slosh stability margins as it may not provide sufficient information to anchor slosh model predictions or validate stability margins. Even when slosh is predicted to be unstable in the frequency domain, slosh instability detection from flight data is elusive due to inadequate excitation and small growth rates. Thus, the lack of observable ascent slosh response is not a demonstration of vehicle stability robustness. Without targeted excitation, sufficient sensing, and dwell time, specific vehicle model response validation (e.g., aero, rigid body, slosh, or flex) is not possible. In-flight response of lightly damped flexible/slosh modes can provide frequency confirmation if sufficient excitation exists, but long dwell times may be needed to identify slosh gain and phase margins. In contrast to slosh, bending-mode models can typically be verified to higher accuracies because the signatures in flight data tend to be cleaner. In summary, flight experience raises confidence but cannot validate slosh models or determine stability margins without targeted provisions (e.g., programmed test inputs).

Methods for Treatment of Low or Negative Slosh Stability Margins

Vehicle stability margins should be reported with the inclusion of all relevant dynamics (i.e., rigid body, slosh, flexible body, and aerodynamics). If slosh stability margins are below industry standards, routine analysis should be augmented by an evaluation of sensitivities and consequences. Targeted sensitivity studies conducted in the frequency and time domains should be designed to analyze the effects of parameter and system variations. In the frequency domain, this can include dispersing the relative slosh frequency in multiple tank scenarios, investigating the effects of flexible body/slosh coupling, evaluating mitigations afforded by nonlinear damping, and computing the time to double. In the time domain, this can include application of a doublet and direct slosh state initialization during stressing flight conditions or periods of instabilities for nominal and worst-case dispersed vehicle parameters. When slosh margin instabilities are present, slosh amplitude doubling times can be compared against the duration of the instability. The purpose is to evaluate opportunities for instability to occur in flight and analyze the relevant indicators (e.g., growth rate/decay, actuator usage, slosh wave amplitude, crew acceleration, abort margins). Stressing cases of concern can then be evaluated for credibility, probability, and consequences from the perspective of overall vehicle risk. Early in a development program, and for pre-flight certification, it is good practice to automate stressing simulations and incorporate them into the standard analyses to increase design confidence and coverage for effects not otherwise captured even when the linear margins indicate stability.

References

1. NESC Technical Bulletin No. 22-05, "Launch Vehicle Flight Control Stability Margin Reduction Considerations," August 2022. https://www.nasa.gov/nesc/technicalbulletins.
2. NESC Report "Treatment of Launch Vehicle Flight Control Stability Margin Reductions for Crewed Missions with Emphasis on Slosh Dynamics," June 2022. https://ntrs.nasa.gov/citations/20220009857.
3. Ottander, J. et al., AIAA SciTech 2018, "Practical Methodology for the Inclusion of Nonlinear Slosh Damping in the Stability Analysis of Liquid Propelled Launch Vehicles."
4. Bauer, H. F., 1964, "Fluid Oscillations in the Containers of a Space Vehicle and Their Influence on Stability," NASA TR R-187.
5. Pei, J., "Analytical Investigation of Propellant Slosh Stability Boundary on a Space Vehicle," Aerospace Research Central. Published April 23, 2021. https://doi.org/10.2514/1.A35024.

For information, contact Dr. Tannen S. VanZwieten tannen.vanzwieten@nasa.gov and Cornelius J. Dennehy cornelius.j.dennehy@nasa.gov and John H. Wall, john.w.wall@nasa.gov.

NESC tech bulletin

Helium Solubility in MMH and NTO

A test program to characterize the solution of helium in nitrogen tetroxide/mixed oxides of nitrogen (NTO)/(MON) and monomethylhydrazine (MMH) at anticipated flight-representative pressures/temperatures was completed. Updated relations for helium solubility in MMH and NTO were generated and documented.

Background

One of the problems encountered in the development of liquid bipropellant rocket engines is the occurrence of low-frequency instabilities, some of which can lead to a phenomenon referred to as chugging. Chugging is caused by a dynamic coupling of the propellant feed system with the combustion dynamics in such a way that it amplifies any disturbance in pressure or propellant flow. Instabilities (e.g., chugging) have been issues for 60 years. Chugging mitigations are often hardware specific and include avoiding the operating regimes that generate instabilities, changing line and manifold volumes, and other design considerations. It has been demonstrated that chugging can be significantly affected by the propellant pressurant, specifically helium, transitioning into and out of solution.

During a literature search for a previous NESC study [ref. 1], it was found that many of the reports containing data on helium transitioning into solution (i.e., MMH, NTO and MON) were reprinted data that were obtained from other sources. Sorting through the reports allowed the original source data to be identified. These various data threads were illustrated to provide improved understanding of the available information and indicated significant scatter in the helium solubility data for both NTO/MON and MMH.

Helium Solubility Testing

A test program was conducted to characterize the solution of helium in NTO/MON and MMH at anticipated flight-representative pressures/temperatures. The testing was conducted at The Aerospace Corporation in El Segundo, California. The testing utilized equipment that had been used for measurements of helium solubility in hydrazine [ref. 2] and was a modified version of the original method used by Chang [refs. 3, 4] (see Figure 1). The major apparatus change from the work of Chang et al. was the use of a steel cylinder instead of a glass bulb, thereby allowing higher pressure test conditions. The current effort used Teflon-lined stainless-steel cylinders that could be safely pressurized to 12.4 MPa (1800 psia). The maximum pressure of the entire system is 6.9 MPa (1000 psia), which is based on the valves as they have the lowest pressure rating.

The experiments used two capacitance manometers (i.e., baratrons), the first ranging from 0.35 to 3.5 kPa (50 to 500 psia) and the second ranging from 0.69 to 6.9 MPa (100 to 1000 psia). Since the stainless-steel cylinders prevented the use of magnetic stirring as utilized by Chang et al., the setup was stirred externally by gently shaking. Tests in deionized water were used to calibrate the apparatus by measuring argon and helium solubility (see Figure 2). The same initial calibration sequence was utilized in the hydrazine solubility work [ref. 2].

Testing Results

The findings from the NESC study include:

- Past MMH datasets underpredicted the helium solubility at lower temperatures (i.e., less than ~20°C).
- The assumption of a linear dependence of mole fraction to pressure is valid for MMH and NTO over the temperature range of -18 to 80 °C and pressure range of 0.1 to 6.8 MPa.
- The updated relations for helium solubility in MMH and NTO from the current assessment are considered an improved prediction of the fully saturated condition compared to prior empirical fits.

References

1. Dorney, D. J., Dickens, K. W., Wentzel, D. J., Guardado, H. J., Fischels, M. V., McNaughton, S. T. C., Pourpoint, T. L., and Gabl, J. R., "Pressurant Gas Evolution from Helium-Saturated Hypergolic Propellants," NASA/TM-20210023030 (also NESC-RP-20-01584), October 2021.
2. DeSain, J. D., Brady, B. B., Curtiss, T. J., Greenberg, L. T., Smith, M. B., and Villahermosa, R. M., "Solubility of Pressurant Gases in Liquid Hydrazine at Elevated," Journal of Propulsion and Power, Vol. 31, No. 4, July–August 2015.
3. Chang, E.T., and Gokcen, N. A., "Thermodynamic Properties of Gases in Propellants and Oxidizers. I. Solubilities of He, N2, 02, Ar, and N203 in Liquid N204," Journal of Physical Chemistry, Vol. 70, No. 7, 1966, pp 2394-2399.
4. Chang, E. T., Gokcen, N. A., and Poston, T. M., "Solubilities of He, N2 and Ar in Hydrazine and Unsymmetrical Dimethyl Hydrazine," The Aerospace Corp. TR-0158(3210-10)-2, El Segundo, CA, 1967.

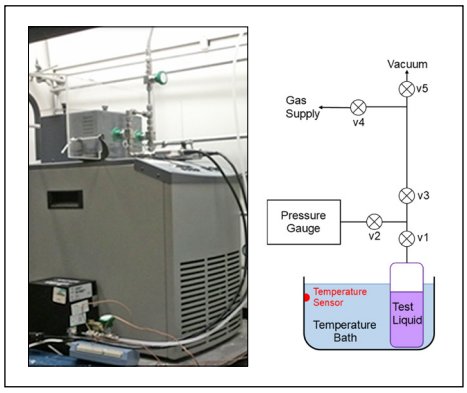


Figure 1: The Aerospace Corporation Test Setup

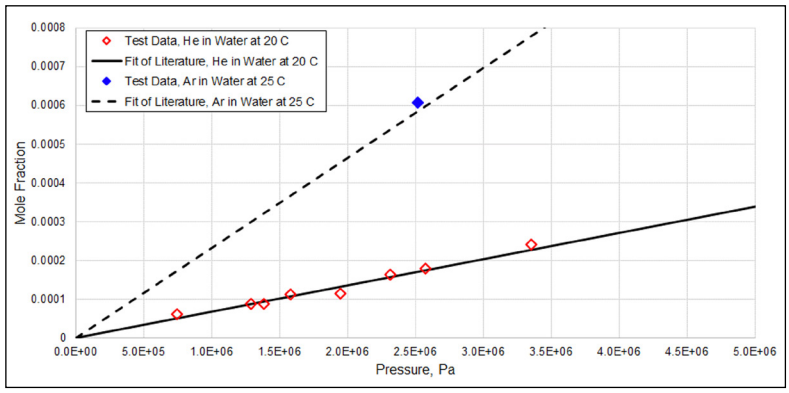


Figure 2: Solubility Tests of Helium and Argon in Water

For information, contact Daniel J. Dorney daniel.j.dorney@nasa.gov.
08/09/22 DOC ID: 20220012296
Back

Contaminant Reduction in High Purity Hydrazine

Hydrazine and its derivatives are used ubiquitously in liquid propulsion systems. In smaller thruster systems, contaminant build up has historically caused flow decay and consequently performance losses. Many of these contaminants are not controlled by the current revision of MIL-PRF-26536 [1], the High Purity Hydrazine (HPH) procurement specification, yet have been observed to be present in HPH at variable concentration and, often exceed potentially problematic levels for small thrusters. This technical bulletin outlines recent work aimed at identifying appropriate separation processes to remove specific target elemental and carbonaceous contamination in HPH.

Background

Following a change in the HPH production process used for US spaceflight application, efforts were undertaken to characterize impurities in the HPH produced by the new method. Results focused on probable identification of extraneous carbonaceous contamination and extended elemental characterization to assess risk to programs and payloads compared to legacy HPH [2-5]. Elemental contaminants, other than iron, are not currently regulated by MIL-PRF-26536 and are not currently required to meet a specific level for HPH procurement. Certain HPH users and missions have required specific low elemental levels that have been largely controlled through testing of cylinders to identify acceptable stocks. Recent discussions throughout the HPH user community have focused on the addition of limits for such contaminants to be added in the next full revision of MIL-PRF-26536. The NESC initiated a study to investigate methods to reduce specific problematic elements should new limitations be implemented and HPH stocks require purification to meet programmatic needs. Additionally, the purification methods were assessed for capacity to simultaneously remove extraneous carbonaceous content in the new HPH. Several lab-scale separation techniques including alumino-silicate-based molecular sieves, ion exchange resins, crystallization, sublimation, and vacuum-assisted distillation were screened for compatibility with HPH, target elemental removal performance, and carbonaceous content reduction.

Testing Conclusions

Alumino-silicate molecular sieves proved to be non-viable as a purification process due to modest removal of the target element and leaching of other problematic elements into the HPH. A selected ion exchange resin was determined to provide excellent target element removal; however, it introduced unacceptable levels of nonvolatile residue (NVR) to the HPH. While the cause of this NVR was not conclusively determined, the ion exchange resin cannot be considered viable without resolving this issue.

The advantage of thermodynamic separation techniques tested in this context is that HPH is not exposed to foreign material, other than the process vessels themselves. Crystallization, sublimation, and vacuum-assisted distillation all displayed the ability to reduce the target element concentration in HPH in non-optimized lab scale testing. Vacuum-assisted distillation also reduced other elemental contaminants and significantly reduced extraneous carbonaceous content. Preliminary data suggested crystallization and sublimation may also achieve carbonaceous content reduction. However, additional work is required to quantify the removal. For use, vessel material considerations are required to avoid using process stabilizers (which become contaminants) on an industrial scale. It is worth noting that crystallization was previously used to purify Viking grade hydrazine [6]. Crystallization and sublimation carry the advantage of being less hazardous than distillation when purifying HPH.

Table 1: Summary of Lab Scale Findings

Method	Target Element Removal*	Carbonaceous Removal	Considerations
Crystallization	28%	Possible Reduction**	Supercooling
Sublimation	97%	Possible Reduction**	Supercooling
Vacuum-Assisted Distillation	99.7%	35%	Stablizer Potentially Necessary for Upscale
Ion Exchange Resin	97%	Additional Contamination	Increase in NVR and Exchange Ion Concentration
Alumino-Silicate Molecular Sieves	N/A***	N/A***	Dissolution into HPH

*Target Element Removal Rates for Non-Optimized Lab-Scale Demonstration
**Further Study Needed to Quantify Reduction
***Study Halted Prior to Full Evaluation Due to Non-Compatibility

Path Forward

NASA programs and thruster manufacturers should continue to assess elements of concern not currently controlled in MIL-PRF-26536 that could impact their HPH thruster systems. Molecular sieves and ion exchange resins should not be considered viable purification methods for HPH without testing the specific material for NVR and carbonaceous material introduction into HPH. In order to build a large-scale purification capability, it is recommended that the thermodynamic separation solutions shown to be successful in this work[2] on a non-optimized bench scale, be further investigated for optimization and upscaling.

References

1. Performance specification - Propellant, Hydrazine, MIL-PRF-26536G w/Amendment 1. Department of Defense. (July 13, 2021).
2. Parker, D., Dorney, D., Coutts, J., Maynard, A., & McClure, M. (2020). State of Hydrazine Synthesis and Its Potential Impact on Spaceflight Applications. NESC Technical Assessment Report NESC-RP-20-01504. Available from the NESC.
3. NESC Technical Bulletin No. 20-08, Assessment of Ketazine Derived High Purity Hydrazine for Spacecraft Propellant Systems, Sept. 2020, https://www.nasa.gov/nesc/technicalbulletins.
4. Lesson Learned 29801, Best Practices for the Elemental Profiling of High-Purity Hydrazine, Dec. 2020, https://llis.nasa.gov/lesson/29801.
5. NESC Technical Bulletin No. 21-03-1, Best Practices for the Elemental Profiling of High-Purity Hydrazine, March 2022, https://www.nasa.gov/nesc/technicalbulletins.
6. Schuler, W.; Pharo, T.; and Hall, C., "The Removal of Impurities from Hydrazine for Control of Contamination Caused by Rocket Engine Exhaust," AIAA/SAE 8th Joint Propulsion Specialist Conference, AIAA Paper No. 72-1046, New Orleans, LA, April 1972, (p. 1046).

For information, contact Donald Parker donald.s.parker@nasa.gov and Janelle Coutts janelle.coutts@nasa.gov.

NESC tech bulletin